Université de Montréal

Protective Signaling of Oxytocin in an *in vitro* Model of Myocardial Ischemia - Reperfusion

by

Araceli Gonzalez Reyes

Department of Biomedical Sciences
Faculty of Medicine

Master's Thesis presented to the Faculty of Medicine
in partial fulfilment of the requirements for the degree of
Master of Science
Biomedical Sciences

December 2012

Université de Montréal

Faculté des études supérieures et postdoctorales

Ce mémoire intitulé:

Protective Signaling of Oxytocin in an *in vitro* Model of Myocardial Ischemia - Reperfusion

Présenté par:

Araceli Gonzalez Reyes

A été évalué par un jury composé des personnes suivantes:

Dr. John Chan, président-rapporteur

Dr. Marek Jankowski, directeur de recherche

Dre. Jolanta Gutkowska, co-directrice de recherche

Dr. Guy Rousseau, membre du jury

Résumé

<u>Introduction</u> : La prévention de la mort de cellules cardiaques contractiles suite à un épisode d'infarctus du myocarde représente le plus grand défi dans la récupération de la fonction cardiaque. On a démontré à maintes reprises que l'ocytocine (OT), l'hormone bien connue pour ses rôles dans le comportement social et reproductif et couramment utilisée dans l'induction de l'accouchement, diminue la taille de l'infarctus et améliore la récupération fonctionnelle du myocarde blessé. Les mécanismes de cette protection ne sont pas totalement compris.

<u>Objectif</u> : Étudier les effets d'un traitement avec de l'ocytocine sur des cardiomyocytes isolés en utilisant un modèle *in vitro* qui simule les conditions d'un infarctus du myocarde.

<u>Méthodes</u> : La lignée cellulaire myoblastique H9c2 a été utilisée comme modèle de cardiomyocyte. Pour simuler le dommage d'ischémie-reperfusion (IR), les cellules ont été placées dans un tampon ischémique et incubées dans une chambre anoxique pendant 2 heures. La reperfusion a été accomplie par la restauration du milieu de culture régulier dans des conditions normales d'oxygène. L'OT a été administrée en présence ou en absence d'inhibiteurs de kinases connues pour être impliquées dans la cardioprotection. La mortalité cellulaire a été évaluée par TUNEL et l'activité mitochondriale par la production de formazan pendant 1 à 4 heures de reperfusion. La microscopie confocale a servie pour localiser les structures cellulaires.

<u>Résultats</u> : Le modèle expérimental de l'IR dans les cellules H9c2 a été caractérisé par une diminution dans la production de formazan (aux alentours de 50 à 70 % du groupe témoin, $p < 0.001$) et par l'augmentation du nombre de noyaux TUNEL-positif ($11.7 \pm 4.5\%$ contre $1.3 \pm 0.7\%$ pour le contrôle). L'addition de l'OT (10^{-7} a 10^{-9} M) au commencement de la reperfusion a inversé les effets de l'IR jusqu'aux niveaux du contrôle ($p < 0.001$). L'effet protecteur de l'OT a été abrogé par : i) un antagoniste de l'OT ; ii) le *knockdown* de l'expression du récepteur à l'OT induit par le siRNA ; iii) la wortmannin, l'inhibiteur de phosphatidylinositol 3-kinases ; iv)

KT5823, l'inhibiteur de la protéine kinase dépendante du cGMP (PKG); v) l'ODQ, un inhibiteur du guanylate cyclase (GC) soluble, et A71915, un antagoniste du GC membranaire. L'analyse confocale des cellules traitées avec OT a révélé la translocation du récepteur à l'OT et la forme phosphorylée de l'Akt (Thr 308, p-Akt) dans le noyau et dans les mitochondries.

Conclusions : L'OT protège directement la viabilité des cardiomyocytes, lorsqu'elle est administrée au début de la reperfusion, par le déclenchement de la signalisation du PI3K, la phosphorylation de l'Akt et son trafic cellulaire. La cytoprotection médiée par l'OT implique la production de cGMP par les deux formes de GC.

Mots-clés : Ocytocine, cardioprotection, ischémie-reperfusion myocardiale

Abstract

Introduction: The prevention of the death of contractile cardiac cells following an episode of myocardial infarction represents the largest challenge in the recovery of myocardial function. Oxytocin, the hormone best known for its roles in reproduction and social behaviour and used commonly for the induction of parturition, has been repeatedly demonstrated to decrease the infarct size and to ameliorate the functional recovery of the injured myocardium. The mechanisms for this protection are incompletely understood.

Objective: To study the effects of oxytocin treatment on isolated cardiomyocytes using an in vitro model simulating the conditions of a myocardial infarction.

Methods: The cardiomyoblastic cell line H9c2 was used as a model of cardiomyocyte. For IR injury, the cells were placed in ischemic buffer and incubated in an anoxic chamber for 2 hours. Reperfusion was achieved by restoring cell media under normoxic conditions. OT was administered in the presence or absence of enzyme inhibitors. Cell death was evaluated by TUNEL and mitochondrial activity by formazan production during 1-4 hours of reperfusion. Confocal microscopy served for localization of cell structures.

Results. The experimental model of IR in H9c2 cells was characterized by decreased formazan production (at the range of 50-70% of normoxic control, $p < 0.001$) and by the increased number of TUNEL-positive nuclei (11.7 ± 4.5 vs. $1.3\pm0.7\%$ in normoxic control). The addition of OT (10^{-7} to 10^{-9} M) at the onset of reperfusion reversed the effects of IR to the control levels ($p < 0.001$). The protective effect of OT was abrogated by: i) an OT antagonist, OTA and siRNA-mediated OT receptor knockout; ii) the phosphatidylinositol 3-kinases inhibitor wortmannin; iii) the cGMP-dependent protein kinase (PKG) inhibitor, KT5823. Soluble guanylate cyclase (GC) inhibitor ODQ and particulate GC antagonist A71915 only partially blocked the protective effects of OT. Confocal analysis of OT-treated cells revealed translocation

of OT receptor and the phosphorylated form of Akt (Thr 308, p-Akt) into the nucleus and mitochondria.

Conclusions: OT directly protects cardiomyocyte viability if administered at the onset of reperfusion by triggering signaling of Pi3K, Akt phosphorylation and its cellular trafficking. OT-mediated cytoprotection involves cGMP production by both forms of GC.

Keywords : Oxytocin, cardioprotection, myocardial ischemia - reperfusion.

Table of Contents

List of Tables

List of Figures

List of Abbreviations

A: Adenine

AF: Alexa Fluor

AMP: adenosine monophosphate

AMPK: AMP-activated protein kinase

ANOVA: analysis of variance

ANP: atrial natriuretic peptide

APS: ammonium persulfate

AR: adrenergic receptors

ARVCM: Adult rat ventricular cardiomyocytes

ATP: adenosine triphosphate

AVP: arginine vasopressin

Bcl-2: B-cell lymphoma 2

BNP: brain natriuretic peptide

BSA: bovine serum albumin

C - cytosine

Ca_i : intracellular calcium

CaM: Ca^{2+}- Calmodulin

CaMKK: CaM kinase kinase

cGMP: cyclic guanosine 3', 5'-monophosphate

CHD: coronary heart disease

CM: cardiomyocyte

CM-H_2DCFDA: 5-(and-6)-chloromethyl-2',7'-dichlorodihydrofluorescein diacetate, acetyl ester

CNP: C-type natriuretic peptide

DAG: 1,2-diacylglycerol

DAPI: 4',6-diamidino-2-phenylindole

DMEM: Dulbecco's modified eagle medium

DMSO: dimethylsulfoxide

DNA: deoxyribonucleic acid

Dox: Doxorubicin

EDTA: ethylenediaminetetraacetic acid

ER : endoplasmic reticulum

Erk1/2 : extracellular-regulated kinases 1 and 2

FBS: fetal bovine serum

eNOS: endothelial nitric oxide synthase

G : guanine

GAPDH: glyceraldehyde-3-phosphate dehydrogenase

GLUT: glucose transporter

GPCR: G-protein coupled receptor

GSK: glycogen synthase kinase

HEPES: 4-(2-hydroxyethyl)-1-piperazineethanesulfonic acid

HR: heart rate

IgG: immunoglobulin G

IL : interleukin

i.p. : intraperitoneal

IP3 : inositol trisphosphate

IPC: ischemic pre-conditioning

IR: simulated ischemia - reperfusion

IRAP: insulin regulated aminopeptidase

i.v.: intravenous

JAK: Janus kinase

KRH: Krebs-Ringer HEPES

KT-5823 **:** (2,3,9,10,11,12-hexahydro 10R-methoxy-2,9-dimethyl-1-oxo-9S,12R-epoxy-1H-diindolo[1,2,3-fg:3',2',1'-kl]pyrrolo[3,4-i][1,6]benzodiazocine-10-carboxylic acid, methyl ester)

L: liter

LSM: confocal laser scanning microscope

LV: left ventricular

MAP: mean arterial pressure

MAPK: mitogen-activated protein kinase

MI: myocardial infarction

min: minute(s)

mitoK$_{ATP}$: mitochondrial ATP-sensitive K$^+$ channels

mPTP: mitochondrial permeability transition pore;

mRNA: messenger RNA

mTOR: mammalian target of rapamycin

MTS: [3-(3,5-dimethylthialzol-2-yl)-5-(3 carboxymethoxypheny)-2-(4-sulphophenyl)-2H-tetrazolium]

NAC: N-acetylcysteine

NHE: Na$^+$/H$^+$ exchanger

NCE: Na$^+$/Ca^{2+} exchanger

NO: nitric oxide

NP: natriuretic peptide

NPR: natriuretic peptide receptor

O$_2$: molecular oxygen

ODQ : 1H-1,2,4- oxadiazolo [4,3-a] quinoxalin-1-one

OT : oxytocin

OTA: oxytocin antagonist

OTKO: oxytocin knockout

OTR: oxytocin receptor

OTRKO: oxytocin receptor knockout

p-Akt: phosphorylated Akt

p-eNOS: phosphorylated eNOS

PBS: phosphate buffered saline

PC: ischemic postconditioning

PDK-1: phosphoinositide-dependent kinase 1

pGC: particulate guanylate cyclase

Pi3K phosphatidylinositol-3-kinase

PIP2 : phosphatidyl inositol 4,5-bisphosphate

PIP3: phosphatidylinositol-3,4,5-triphosphate

PKC: protein kinase C

PKG: cGMP-dependent protein kinase

PLB: phospholamban

PLC-β: phospholipase C type β

PMSF : phenylmethanesulphonylfluoride

RAAS: renin-angiotensin-aldosterone system

RIPA: radio immunoprecipitation assay

RISK: reperfusion injury salvage kinases

RNA: ribonucleic acid

ROS: reactive oxygen species

rpm: revolutions per minute

RT: room temperature

RT-PCR: Real time polymerase chain reaction

s.c.: subcutaneous

SDS: sodium dodecyl sulfate

SERCA: sarcoplasmic reticulum Ca^{2+} ATPase

SEM: standard error

sGC: soluble guanylate cyclase

IR: simulated ischemia - reperfusion

siRNA: small interfering RNA

STAT: signal transducer and activator of transcription

T: thymine

TBS: tris buffered saline

TCA: trichloroacetic acid

TEMED: tetramethylethylenediamine

TGF: transforming growth factor

TNF: tumor necrosis factor

Tris: trisaminomethane

TUNEL: Terminal deoxynucleotidyl transferase-mediated dUTP nick end-labeling

V1a: vasopressin receptor type 1a

VEGF: vascular endothelial growth factor

Acknowledgements

I would like to thank my supervisors, Dr. Marek Jankowski and Dr. Jolanta Gutkowska for so generously accepting me into their laboratory and for their continued support and encouragement throughout the course of my master's project. I thank them for sharing their knowledge and enthusiasm with me. Thank you for believing in me and inspiring me to improve myself.

I would also like to thank all the members of the laboratory, in particular Christophe Fadainia, Dominique Genest and Dr. Eric Plante, whose encouragement and moral support have been invaluable to me; Dr. Bogdan Danalache and Dr. Alexandre Popov for so generously sharing their incredible expertise, and Dr. Ahmed Menaouar and Julien Durand for both moral and technical support.

I extend a special thank you to my family, including my new Canadian family, whose love and support have allowed me to thrive. Lastly I thank my loving husband, whose constant love, patience and inspiration mean the world to me.

Dedication

I dedicate this work to my parents, whose love, inspiration and support have always encouraged me to aim high and pursue my dreams. I am eternally grateful.

I. INTRODUCTION

I.1. Myocardial ischemia - reperfusion injury

Coronary heart disease (CHD) is the leading cause of death in the world[1]. A serious manifestation of CHD is cardiac ischemia, caused by the interruption of blood flow to the cardiac tissue and an inadequate O_2 supply to the heart. Acute ischemia as in the case of acute myocardial infarction (MI) is treated by the rapid restoration of blood flow through reperfusion strategies. Although reperfusion is necessary for cardiac rescue, the abrupt restoration of blood flow results in ischemia-reperfusion injury of the myocardium[2,3]. The ensuing cell death is triggered by several factors including cellular and mitochondrial calcium overload, oxidative stress, reduction in nitric oxide (NO) production, and inflammatory response. The loss of contractile cardiac cells, cardiomyocytes, remains the largest challenge to functional recovery from an episode of acute MI[1]. Even with current reperfusion strategies, 10% of acute MI patients die and 25% progress to heart failure[1], with 7 million deaths each year directly attributable to MI around the world[4].

I.1.1. Pathophysiology of ischemia - reperfusion injury

Mitochondrial damage is a major factor triggering the loss of myocardial cells[5]. Under normal physiological conditions myocardial tissue produces more than 90% of its ATP by mitochondrial oxidative phosphorylation[6]. During ischemia cardiomyocytes rely on anaerobic glycolysis, leading to intracellular acidosis[7,8]. This acidosis causes a stimulation of the activity of the

sarcolemmal Na^+/H^+ exchanger (NHE-1) to extrude excess H^+ ions from the cytosol, with concomitant Na^+ overload of the cytosol[8]. The excess of intracellular Na^+ in turn causes an increase in intracellular Ca^{2+} due to the action of the Na^+/Ca^{2+} exchanger (NCE)[8]. The depletion of ATP during ischemia prevents the activity of pumps such as the Na^+/K^+ ATPase, as well as active Ca^{2+} excretion which prevents the re-establishment of normal cellular ionic homeostasis[5,8,9]. The intracellular Ca^{2+} overload causes calpain activation, apoptotic cascades, mitochondrial permeability transition pore (mPTP) opening and hypercontracture. However, the intracellular acidosis present during ischemia causes a decrease in the affinity of troponin to Ca^{2+} and phosphofructokinase, which hinders the functioning of the myocardial contractile apparatus[7] preventing hypercontracture. Similarly, cell death during ischemia is prevented as a lower intracellular pH inhibits the formation of the mitochondrial permeability transition pore.

Lethal reperfusion injury arises from the rapid normalization of physiological conditions after a period of ischemia. As the extracellular pH normalizes it causes a massive efflux of H^+ from the cell and influx of Na^+, causing the Na^+/Ca^{2+} exchanger to operate in reverse mode and further increase intracellular Ca^{2+} overload. Furthermore, there is an increase in reactive oxygen species (ROS) production in the first minutes of reperfusion as O_2 is re-introduced into damaged mitochondria[9]. High intracellular $[Ca^{2+}]$ and ROS trigger the opening of the mitochondrial permeability transition pore (mPTP)[5,10]. The mPTP is a large conductance pore that forms on the mitochondrial membrane, releases mitochondrial proteins into the cytosol and triggers cell death[11] by apoptosis and necrosis. Sustained opening of mPTP is considered the irreversible point in the commitment of a cell to death[10].
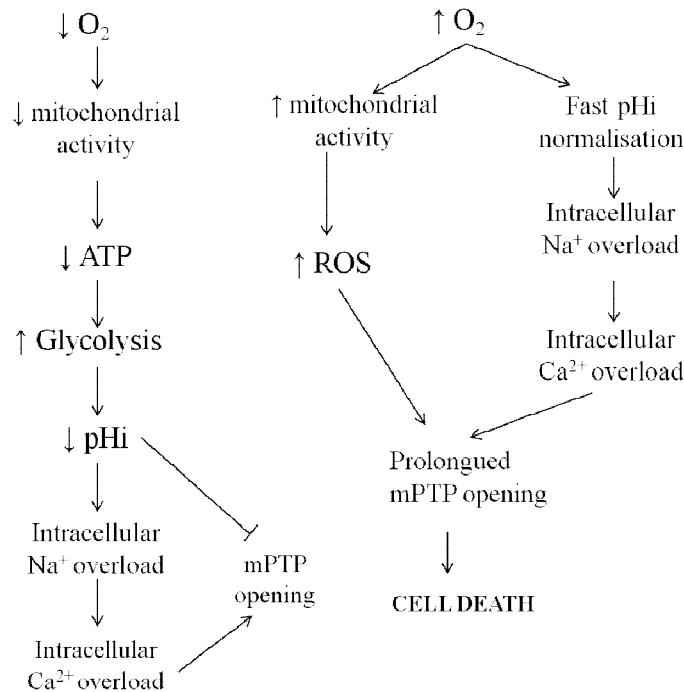
Figure 1. Pathophysiology of Myocardial Ischemia - Reperfusion injury. During ischemia, the reduced O_2 supply causes an increase in the rate of glycolysis, generating H^+ and lactate and decreasing intracellular pH (pHi). The Na^+/H^+ exchanger, NHE, overloads the cytosol with Na^+ as the excess H^+ are extruded, causing the reversal of the Na^+/Ca^{2+} exchanger, which extrudes excess Na^+ but overloads the cytosol with Ca^{2+}. The use of ATP-dependent pumps is limited by lack of ATP. However, the intracellular acidosis inhibits mPTP opening. During reperfusion, abrupt restoration of the extracellular pH causes an even more pronounced efflux of H^+ from the cell, aggravating further the mechanisms outlined above. As the pHi is normalized, and a ROS burst is created as O_2 is reintroduced, the inhibition of mPTP opening is lifted and lethal reperfusion injury can arise.

I.1.2. Cardioprotection by ischemic pre- and postconditioning

A significant reduction in infarct size is observed when the myocardium is exposed to brief intermittent periods of ischemia and reperfusion, both at a time prior to ischemia, known as ischemic preconditioning (IPC), or immediately after reperfusion, known as ischemic postconditioning (PC). For the first time, Murry *et al.* reported that four cycles of brief intermittent ischemia before the onset of a sustained episode of ischemia followed by reperfusion reduced infarct size to 25% of that seen in control animals[12]. They termed this phenomenon ischemic preconditioning (IPC) and much work has been devoted ever since to identify the mechanisms involved in this phenomenon. Intracellular signaling pathways that are activated during IPC and create a conditioned phenotype are responsible for cell protection and the reduction in infarct size[13]. Adenosine, bradykinin and opioids acting via their respective G-protein coupled receptors (GPCRs) can mimic the IPC response, which is thought to converge on protein kinase C (PKC) activation, likely via the opening of mitochondrial ATP-sensitive K^+ channels[14] and prevention of mPTP opening[13]. The signaling cascades recruited by IPC appear to be active during the reperfusion phase and mediate IPC-induced protection at reperfusion[15].

More recently, a cardioprotective effect of performing an intermittent ischemia protocol at the onset of reperfusion following a prolonged ischemic episode in anesthetized dogs was reported by Zhao *et al.*[16]. They termed this effect ischemic postconditioning (PC) and it was shown to be equally effective as IPC at reducing final infarct size. Approximately 50% of the final infarct size is believed to be preventable through conditioning strategies[1].

Two mechanisms of cardioprotection by PC have been proposed: passive mechanisms, in which the protection results from a gradual restoration of the pre-ischemic conditions rather than an abrupt reperfusion, and active, in which cardioprotective signaling mechanisms are triggered within the cardiomyocytes[17]. Active mechanisms include the recruitment and activation of kinase-mediated signaling pathways within the injured cardiomyocytes, such as the RISK and SAFE pathways (see section I.1.4. below).

I.1.3. Cardioprotective signaling involved in pre- and postconditioning

IPC is believed to act by activating pro-survival kinases at reperfusion[15,18]. Several signaling pathways have been shown to be activated by PC, and inhibitors of key kinases in these pathways can block the protective effect of IPC and PC. The reperfusion injury salvage kinase (RISK) pathway includes pro-survival kinases such as phosphoinositide 3-kinases (Pi3K)/Akt, AMP-activated protein kinases (AMPK) and extracellular signal-regulated kinases 1 and 2 (Erk ½), whose signalisation is thought to converge on the activation of cGMP-dependent protein kinase (PKG) and protein kinase C (PKC) ε, causing the inhibition of prolonged mPTP opening[8]. Similarly, the survivor activating factor enhancement (SAFE) pathway involving Janus kinase (JAK) and signal transducer and activator of transcription (STAT) signaling can provide protection separately from the RISK pathway[8]. The degree of crosstalk between the RISK and SAFE pathways is presently unclear, but both are believed to ultimately protect mitochondrial function[19]. The pharmacological manipulation of these pathways represents a more clinically - applicable alternative to ischemic conditioning[20].

I.1.3.1. Reperfusion injury salvage kinase (RISK) Pathway

I.1.3.1.1. Pi3K/Akt

Pro-survival kinases known to be involved in PC include phosphatidylinositol 3-kinases (Pi3K), which causes the phosphorylation and activation of Akt[8]. Pi3Ks are a family of intracellular signal-transducing lipid kinases with a wide variety of roles in the regulation of cellular processes. Three classes of Pi3K (Class I, II and III) have been identified based on the specificity of the lipid substrate they phosphorylate[21].

Akt kinase, also known as protein kinase B, is known to be a critical kinase at the core of cellular signal integration in survival, growth and proliferation[22]. Akt activity is modulated by its phosphorylation status at residues Thr308 and Ser473[23]. Accordingly, Akt activity is regulated through the activity of intracellular phosphatases and kinases that can directly or indirectly alter its phosphorylation status.

Upon a variety of stimuli including GPCR activation, class I Pi3Ks phosphorylate phosphatidylinositol-4,5-biphosphate (PIP2) and convert it to phosphatidylinositol-3,4,5-triphosphate (PIP3) at the inner surface of the plasma[23] and nuclear[24] membranes. PIP3 binds intracellular enzymes with a pleckstrin homology (PH) domain[25], such as Akt and phosphoinositide-dependent kinase 1 (PDK-1). PH domains are conserved protein sequences of approximately 100 amino acids which are present in a wide range of proteins and mediate their interaction with other intracellular components such as proteins and lipids[26,27]. The interaction of PIP3 with Akt and PDK-1 allows for the PDK-1-mediated phosphorylation and activation of Akt at Thr308[23]. For full activation, Akt must also be phosphorylated at a second residue, Ser473,

which is thought to be mediated at the plasma membrane by mammalian target of rapamycin (mTOR) protein complex 2[28]. Upon activation, Akt accumulates in different cellular compartments, including mitochondria[29,30] and nuclei[31,32].

Akt phosphorylation and activation reduces cardiomyocyte death from ischemia-reperfusion injury and regulates glycogen synthesis, glucose transport, glycolysis, protein synthesis, cell enlargement, mitochondrial integrity and cell death[28,33]. However, studies demonstrating negative effects of constitutive and sustained active Akt expression in cardiomyocytes, such as hypertrophy, suggested that there could be an important spatial and temporal regulation of Akt activation[28].

It was recently discovered that Pi3K activation resulted in a rapid accumulation of Akt in the mitochondria in neuroblastoma and embryonic kidney cell lines, preventing the release of apoptotic proteins from the mitochondria[34]. It appears that translocation of phosphorylated (activated) Akt to the mitochondria preserves mitochondrial integrity[35]. In mice hearts, translocation of phosphorylated Akt from the cytosol to the mitochondria was associated with ATP-dependent mitochondrial K^+ channel (mitoK$_{ATP}$) opening[36]. Similarly, insulin stimulated phosphorylation and translocation of Akt to the mitochondria of mice cardiomyocytes[37], and constitutively active mitochondria-targeted Akt over-expression prevented cell death in rat neonatal cardiomyocytes[29]. A mitochondria-targeted constitutively active Akt protected mitochondrial integrity as indicated by the prevention of the loss of mitochondrial membrane electrochemical gradient in cardiomyocytes exposed to H_2O_2 or Doxorubicin[29].

There exist several known mitochondrial targets for Akt such as Bcl-2 family members[22] and hexokinase II[38] whose phosphorylation by Akt favours survival. Other downstream targets of Akt are nitric oxide (NO) synthase (NOS)[22] isoforms (such as mitochondrial NOS)[39], which become active upon Akt - mediated phosphorylation, as well as glycogen synthase kinase (GSK) and caspase-9, both of which become inactive through phosphorylation by Akt[30].

I.1.3.1.2. eNOS-cGMP/PKG

Activation of the cGMP/PKG pathway plays a critical role in the pro-survival signaling triggered by IPC and PC. The second messenger cyclic guanosine 3', 5'-monophosphate (cGMP) is generated by soluble or particulate guanylyl cyclases (sGC or pGC). pGC are natriuretic peptide receptors (NPR), whereas sGC is a cytoplasmic heterodimeric haemoprotein activated by nitric oxide (NO) and carbon monoxide (CO). The subcellular localization of cGMP generation and accumulation plays a role in determining its effect[40].

An important mediator of the effects of cGMP is cGMP-dependent protein kinase (PKG). PKG inhibits NHE activity[41], delaying normalization of intracellular acidosis during reperfusion which is unfavourable for mPTP opening. Other downstream targets of PKG include the opening of mitoK$_{ATP}$[14]. Inhibition of PKG activity with inhibitor KT-5823 blocks the cardioprotective effect of insulin[42], of B-type natriuretic peptide and of NO[43].

Additionally, nitric oxide (NO) production is known to be a mediator of IPC[19], and exogenous NO can induce pharmacological postconditioning[44] independently of PKG activity through S-

nitrosylation of protein thiol groups[45]. The phosphorylation-based activation of eNOS (at residue Ser1177) is known to be involved in the protection by IPC, PC and pharmacological conditioning[19].

I.1.3.2. Survivor activating factor enhancement (SAFE) pathway

Activation of the JAK/STAT pathway is necessary for the infarct-reducing effects of ischemic preconditioning[46] and plays important roles in postconditioning[8]. In the canonical model of JAK/STAT signaling the binding of cytokines, such as tumor necrosis factor alpha (TNFα), to plasma membrane cytokine receptors causes dimerization of the receptors. JAK proteins associated to these receptors trans-phosphorylate each other upon dimerization and become activated, allowing them to phosphorylate the cytoplasmic part of the associated cytokine receptor at specific tyrosines. STAT proteins can then specifically bind the phosphotyrosine motifs on the receptors, and get phosphorylated by JAKs. Phosphorylated STAT proteins dimerize and translocate to the nucleus, where they regulate the transcription of target genes[47].

TNFα activation in the heart is necessary for the induction of cardioprotection by IPC, and TNFα treatment mimics IPC independently of RISK pathway activation[48]. TNFα is believed to trigger signaling through the activation of STAT-3 proteins[48] which cause the inactivating phosphorylation of glycogen synthase kinase 3β (GSK3β) and Bad, a pro-apoptotic protein, as well as an increase in Bcl-2 and a decrease in bax expression[48]. Cardioprotective STAT-3 signaling confers cellular protection in a timeframe that indicates actions independently of but concomitant to its transcription factor activities[48].

I.1.3.3. Mitochondria as the target for IRI and postconditioning

As mentioned above, cardiomyocytes are highly reliant on oxidative phosphorylation. The mitochondrial permeability transition pore (mPTP) is a large conductance channel of unclear identity that forms across the mitochondrial membranes, collapses the mitochondrial membrane potential and allows for the release of mitochondrial proteins to the cytosol, which trigger caspase cascades and cell death[8,10]. Under normal physiological conditions, the mPTP remains closed, and it is well-established that mPTP opening occurs during reperfusion after myocardial ischemia[11,49]. The conditions that favour mPTP opening at reperfusion are a burst in ROS production when oxygen is re-introduced into damaged mitochondria, high intracellular and intra-mitochondrial Ca^{2+} levels and the normalization of the intracellular pH, since acidosis inhibits its opening[8]. Since mPTP opening is viewed as the irreversible commitment of a cell to death, prevention of its opening is seen as the key endpoint of cardioprotection[10]. Indeed, mPTP prevention is viewed as the effector of pre- and postconditioning[10].

Activation of the reperfusion injury salvage kinases (RISK) pathway at reperfusion is thought to prevent mPTP opening[8,50]. Similarly, the opening of mitochondrial ATP-dependent K^+ channels (mitoK$_{ATP}$) has been linked to the prevention of mPTP opening, and mitoK$_{ATP}$ channels are modulated by known cardioprotective kinases of the RISK pathway such as PKG[14] and Akt[36].

I.1.3.3.1. Mitochondrial ATP-sensitive K^+ channels (mitoK$_{ATP}$) and PKC

The opening of mitoK$_{ATP}$ channels causes an influx of K^+ and water into the mitochondrial matrix, which causes ROS generation by the respiratory complex I and activation of PKC, p38

MAPK[19] and phosphorylation of phospholamban (PLB) at Ser16, which modulates the sarcoplasmic reticulum Ca^{2+} ATPase (SERCA) and normalizes Ca^{2+} handling, preventing hypercontracture and opening of the mPTP[8]. The molecular identity of mitoK$_{ATP}$ remains unclear, but they are known to be causally involved in IPC and PC[19].

I.1.3.3.2. Signalosome hypothesis of cardioprotective signaling

The question remains as to how the activation of cytosolic kinases (such as those in the RISK pathway) could rapidly modulate the appearance of the mPTP in the mitochondrial membranes. To address this problem, Garlid *et al.*[51,52] proposed the Signalosome hypothesis of cardioprotective signaling. This hypothesis proposes that GPCR signaling at the plasma membrane results in the caveolar assembly of vesicles containing various kinases, forming signaling complexes that are then translocated intracellularly to the mitochondria and phosphorylate receptors on the outer mitochondrial membrane. This triggers the phosphorylation of a mitochondrial pool of protein kinase C-ε which in turn phosphorylates and opens mitoK$_{ATP}$ channels[51]. These signalosomes are formed upon various cardioprotective stimuli, such as IPC, PC, bradykinin; they can be isolated and when added to untreated hearts can cause mitoK$_{ATP}$ opening and prevention of mPTP formation. These 100-140 nm vesicles contain caveolin 3, Akt, PKG, eNOS and GC[51].

I.2. Oxytocin System

Oxytocin (OT) is a small peptide known to mediate a wide variety of physiological functions, both as a hormone and as a neurotransmitter, from childbirth and lactation to socialization and appetite modulation[53]. Clinically, oxytocin analogues are widely used in the induction of labour during childbirth and for the prevention of post-partum hemorrhage. Synthetic analogues of oxytocin are amongst the most commonly used pharmaceuticals in the world and are listed in the World Health Organization's list of essential medications[54].

Initially discovered by Dale in 1906 for its uterotonic and milk ejection effects, OT was the first peptide hormone whose structure was elucidated in 1953[55]. OT is highly conserved in all animal species with the amino acid sequence Cys-Tyr-Ile-Gln-Asn-Cys-Pro-Leu-Gly-NH_2 and a disulfide bridge between Cys residues 1 and 6[56]. In mammals, OT is primarily synthesized in the supraoptic and paraventricular nuclei of the hypothalamus. OT is transcribed as a long precursor protein, preprooxytocin, of 160-170 amino acid residues. This preprohormone includes the signaling peptide and the OT carrier protein neurophysin I which is synthesised from the same gene as OT. OT is then processed and transported by neurophysin I to the posterior pituitary and stored in neurosecretory granules at high concentrations (0.1 M) until its release into circulation[56] in a pulsatile manner[57]. The intermediate form of OT is the tri-aminoacid extended OT-Gly-Lys-Arg (OT-GKR) and has recently been shown to also exert significant biological activity[58].

Figure 2. Neurophysin - Oxytocin. Larger ribbon structure depicts neurophysin; stick-and-ball structure depicts oxytocin. Taken from Wikimedia Commons.

Traditionally, OT has been considered a female reproductive hormone although the observations that OT is released in men and women to the same degree and through the same stimuli have revealed OT to be involved in many processes distinct from reproduction in both men and women. OT plays a role in the regulation of food intake, stress responses, immune modulation, cardiovascular regulation and in complex social behaviours such as bonding and relationship maintenance[56,59].

OT is related to a second neurohypophyseal hormone, arginine vasopressin (AVP). AVP is also a nonapeptidic hormone differing from OT in residues 3 and 8 (Cys-Tyr-<u>Phe</u>-Gln-Asn-Cys-Pro-<u>Arg</u>-Gly-NH_2). AVP induces vasoconstriction, water retention and corticotrophin release[60], whereas OT causes natriuresis, vasodilatation, decreases in blood pressure, negative cardiac inotropic and chronotropic effects[61], and decreases cortisol levels[62].

I.2.1. Oxytocin receptors

Only one receptor specific for OT has been discovered so far. This receptor, OTR, is a member of the class I family of G protein - coupled receptors (GPCR) with seven trans-membrane domains[56].
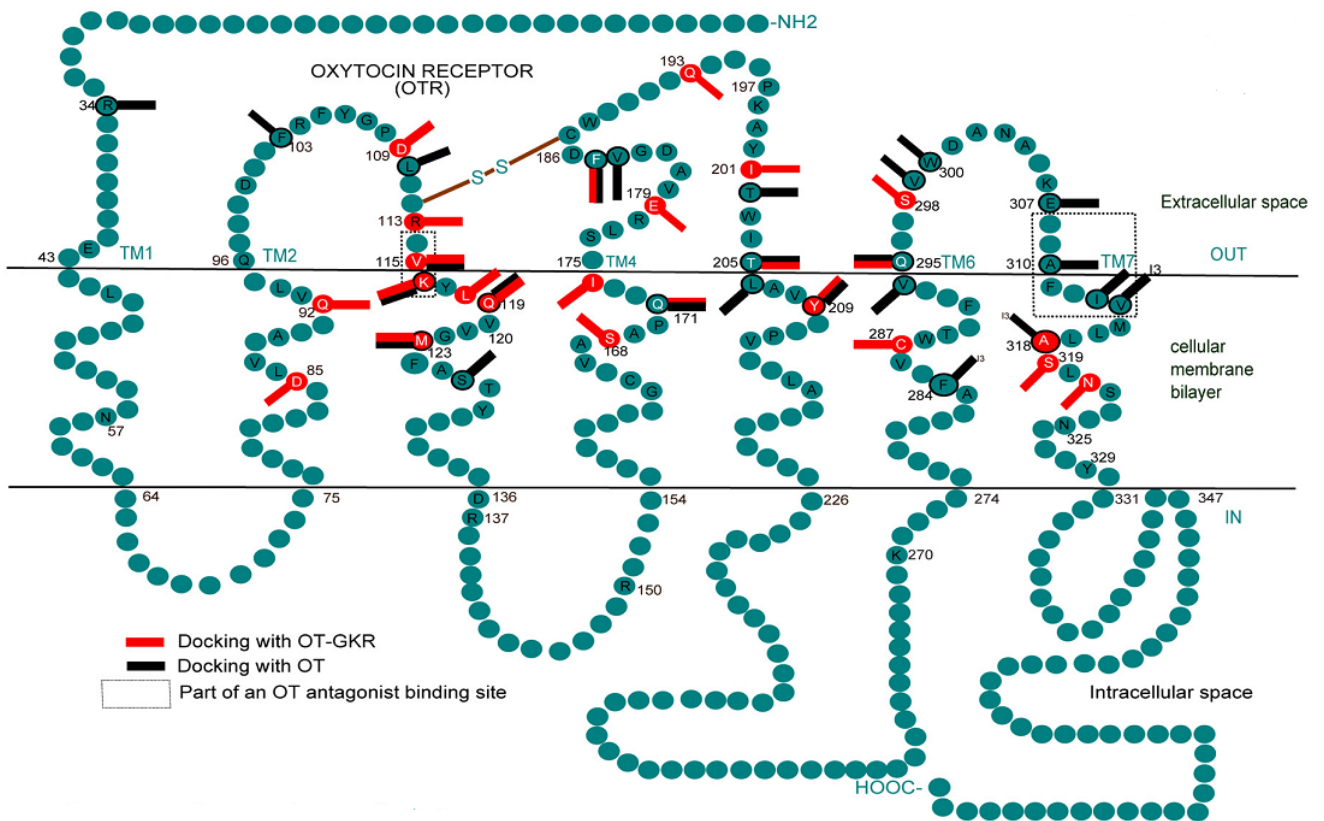
Figure 3. Schematic model of the human OTR spanning the membrane. The amino acid residues in black circles have been proposed as OT docking sites, and the red bars represent docking sites of OT-GKR. Figure taken from Danalache *et al.*, 2010[58].

The regulation of OTR expression is species-specific[56]. OTR expression has been described in a variety of tissues and cell types such as myometrial smooth muscle cells, myoepithelial cells of

mammary glands, vascular endothelium, kidney epithelium, hypothalamus, anterior pituitary, astrocytes, osteoblasts, adipocytes[56] and, recently, cardiomyocytes[63]. Additionally, OT can trigger signalisation via vasopressin receptors V1 and V2a but with lower affinity[64].

The OTR gene is composed of a 17 kb region and contains four exons and three introns, one of which (intron 3) is believed to be involved in OTR transcriptional suppression. The promoter region of the OTR gene contains interleukin response elements as well as estrogen response elements in rats, mice and humans[56]. It is believed that the OTR promoter is constitutively active. Introns 1 and 3 are probably involved in methylation-based suppression of OTR expression[57].

OTR, like other GPCRs, undergoes a rapid desensitization upon OT stimulation (>60% decrease in 5-10 minutes of OT stimulation of Hek293 cells) that is based on receptor internalization[56]. OTR is associated to caveolae on the plasma membrane.

I.2.2. OT/OTR in cytoprotective signaling

OT has been shown to protect various tissues and cell types from ischemia-reperfusion injury. After the initial report that OT administration had anti-inflammatory, pro-survival effects on rat musculocutaneous flaps[65], Tugtepe *et al.*[66] showed that OT, given before the onset of renal ischemia and again before reperfusion was started, improved kidney function and decreased damage to the tissue and oxidative stress through decreases in neutrophil infiltration and fibrosis. Similarly, in a rat model of hepatic ischemia-reperfusion OT (500 μg/kg, i.p.) given 24 and 12 hours before an ischemic insult and again just prior to the onset of reperfusion alleviated hepatic

damage, fibrosis and neutrophil infiltration[67]. More recently, OT (1 µM administered during the ischemic insult) was shown to protect immature hippocampal cell cultures *in vitro* from loss of viability resulting from oxygen-glucose deprivation, and this effect was fully blocked by the use of an OT antagonist[68].

I.2.3. OT as a cardioprotective hormone

Following the observation by our laboratory that OT is a cardiovascular hormone[63,69], a cardioprotective effect of OT has been revealed. OT stimulates release of the cardioprotective atrial natriuretic peptide (ANP) from isolated dog atria in an OTR-mediated mechanism that appears to be dependent on the action of intrinsic parasympathetic postganglionic neurons[63]. OT was also shown to have transient negative inotropic and chronotropic effects on perfused isolated dog right atria in a mechanism independent of ANP release and mediated by nitric oxide (NO) production and acetylcholine release at cardiac parasympathetic postganglionic neurons[61].

Ondrejcakova *et al.* [70] showed for the first time that in isolated rat hearts, a 25 minute perfusion with OT preceding the induction of an ischemic insult reduced infarct size by 66% as compared with control hearts. In the same study the elimination of the negative chronotropic effect of OT by the electrical stimulation of heartbeat eliminated the infarct reduction, which led the authors to conclude that OT- induced protection of ischemic myocardium is dependent upon its negative chronotropic effects. Kobayashi *et al.*[71] demonstrated in a rabbit model of *ACUTE MI* that daily subcutaneous treatments with OT (10 mg/kg, s.c.) immediately following reperfusion

significantly reduced infarct size, had pro-angiogenic and anti-fibrotic effects and increased the activation of pro-survival kinases Akt, Erk1/2 and STAT3, as well as eNOS; anti apoptotic Bcl-2 was up-regulated in the ischemic myocardium following OT treatment, indicating potential anti-apoptotic effects. Interestingly, Akt, Erk1/2, eNOS and STAT3 have all been previously shown to be mediators of cardiac pre- and postconditioning[8].

Further supporting a cardioprotective role for OT, the expression of OT and its receptor was strongly induced both in the heart and hypothalamus of ovariectomized and sham-operated rats following exercise training, indicating a possible involvement of OT in exercise's cardioprotective effects[72], and down-regulated by 40-50% in the injured left ventricle of mice[73] and rats[74] following MI. Jankowski *et al.* found that this down-regulation following MI could be reversed by administration of OT (25 ng/kg/h, s.c.) given before the onset of ischemia and during one week of reperfusion in a rat model of myocardial infarction[74]. In the same study, OT was revealed to reduce the expression of pro-inflammatory cytokines (TNFα, IL-1β and IL-6) produced by MI back to the levels seen in sham-operated rats; OT could also reduce immune cell infiltration (especially of neutrophils), induce eNOS production and normalize ANP mRNA expression in the scar area, and had pro-proliferative, anti-apoptotic and anti-fibrotic effects on injured hearts. OT was found to decrease IL-6 secretion from macrophages and endothelial cells in a dose-dependent manner, and to attenuate superoxide production in aortic endothelial and smooth muscle cells, monocytes and macrophages[75]. OT was also shown to induce glucose uptake *in vitro* in neonatal rat cardiomyocytes under conditions of chemical hypoxia by a pathway involving Pi3K[76].

Work by Alizadeh *et al.*[77] showed that the infarct size reduction in the anesthetized rat heart induced by a pre-treatment with OT ($0.03\mu g/kg$ i.p.) 25 minutes prior to ischemia was eliminated by the co-treatment with an inhibitor of the opening of mitoK_{ATP} channels, which have been proposed as the end-effectors of cardioprotective ischemic pre- and postconditioning[78]. Interestingly, the same group found that the protective effects of ischemic preconditioning (IPC) were completely eliminated by the administration of an antagonist specific to the OT receptor at the start of IPC, suggesting a role for endogenous OT in cardiac ischemic preconditioning[79]. No reports exist on the role of endogenous OT signaling in postconditioning.

Table 1. Oxytocin-mediated cardioprotection in myocardial ischemia - reperfusion.

Ref.	Myocardial Infarction model	Ischemia - Reperfusion Protocol	Dose and mode of OT administration	Timing of administration	Effect
[70]	Isolated perfused rat heart	25 min ischemia; 120 min reperfusion	90 µg/L	Perfused with OT for 25 min before ischemia	↓ infarct size by 66% ($p < 0.01$) Improved LV functional recovery
[71]	Rabbit MI	30 min ischemia; 2 and 14 days reperfusion	10 mg/kg/day s.c.	Immediately after reperfusion and once per day for 5 days after MI	↓ infarct size, ↓ fibrosis Normalized LV diastolic and systolic dimensions, ejection fraction, fractional shortening, +dP/dt , heart rate as well as systolic and diastolic blood pressure on day 14 post-MI Increased activating phosphorylation of anti-apoptotic Akt, Stat3, eNOS and Erk ½ on day 2 and 14 post-MI ↑ expression of VEGF, Bcl-2 ↑ expression of CD-31 positive microvessels in infarct border zone
[74]	Rat MI	Partial ischemia for 7 days	25 and 125 ng/kg/h s.c.	Prior to ischemia and then for 3 to 7 days of reperfusion	↑ Cell proliferation in infarct one (measured by PCN expression) ↓ apoptosis, ↓ fibrosis in remote myocardium ↓ neutrophil, macrophage and T lymphocyte infiltration ↓ inflammatory cytokine TNF and IL-6 ↑ TGF-β, ↓ ANP and BNP mRNA level

[77,80–82]	Rat MI	25 min ischemia; 120 min reperfusion	0.03 mg/kg i.v.and 0.03μg/kg i.p.	10 or 25 min prior to induction of ischemia	↓ infarct size to nearly 50% of control ↓ severity of ventricular arrhythmias, tachycardia and fibrillation ↓ CK-MB in blood OT effect blocked by:1. mitoK$_{ATP}$ blocker 5-hydroxydecanoate; 2. OTR antagonist; 3. mPTP opener atractyloside; 4. NOS inhibitor L-NAME; 5. PKC inhibitor chelerythine; 6. ROS scavenger N-acetylcysteine.
[83]	Isolated perfused rat heart	30 min ischemia; 120 min reperfusion	10^{-12} to 10^{-10} M	5 min prior to reperfusion and continued for 25 min	↓ infarct size, ↓ CK-MB and malondialdehyde at concentrations of 8×10^{-12}, 10^{-11} and 2×10^{-11} M

I.2.4. Atrial natriuretic peptide

Atrial natriuretic peptide (ANP) is a 28 amino acid peptide that was first isolated from atrial muscle and identified to elicit potent diuretic and natriuretic effects[84]. Other natriuretic peptides identified include brain natriuretic peptide (BNP) and C-type natriuretic peptide (CNP). ANP and BNP are predominantly synthesized in the heart, CNP in the central nervous system[85]. Three known natriuretic peptide receptors have been identified: natriuretic peptide receptor A (NPR-A), B, and C. NPR-A and -B act as membrane-bound guanylate cyclases that upon stimulation signal intracellularly through the generation of cyclic guanosine monophosphate (cGMP); NPR-C is considered a clearance receptor because it internalizes and removes natriuretic peptides from the circulation[85,86]. ANP preferentially acts via NPR-A to stimulate cGMP production[85].

ANP is synthesized as a 126 amino acid peptide pro-ANP and stored in dense secretory granules in the atria[87]. ANP secretion is mainly induced by mechanical stretching of the atria[88]. Cardiac ischemia and endothelin also stimulate, whereas NO inhibits, ANP secretion[88]. Importantly, elevated concentrations of oxytocin (10^{-6} M) have been reported to elicit ANP release from isolated perfused female rat hearts[63].

The immediate effect of ANP is to increase diuresis (water excretion) and natriuresis (sodium excretion) by inhibiting Na^+ and water re-absorption in the kidney, antagonising the effects of the renin - angiotensin - aldosterone system (RAAS)[85]. ANP acts as an endothelium-independent vasodilator and inhibits sympathetic nerve activity[89]. Furthermore, ANP can act as an autocrine and paracrine factor and directly stimulate cardiomyocytes mostly through NPR-A signaling[85].

Treatment of cardiomyocytes with ANP antagonises the hypertrophic response to norepinephrine[90] and phenylephrine as well as in basal conditions[85] via the generation of cGMP. The importance of ANP-NPR-A signaling is demonstrated by the lethality of the NPR-A knockout in mice, at 6 months of age, due to congestive heart failure or aortic dissection[91].

I.2.4.1. ANP in myocardial ischemia-reperfusion

The action of ANP opposes several detrimental effects of myocardial reperfusion injury. Plasma ANP levels are increased in patients with acute MI[89], and infusion of ANP in patients with MI causes a decrease in plasma concentrations of aldosterone, angiotensin II and endothelin, and inhibits cardiomyocyte cell death[89]. ANP also decreases macrophage and neutrophil-mediated inflammation. In isolated cardiomyocytes, ANP causes an elevation of cGMP and the nuclear accumulation of phosphorylated Akt[31], which is an key kinase with multiple cardioprotective effects in the context of myocardial ischemia-reperfusion (see section I.1.3.1.1). ANP has an anti-proliferative effect on cardiac fibroblasts[86], helping to decrease fibrosis. Treatment of isolated hearts with ANP reduced infarct size via the NO - cGMP - mitoK$_{ATP}$ pathway and significantly improved the post-ischemic recovery of cardiac output and coronary flow[85]. A clinical trial with acute MI patients receiving an intravenous infusion of ANP (0.025μg/kg/min) immediately after reperfusion and during 3 days showed a significant decrease of 14.7% in infarct size and a 5% improvement in left ventricular ejection fraction 6-12 months after acute MI[92].

I.2.5. Cardiovascular effects of OT and OTR gene knockouts

Mouse models of both OT and OTR knockout mice have been developed; these mice are viable and display no clear developmental changes, but are incapable of nursing their offspring[93,94] and display clear metabolic changes[95–97].

I.2.5.1. OT knockout

OT-/- (OTKO) mice were developed by Young *et al.*[98] who reported that these mice present a mild hypotension. In this initial study baseline heart rate (HR) was unchanged, but intrinsic HR (HR following adrenergic and cholinergic blockade) was significantly higher in OTKO mice[99]. Vagal tone did not differ significantly, but OTKO mice showed lower levels of sympathetic activity, leading to a higher sympathetic reserve[99]. OTKO mice presented an increase in baroreflex gain[99]. Furthermore, OTKO mice consume higher quantities of salt, but not water, under overnight fluid deprivation[100], in normal conditions[101], and following fluid depletion induced by polyethyleneglycol[102]. Others found a slight decrease in BP and HR in OTKO mice[102] and central stimulation with angiotensin II caused a similar increase in BP in both OTKO and control groups[102]. Mean arterial blood pressure (MAP) and heart rate (HR) averages over 24 hours were significantly lower in OTKO mice; upon induction of chronic shaker stress for 3 and 7 days, OTKO mice presented an increase in average MAP in OTKO, but not control, mice[103]. Basal levels of plasma corticosterone remained unchanged in OTKO mice compared to control, but stress-induced corticosterone increase was less pronounced in OTKO mice[103].

OTKO mice displayed an unaltered expression level and distribution of oxytocin receptors (OTR)[104]. Vasopressin (AVP) can elicit physiological effect via the activation of OTR. It was therefore proposed that the lack of overt deficiencies induced upon knockout of the OT gene could be partially compensated by the direct stimulation of OTR by AVP[96,104].

I.2.5.2. OTR knockout

There were no changes to the overall health, sensorimotor functions or anxiety behaviour in OTRKO mice[94]. OTRKO females displayed normal parturition[96,105], mating and litter size[105], but lacked the milk let-down reflex and maternal behaviour[96,105], and the pregnant myometrium did not contract upon AVP stimulation[105]. Furthermore, OTRKO mice displayed increased obesity with increased white adipose tissue and adipocyte enlargement with no differences in food intake, as well as the inability to regulate internal temperatures upon cold exposure[96]. The expression of α2A adrenergic receptors (AR) was markedly increased, while β3 AR expression decreased in brown adipose tissue[96].

I.3. The use of isolated cardiomyocytes for the study of cardioprotective signaling: advantages and limitations

The myocardium is composed of a variety of cell types, including fibroblasts, endothelial cells, vascular smooth muscle and macrophages. Cardiomyocytes represent between 70-80% of the myocardial volume; however, the relative number of cardiomyocytes in the myocardium is a lot

lower, estimated between 35 and 55% of all cells, with fibroblasts representing up to 27% of myocardial cells[106]. Thus, interventions such as ischemic conditioning are likely to affect the variety of cells present in the myocardium, and the cardioprotective phenotype triggered is likely the result of the interplay between the different cells' response to protective stimuli[4] through interactions and paracrine signaling between them. For example, using a transgenic mice model that only expressed erythropoietin (EPO) receptor in endothelial and hematopoietic cells, Teng *et al.* reported that the acute infarct-sparing effect of erythropoietin was mediated by endothelial cells[107]. On the other hand, ischemic preconditioning of isolated cardiomyocytes has been reported to protect their viability[108,109], indicating an endogenous protective response of cardiomyocytes independently of other cell types.

In order to discern the specific intracellular signalisation elicited upon cardiomyocytes by cardioprotective stimuli, isolated cardiomyocytes studies are of great importance[4]. Furthermore, isolated cardiomyocytes in culture allow for a detailed study of the intracellular structures involved in cardiomyocyte survival in the context of ischemia-reperfusion injury[109].

I.4. Hypothesis and Aims

I.4.1. Hypothesis

1. Oxytocin directly triggers protective signaling in cardiomyocytes during the acute phase of ischemia - reperfusion.

2. This protective signaling is mediated by the interaction of oxytocin with its receptor, OTR, that is expressed by cardiomyocytes.

3. Oxytocin causes the phosphorylation - dependent activation of pro-survival kinases involved in cardiomyocyte salvage from ischemia - reperfusion injury, such as those termed reperfusion injury salvage kinases (RISK), including Pi3K-Akt and cGMP-dependent protein kinase, PKG.

4. Oxytocin also induces protection indirectly through the release of ANP from intracellular stores, causing activation of natriuretic peptide receptor A (NPR-A) and subsequent cGMP-dependent cardioprotective signaling.

I.4.2. Aims

To establish an *in vitro* model that adequately simulates the damage induced by ischemia - reperfusion on isolated cardiomyocytes.

To study the detailed cellular effects of oxytocin signaling on cardiomyocytes during the acute phase of ischemia - reperfusion injury.

II. MATERIALS AND METHODS

II.1. Cell Culture

II.1.1. H9c2 myoblastic cell line from rat embryonic heart

Commercially available H9c2 rat embryonic cardiac myoblasts were purchased from ATCC and grown in Dulbecco's modified Eagle medium (DMEM) supplemented with 10% (v/v) fetal bovine serum (FBS, GIBCO Lot. 755216) and 1% (v/v) penicillin/streptomycin (Gibco 15140) at 37°C and 5% CO_2 containing 4 mM L-glutamine, 4500 mg/L glucose, 1 mM sodium pyruvate, and 1500 mg/L sodium bicarbonate. Cells were subcultured at 70-80% confluence to preserve the myoblastic phenotype.

For the majority of experiments, cells were seeded on the preceding day at a density of 10^4 cells/cm^2 and allowed to attach overnight. For experiments where conditions required longer incubation times (e.g. siRNA treatments for 48 hours), the cells were seeded at 5,000 cells/cm^2 to maintain the confluence below 80%. All cells were maintained in a humidified incubator (Sanyo MCO-17AC) at 37°C containing 5% CO_2.

Table 2 summarizes the reagents used in routine care and culture of cells.

Table 2. Reagents employed in cell culture

Product	Company	Reference
Dulbecco's modified Eagle medium (DMEM)	ATCC	30-2002 (Lot 30201224)
Fetal Bovine Serum (U.S.)	GIBCO	26140
Penicillin/Streptomycin	GIBCO	15140-122
Trypsin 0.25%/EDTA 0.1%	Multicell	325-043-EL
Dimethyl sulfoxide (DMSO)	Sigma	D8418 - 100 mL

II.1.2. Isolation of rat adult ventricular cardiomyocytes

Some key experiments were performed on primary cultures of adult rat ventricular cardiomyocytes (ARVCMs) in order to validate our use of H9c2 as a model of adult cardiomyocyte. A non-perfusion cell isolation procedure (Cellutron #ac-7018) was attempted repeatedly, but gave unsatisfactory cell yields and very high mortality of the cardiomyocytes in culture. A perfusion - based isolation procedure was followed instead.

The chest cavity of anesthetized female adult Sprague-Dawley (250-290 g) rats was surgically opened; the ascending aorta was cut and cannulised. The heart was then excised, the atria were removed with scissors, and the ventricles were perfused with a KH-Ca^{2+} solution at 37°C for 5 min, followed by a 20 minute perfusion (Gemini PC-1 perfusion pump controller) with a digestion solution containing collagenase, hyaluronidase and BSA. The ventricles were then transferred to a Petri dish containing a second digestion solution, with trypsin and DNAse I, cut longitudinally with new blades, and incubated with light agitation at 37°C for 10 minutes. Cell suspensions were filtered using a syringe attached to a Swinnex filter to remove debris. After a light centrifugation (1 min, 1000 rpm) to separate fibroblasts, the remaining cell suspension, containing an assortment of cell types present in the adult ventricle, was purified for cardiomyocytes by sequential washes and decanting onto a 10 mL cushion of 6% BSA (3 g BSA in 50 mL M199 media). After allowing cells to settle based on density, myocytes accumulated at the bottom of the BSA cushion, with non-myocytes present in the upper phase. The myocyte phase was re-suspended in M199 media with 10% FBS, counted and plated at a density of 10^5 cells in each well of a laminin-coated 12-well plate (25,000 cells/cm^2). When necessary, cells were pipetted using cut plastic micropipette tips to minimize mechanical damage to the cells.

Table 3. Cell culture media used for ARVCM isolation and culture

Product	Concentration	Reference
M199 with Phenol red		Invitrogen 11150
Sodium bicarbonate	0.026 M	Sigma S4019
HEPES buffer solution 1M	0.02M	Sigma H3375
BSA	0,20%	Serologicals FrV, Very low endotoxin. Code 81-068-3
Pen-Strep (10 000U/10 000μg)	1.0%	Gibco 15140-148
L-Ascorbic Acid (free-acid)	0.1mM	Sigma A-7631
Creatine	5mM	Sigma C-3630
Carnitine	2mM	Sigma C-0283
Taurine	5mM	Sigma T-9931
FBS	0 or 10%	Gibco 26140-079

Table 4. Krebs-Henseleit (KH) buffer used for perfusion, with and without Ca^{2+}

Product	Final Concentration	Reference
NaCl (MW 58.44)	118mM	ACL S-2838
KCl (MW 74.6)	4.7mM	Fisher Scientific P-217
$MgSO_4*7H_2O$ (MW 246.48)	1.19mM	Acros Organics 213115000
$NaHCO_3$ (MW 84)	25mM	Sigma S4019
Dextrose (MW 180.2)	11mM	ACP D-0660
KH_2PO_4 (MW 136.1)	1mM	Fisher Scientific P-285
$CaCl_2$ 100x	100mM *	J.T. Baker

* only used for KH-Ca^{2+} at a concentration of 100 mM

Table 5. Perfusion Digestion Solution prepared in KH buffer

Perfusion Digestion Solution	**Final Concentration**	**Reference**
Collagenase	1 mg/mL	Worthington S4B7097 205u/mg
Hyaluronidase	0.3 mg/mL	Roche 10 106 500 001
BSA	1 mg/mL	Serologicals FrV, Very low endotoxin. Code 81-068-3

Table 6. Incubation Digestion Solution prepared in KH buffer

	Final Concentration	**Reference**
DNAse I	≤ 0.13 mg/mL	Sigma DN-25
Trypsin	≤ 0.13 mg/mL	Difco 215240

II.2. Simulated Ischemia - Reperfusion

Sub-confluent plates were placed in warm ischemic buffer in a sealed chamber (Billups-Rothenberg Modular Incubator Chamber, California, USA) saturated with 95% N_2 + 5% CO_2 for 2 hours at 37°C. Table 7 presents the composition of the ischemic buffer.

Figure 4 presents the treatment schedule for the simulated ischemia-reperfusion (IR) experiments. After 2 hours of ischemia, the plates were quickly processed and reperfusion of all conditions was performed within 3 minutes of the opening of the anoxic chamber. Reperfusion was simulated by the replacement of the ischemic buffer with DMEM supplemented with 1% FBS with or without oxytocin, under normoxic conditions (5% CO_2),

and cells were incubated for an additional 1 - 4 hr. Inhibitors and antagonists were provided at the induction of ischemia, dissolved in ischemic buffer, and re-administered in the reperfusion media (Figure 4). All controls were treated with the appropriate concentrations of vehicle. Additionally, OT antagonist OTA was administered 15 minutes prior to the induction of ischemia and maintained throughout the experiment.

Table 7. Ischemic Buffer composition

Product	Concentration (mM)
NaCl	128
KCl	5
$MgSO_4$	0.4
KH_2PO_4	0.3
$MgCl_2$	0.5
$CaCl_2$	1.3
HEPES	10
Na L-Lactate	20
$NaHCO_3$	4
pH	6.8
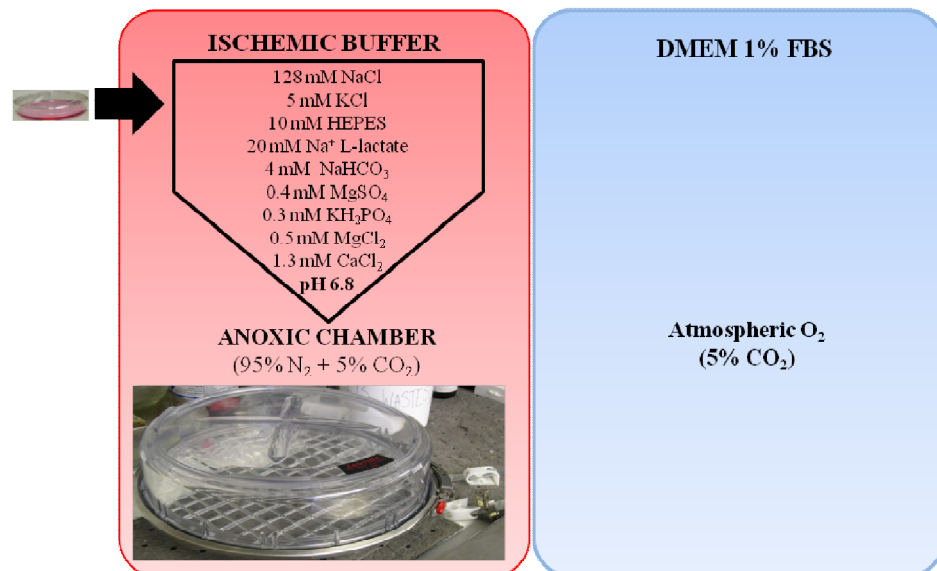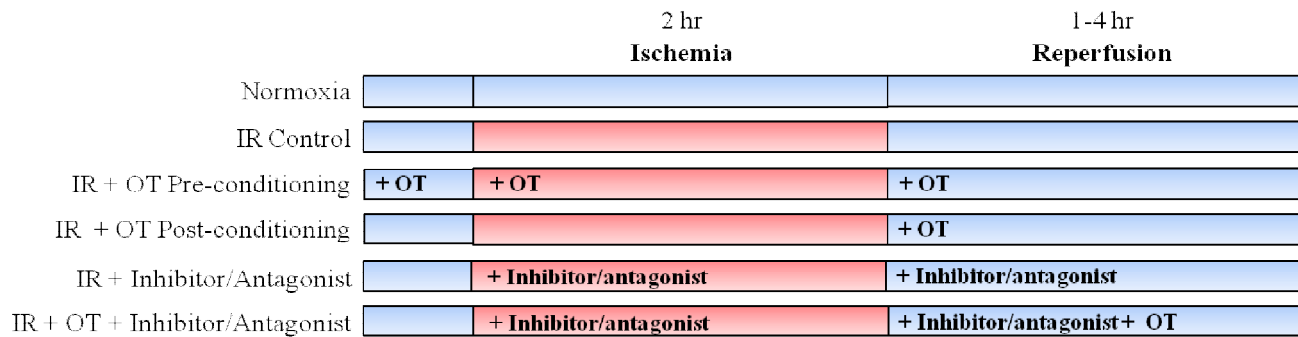
Figure 4. Simulated Ischemia - Reperfusion (IR) protocol. Sub-confluent monolayers of H9c2 cells were covered in warm ischemic buffer and placed inside an anoxic chamber for 2 hours at 37°C. The cells were "reperfused" with pre-equilibrated warm DMEM containing 1% FBS under normal atmospheric oxygen conditions and further incubated for 2 - 4 hours.

II.3. Cell viability and DNA fragmentation

Cell viability was measured by the conversion of the tetrazolium salt MTS [3-(3,5-dimethylthialzol-2-yl)-5-(3 carboxymethoxypheny)-2-(4-sulphophenyl)-2H-tetrazolium] into a formazan product that is soluble in culture medium (Promega CellTiter Aqueous 96 # G3580) according to manufacturer's instructions. 20 µL of MTS were added to 100 µL cell culture medium in each well of a 96-well plate (Corning Costar #3595) where cells were grown. Absorbance at 490 nm was measured using a Symantek plate reader. Blank absorbance values resulting from the cell-free oxidation of MTS were subtracted from all experimental values.

TUNEL (Terminal deoxynucleotidyl transferase-mediated dUTP nick end-labeling) assay was performed using DeadEnd™ Fluorometric TUNEL System (Cat. No. G3250, Promega, Montreal, QC, Canada) according to the manufacturer's protocol. Briefly, cells were grown on poly-L-lysine - treated cover slips in 6 well plates and after the proper treatment, cells were fixed with a solution containing 6% formaldehyde and 2% methanol in PBS, pH 7.4, for 10 min at RT and permeabilized with 0.2% Triton X-100 in PBS, pH 7.4. Cells were incubated in the TUNEL reaction mixture for 1hr in the dark at 37°C, washed and mounted on Prolong Gold anti-fade reagent with DAPI (Cat. No. P36931, Invitrogen, Montreal, QC, Canada).

Cells were visualized using an inverted light fluorescent microscope (Olympus IX51) and images were captured at 10 and 20X magnifications for analysis using a digital charge-coupled device camera (Q IMAGING #Q23774). The quantification of TUNEL-positive

cells as a proportion of total DAPI-stained nuclei was performed using ImageJ software particle analysis.
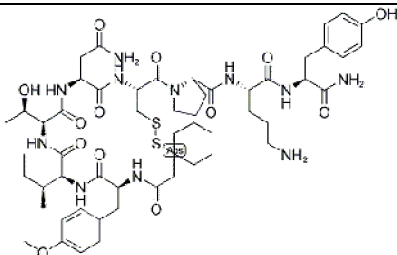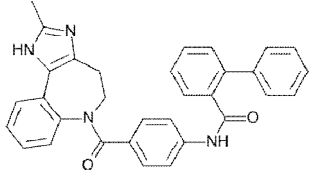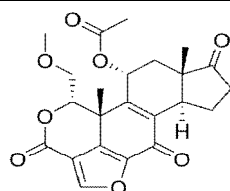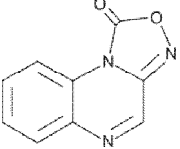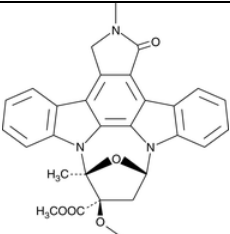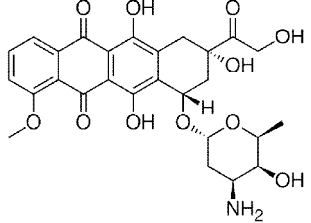
Oxytocin used in all experiments was purchased from Sigma (06379-1mg) and dissolved at a final concentration of 10^{-3} M in sterile cell culture-grade ddH_2O.

II.4. Antagonists and Inhibitors

As presented in Figure 4, the simulated ischemia - reperfusion (IR) protocol was followed in combination with oxytocin treatments. In order to elucidate the signaling pathways affected by OT treatment of the cells, different chemical antagonists and inhibitors were employed. Table 8 summarizes all receptor antagonists and signaling pathway inhibitors used throughout the experiments.

Antagonists OTA and Conivaptan were applied to cells in DMEM with 1% FBS for 15 minutes prior to the induction of ischemia, and then added again to the simulated ischemia buffer as well as to the reperfusion medium. All inhibitors were initially applied to the cells dissolved in the ischemic buffer as well as in the reperfusion medium.

Table 8. Antagonists and inhibitors used

Product	Description	Reference	Structure
OTA ((d(CH$_2$)$_5$^{1} Tyr(Me)^2 Thr^4 Orn^8 Tyr-NH$_2$^{9})-Vasotocin)	Oxytocin antagonist	Bachem H-9405	
Conivaptan	V1a and V2 antagonist	Astellas Pharma YM-087	
Wortmannin	Covalent Pi3K inhibitor	Sigma W1628	
ODQ (l'1H-(1,2,4)oxadiazolo[4,3-a]quinoxalin-1-one)	Soluble Guanylate Cyclase inhibitor		
A71915 (H-Arg-Cys-β-cyclohexyl-Ala-Gly-Gly-Arg-Ile-Asp-Arg-Ile-D-Tic-Arg-Cys-NH$_2$ Trifluoroacetate salt)	ANP antagonist	Bachem H3048	Arg-Cys-β-Cha-Gly-Gly-Arg-Ile-Asp-Arg-Ile-D-Tic-Arg-Cys-NH2 (Amidation of C-terminal cysteine; D-Tic- D-3-carboxyisoquinoline; alanine residue is β cyclohexylalanine (Cha))
KT-5823 (2,3,9,10,11,12-hexahydro 10R-methoxy-2,9-dimethyl-1-oxo-9S,12R-epoxy-1H-diindolo[1,2,3-fg:3',2',1'-kl]pyrrolo[3,4-i][1,6]benzodiazocine-10-carboxylic acid, methyl ester)	PKG Inhibitor	Sigma K1388	
Doxorubicin	Antitumor antibiotic	Sigma D1515	

II.5. siRNA-mediated knockdown of OTR

Two different siRNA sequences were used to knockdown OTR expression in order to minimize potential off-target effects of each sequence. The final OTR siRNA concentration was used at 5 nM; of which 2.5 nM corresponded to each one of the two sequences targeting OTR (i.e., 5 nM siOTR = 2.5 pmol sequence 1 + 2.5 pmol sequence 2 in 1mL medium). Table 9 presents the siRNA sequences used in all knockdown experiments.

A negative control (scrambled) sequence labelled a with red fluorescent Alexa Fluor 555 tag was selected as a transfection control in order to visualize siRNA incorporation. A positive control sequence (All Stars Cell Death #SI04939025) targeting genes essential for cell survival was also used to 1) obtain additional visual confirmation of the transfection efficiency and 2) in combination with the TUNEL experiments as a positive control for cell death.

H9c2 cells were plated in 24-well plates and shortly after plating (<1hr), transfection complexes containing siRNA sequences and transfection reagent (1.25 % v/v to obtain 0.25%v/v final) were added to the cells to a final concentration of 5 nM siRNA. Positive and negative control sequences were used in each experiment to monitor transfection efficiency.

Table 9. siRNA sequences used

siRNA	Reference	Target Sequence	Final concentration
Oxytocin Receptor	Rn_Oxtr_7 SI03106894	5'-GTGGAGCGTTTGGGACGTCAA-3'	2.5 nM
Oxytocin Receptor	Rn_Oxtr_6 SI03054527	5'-CAAGGCCTACGTCACATGGAT-3'	2.5 nM
Negative Control AF555	AllStars Neg. siRNA AF555 1027286	Proprietary - not disclosed	5 nM
Positive Control	Ctrl_AllStars_3 SI04939025	Proprietary - not disclosed	5 nM
HiPerfect Transfection reagent	301705	NA	0.25% v/v

II.6. Immunofluorescence and confocal microscopy

The fluorescently-labelled secondary antibodies were used to study the intracellular signalisation triggered upon OT treatment. In these experiments, round glass cover slips were placed in each well of a 12-well plate, UV-sterilized for 1 hr and coated with 0.5 mL sterile poly-L-lysine solution for 5 minutes at room temperature, after which they were rinsed with sterile dH$_2$O and allowed to dry for at least 2 hr. Alternatively, UV-sterilized poly-lysine treated glass slides were used in combination with the flexiPERM tissue culture inserts. H9c2 cells were plated at a density of 5 x10^3 cells/cm^2 on the poly-lysine treated cover slips or glass slides. After treatments, cells were fixed with a solution containing 3% formaldehyde and 1% methanol in PBS, pH 7.4, for 10 min at RT or overnight at 4°C. Slides were then blocked in a solution containing non-immune 5% serum of the host of the secondary

antibody. Primary antibody dilutions were applied according manufacturer's instructions at room temperature for 2 hr or overnight at 4°C in antibody incubation buffer and covered with parafilm. Slides were washed 3X in washing buffer and secondary antibodies conjugated to fluorescent dye were applied for 1 hr at RT in the dark. Slides were washed and mounted on Prolong Gold anti-fade reagent with DAPI.

Table 10. Solutions used in immunofluorescent staining

Solution	Description
Wash Buffer (PBS-GSA)	1X DPBS (Gibco #14190) with 10 mM glycine and 0.2% NaN_3.
Permeabilization solution	PBS-GSA with 0.5% Triton X-100
Blocking solution	PBS-GSA containing 5% serum of the host animal of the secondary antibody used
Antibody incubation buffer	PBS-GSA with 1% BSA

Table 11. Commercial products used in immunofluorescence

Product	Company	Reference
Round glass cover slips, #1.5, 18 mm	Warner Instruments	CS-18R15 (Cat. 64-0714)
Poly-lysine coated glass microscope slides	Thermo Scientific	P4981-001
FlexiPerm 8 and 12 wells	Sarstedt	94.6032.039; 94.6011.438
Poly-L-Lysine 0.01% solution	Sigma	P4832
TissuFix (6% formaldehyde, 2% Methanol solution)	Chaptec	NA
ProLong Gold anti-fade reagent with DAPI	Invitrogen	P36931
Glycine	BioShop	GLN001.5
Triton X-100	Sigma	T-8787

Table 12. Antibodies and sera used for immunofluorescence

Antibody	Host	Company	Ref.
OTR (N-19)	Goat polyclonal	Santa Cruz	Sc-8103
OTR	Rabbit	Sigma	O4389
V1a	Goat	Santa Cruz	Sc-18096
GATA4 (G4)	Mouse monoclonal	Santa Cruz	Sc-25310
Troponin T	Mouse monoclonal	Abcam	Ab27217
p-Akt (Thr 308) C31E5E	Rabbit	Cell Signaling	2965S
Cox IV	Mouse	Abcam	14744
p-eNOS	Mouse	BD Pharmigen	612392
Normal Goat IgG	Goat	Santa Cruz	Sc-2028
Normal Rabbit IgG	Rabbit	Santa Cruz	sc-2027
Normal Mouse IgG	Mouse	Santa Cruz	sc-2025
Anti mouse Alexa Fluor 568	Goat	Invitrogen	A11004
Anti rabbit Alexa Fluor 488	Donkey	Invitrogen	A21206
Anti-rabbit Alexa Fluor 488	Goat	Invitrogen	A11008
Anti goat Alexa Fluor 568	Donkey	Invitrogen	A11057
Normal Donkey serum	Donkey	Millipore	S30
Normal Rabbit serum	Rabbit	GIBCO	16120-099
Normal Goat serum	Goat	GIBCO	16210-064
Normal Mouse serum	Mouse	Invitrogen	10410

II.6.1. Image capture and processing

Slides were observed using an inverted microscope (Olympus IX51) and images were captured using a digital charge-coupled device camera (Q IMAGING #Q23774).

Confocal microscopy was performed using a Zeiss LSM 510-META confocal microscope equipped with a Laser line Argon 488 nm, HeNe 543 nm and diode 405 nm. Captured images

were analyzed with Zen2011 software. Appropriate training in the use of the confocal microscope, as well as additional imaging sessions were hired at an hourly fee from the McGill Anatomy and Cell Biology Confocal Microscopy facility.

II.7. Intracellular ROS production

Cells were seeded on 96-well plates with black walls (Nunc # 165305) and allowed to attach overnight. The cells were then incubated with the CM-H_2DCFDA probe in warm KRH buffer at 37°C for 30 minutes, washed and returned to normal growth conditions in the presence and absence of OT. Fluorescence was monitored at the indicated times using a fluorescence plate reader set at excitation 485/20 nm, emission 528/20 nm.

II.8. Western Blot

II.8.1. Protein extraction

Plates containing monolayers of H9c2 cells were placed on ice and washed 2X with ice-cold PBS, gently so as to not detach the cells. 100µL of RIPA lysis buffer containing protease and phosphatase inhibitors were added per 100-mm Petri plate and cells were scraped with a cell scraper (Sarstedt 83.1830) and transferred to pre-chilled Eppendorf tubes kept on ice. The samples were vortexed every 5 minutes for 30 minutes while kept on ice. Two sonications of 10 seconds each were performed and the samples were centrifuged at 12,000 rpm at 4°C for 20 minutes. The supernatant was recovered, an aliquot taken for protein quantification and the remainder kept at -80°C until use.

Table 13. RIPA buffer composition

Ingredient	Concentration	Reference
NaCl	150 mM	ACP S-2838
Triton X - 100	1% v/v	Sigma T-8787
Na deoxycholate ($C_{24}H_{39}NaO_4$)	0.5 % w/v	Sigma D6750
SDS	0.1% w/v	Invitrogen 15525-017
Tris	50 mM	Invitrogen 15504-020
Protease/phosphatase inhibitors		ZmTech Scientifique I208052

II.8.2. Protein quantification

The protein concentration in the samples was measured using the Bradford method, in which the dye Coomasie Blue binds to the positive amine groups in solution through ionic interactions. This interaction stabilizes the dye in a conformation which absorbs light of 595 nm. The absorbance of the solution is linearly related to the amount of protein in solution up to 2 mg/mL. A BSA standard curve ranging from 40 µg/mL to 200 µg/mL was prepared using the same buffer as used to extract the protein.

II.8.3. Electrophoretic migration of protein samples

II.8.3.1. Sample preparation

After protein quantification, the samples were prepared for electrophoresis by diluting each one to the same final concentration (50µg protein/mL) with 5X Laemmli and water to obtain

150 µL of each sample. (ie, 150 µL loading sample = 30 µL Laemmli 5X + x µL sample + (120-x) µL water). The concentrations were equalized in order to load on the gel the same volume in each well. The samples were then boiled in a water bath for 5 min.

Table 14. 5X Denaturing reducing Laemmli protein loading dye

Component	Concentration	Reference
1.5 M Tris HCl	300 mM	Invitrogen 15504-020
Glycerol	50%	Sigma G6279
β-mercaptoethanol	5%	Gibco 21985-023
SDS	10%	Invitrogen 15525-017
1% Bromophenol Blue	0.050%	Sigma B-5525
pH 6.2 (adjust)		

II.8.3.2. Preparation of SDS polyacrylamide gels

Separation gels were prepared at different acrylamide concentrations (7.5, 10 or 12.5%) and cast on BioRad glass supports with 0.5 mL isobutanol poured gently on top of each gel. After polymerisation of the separation gel, a 4% acrylamide stacking gel was cast on top of the separation gel. All gels had a final width of 1.0 mm.

Table 15. Solutions used in SDS-PAGE preparation

Solution	Use
1.5 M Tris pH 8.8	Separation gel
0.5 M Tris pH 6.8	Stacking gel
Acrylamide stock (29% acrylamide, 1% bisacrylamide)	Invitrogen 15512-023
SDS 10%	Invitrogen 15525-017
APS (0.1 g/mL)*	Sigma A3678
TEMED	Sigma T-8133

* APS solution freshly prepared each time.

Gels were mounted on an electrophoresis apparatus (Bio-Rad Mini Protean Tetra Cell). The chamber was filled with electrophoresis running buffer (192 mM glycine, 25 mM Tris, 1% SDS, pH 8.3) and the gels were cast inside. 5 to 10 µg protein in 1X Laemmli buffer were loaded in each well. All wells contained the same final volume to favour a straight migration. Volumes were adjusted with 1X Laemmli as required.

The electrophoresis chamber containing the loaded gels was placed at 4°C and connected to a power source. The electrophoresis was carried out at 80V for 30 minutes and then at 120V for 1-3 hours until the band of interest reached the middle of the gel.

Table 16. 10X Electrophoresis Buffer solution

Component	Concentration
Glycine	1920 mM
Tris	250 mM
SDS	1.0%
pH 8.3	

II.8.4. Transfer of proteins to nitrocellulose membrane

A transfer buffer was freshly prepared containing 192 mM glycine, 25 mM Tris, 20% methanol and kept cold (4°C) until use. For larger (>100kDa) proteins, 1 mL of SDS 10% was added to 3L of transfer buffer to facilitate the transfer. When the electrophoresis was done, the gels were cut and placed in transfer buffer to equilibrate, along with the membranes, for 15 minutes at room temperature. Three pieces of blotting paper, cut to the size of the membrane were soaked in transfer buffer and placed one by one on the anode (+) side of the transfer cassette. The membrane was carefully placed on top of the blotting paper, then the gel on top of the membrane and three pieces of blotting paper. Any bubbles formed were carefully rolled out with the use of a glass pipette rolled along the blotting paper. The transfer was carried out at 20V for 1.5 hr.

II.8.4.1. Ponceau red transfer verification, blocking and incubation with antibodies

All incubations of the membranes were performed with light agitation on a shaker. The membranes were placed in Ponceau red stain (aqueous solution containing 0.2% w/v Ponceau red and 0.75% w/v trichloroacetic acid) for 2-3 minutes and rinsed with distilled water until protein bands were visible against a white background. This step allows for the verification of an equal transfer of proteins onto the membrane.

The membranes were then washed 3X with tris buffered saline (25 mM tris, 150 mM NaCl, pH 7.4) containing 0.1% Tween 20 (TBS-T; Tween 20 from Sigma #P1379). Non-specific binding sites for the antibody were blocked by incubating the membrane for 1 hr at room

temperature in a solution, prepared in TBS-T, containing 5% fat-free milk or 2% blocking powder (ECL Advance blocking reagent) when phosphorylated proteins were the subject of the investigation.

After blocking, the membranes were washed 3X 5 minutes with TBS-T and covered in a solution containing the primary antibody at the appropriate dilution in TBS-T with 2% BSA and incubated overnight at 4°C on a shaker. The membranes were then washed 6X 5 minutes each wash in TBS-T and incubated with appropriate dilutions of horseradish peroxidase-linked secondary antibodies prepared in 5% milk or 2% blocking solution.

The detection method used in all membrane developments was ECL Advance (GE RPN2135). The product was applied to the membranes as per manufacturer's instructions. Autoradiography films were placed against the membranes to detect the chemiluminescent signal emanating from bound secondary antibody.

Developed films were scanned as images of TIFF format, without compression, for quantification of the bands. Using ImageJ software (v. 1.45s), the film images were opened, inverted and quantified using the software's "Gel" function. With this method, each selected lane is quantified (upon the command "Plot lanes") and the intensity of each lane is provided. The relative expression of the proteins of interest in each lane was calculated with the ratio of the intensity of the protein of interest over the expression of a housekeeping protein such as GAPDH.

II.9. Statistical Analysis

All results are presented as the mean ± SEM. All data were processed using Prism 5 software (GraphPad Software, California, USA). One-way ANOVA with Tukey's post-test was performed when specified. Grouped data were analyzed using two-way ANOVA. When significance was obtained, groups were further compared using unpaired student t-test. Results were considered significant when $p < 0.05$.

III. RESULTS

III.1. Standardization of Experimental Conditions

III.1.1. H9c2 cells are a good model of cardiomyocyte in simulated ischemia-reperfusion experiments

Commercially available H9c2 cells were examined for their applicability in the present study by immunofluorescent detection of cardiomyocyte and functional markers. As presented in

Figure 5, all the cells expressed cardiac transcription factor GATA-4 (Fig. 5A) cardiomyocyte contractile protein troponin (Fig. 5B) as well as oxytocin receptor (OTR, Fig. 5C) and vasopressin receptor type 1a (V1a, Fig. 5D).
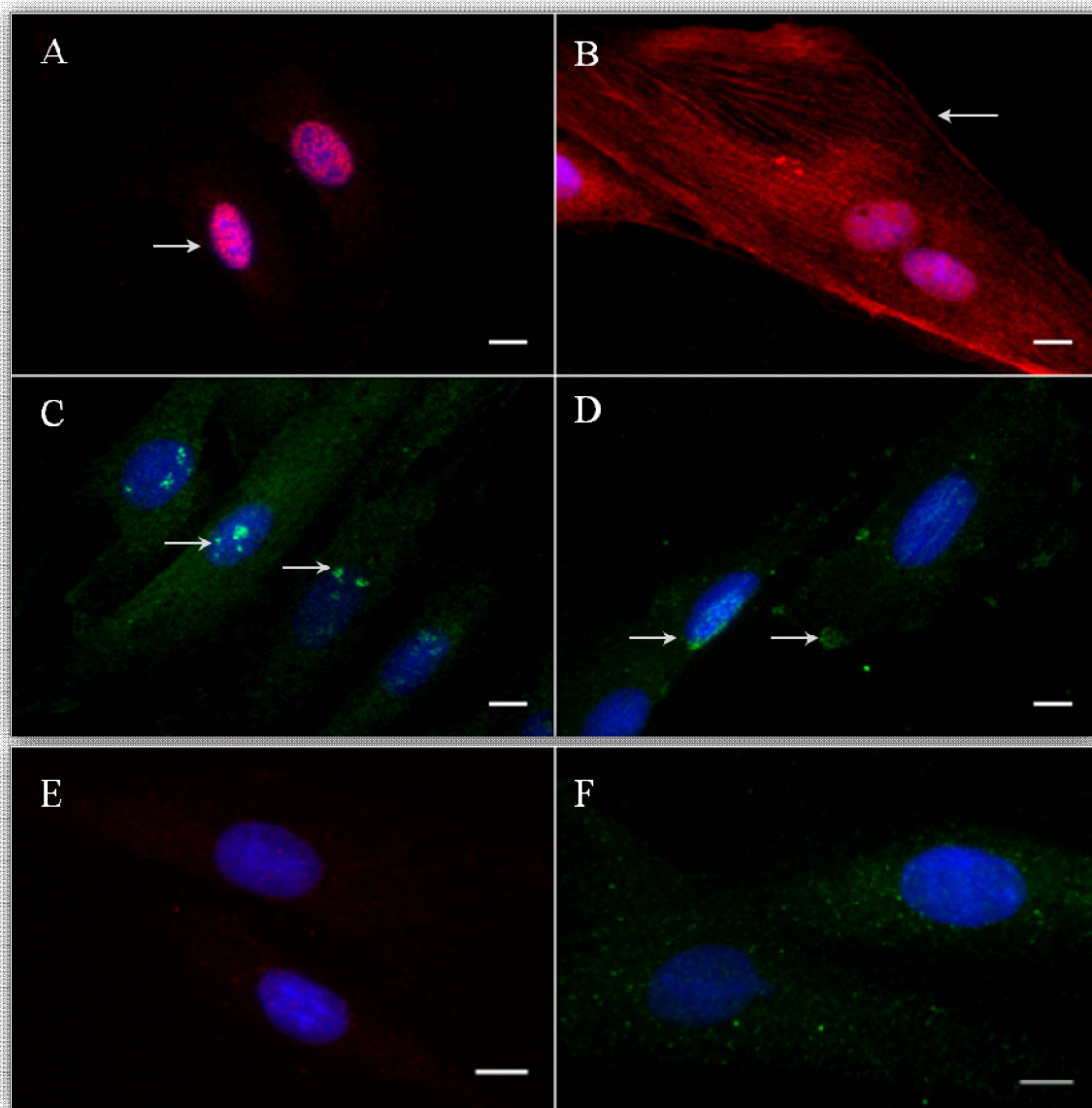
Figure 5. H9c2 cells express cardiomyocyte proteins and receptors of the oxytocin system. 20X micrographs of immunofluorescent staining of H9c2 with **A.** Mouse anti-GATA-4; **B.** Mouse anti-Troponin T; **C.** Goat anti-oxytocin receptor (OTR); **D.** Goat anti-vasopressin type 1a receptor (V1a); **E.** Mouse IgG; **F.** Goat IgG. Arrows indicate specific staining of the receptors. Bars represent 10 μm.

III.1.2. Viability of H9c2 cells

In order to routinely study the effects of oxytocin on cardiomyocyte survival, we required a reliable method to assess cellular viability. One such method is the colorimetric detection of formazan production, which is an indicator of cellular metabolic viability[110].

As presented in Figure 6, the assay provides a linear correlation between the number of H9c2 cells seeded and the absorbance at 490 nm between 400 and 6400 cells per well of a 96-well plate ($r^2 = 0.9942$ for the linear regression between 400 - 6400 cells/well). The optimal seeding density for accurate viability estimation was determined to be 3,200 cells per well of a 96-well plate, equivalent to 10^3 cells/cm^2, as this provided a detectable signal ≥ 0.150 absorbance units after 2 hours of reperfusion while maintaining $< 80\%$ confluence in all experimental wells. The production of formazan is no longer linearly related to seeding density at 12800 cells/well (40,000 cells/cm^2).
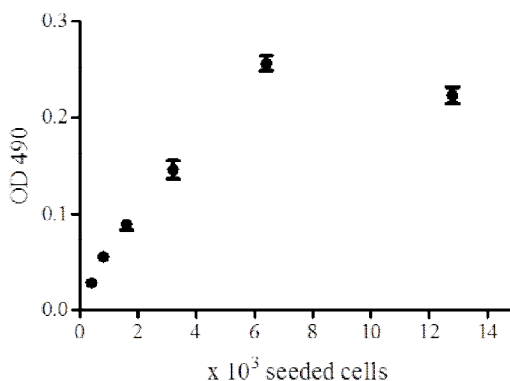
Figure 6. Formazan production is linearly related to H9c2 seeding density up to 20,000 cells/cm^2. Effect of H9c2 seeding density on tetrazolium salt reduction capability. Cells were seeded at the indicated densities in each well of a 96-well plate (0.32 cm^2) and allowed to attach overnight. Cells were incubated for 2 hours with MTS tetrazolium salt and the absorbance at 490 nm was measured with a microplate reader. The absorbance of the blank (no cells) control was subtracted from all values.

III.1.3. Simulated ischemia-reperfusion (IR) protocol

We sought a simulated ischemia-reperfusion protocol that produced a significant reduction in cell viability. Using the protocol presented in Figure 7, different lengths of incubation under hypoxic conditions were tested in the presence of DMEM 1% FBS or in an ischemic buffer[111] that simulates the conditions of the ischemic myocardium.
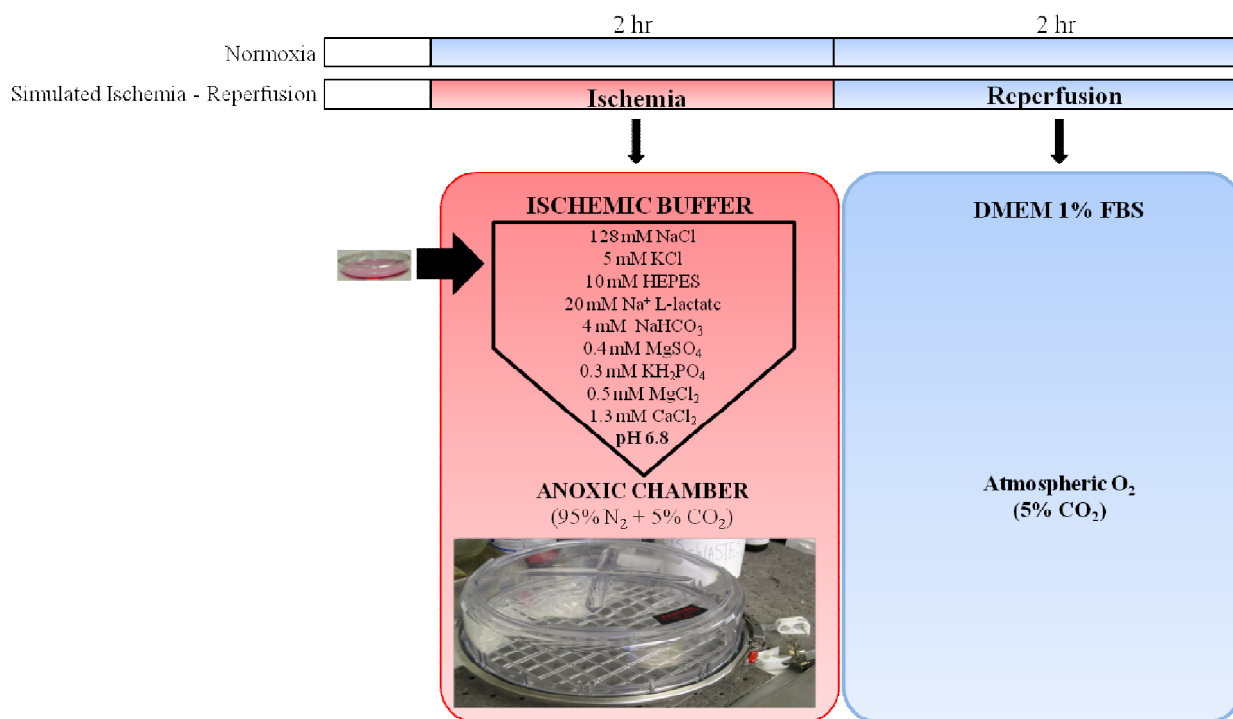
Figure 7. Experimental simulated ischemia-reperfusion (IR) protocol. Sub-confluent monolayers of H9c2 cells were covered in warm ischemic buffer and placed inside an anoxic chamber for 2 hours at 37°C. The cells were "reperfused" with pre-equilibrated warm DMEM containing 1% FBS under normal atmospheric oxygen conditions and further incubated for 2 - 4 hours.

As presented in Figure 8A, two hours of hypoxia in the presence of DMEM with 1% FBS yielded a 5.6 ± 1.1% reduction in cell viability, whereas the same length of hypoxia in combination with the simulated ischemia buffer provided a 14.2 ± 2.6% reduction in cell

metabolic viability (Fig. 8B, p = 0.0131 vs. DMEM 1% FBS). In addition, viability in the simulated ischemia buffer, but not in DMEM, decreased steadily as a function of the time of exposure to hypoxia (Fig. 8).
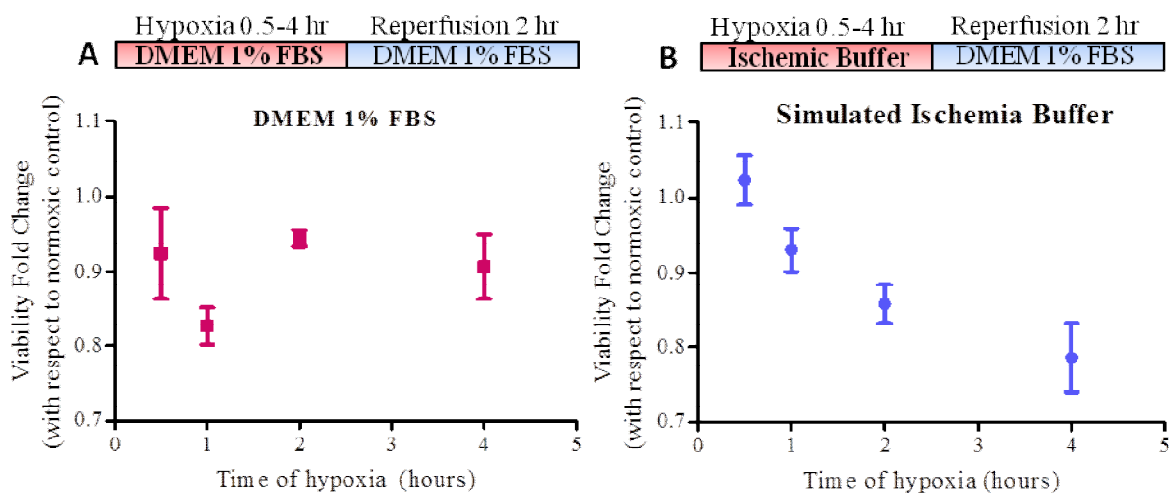
Figure 8. H9c2 viability after various times under hypoxic conditions. Cells were covered either in **A.** DMEM 1% FBS or in **B.** simulated ischemia (SI) buffer and placed inside a humidified hypoxic chamber (Billups-Rothenberg Modular Incubator Chamber) for 0.5, 1, 2 and 4 hours. After the indicated times, the cells were removed from the hypoxic chamber and moved into normal incubation conditions, and the cells' medium or SI buffer was replaced with fresh DMEM containing 1% FBS. After a brief equilibration period (10-20 minutes), MTS was added to each experimental well. Plates were then incubated at 37°C for the remainder of 2 hours of reperfusion (1 hr 40 min to 1 hr 50 min). Results are presented normalized to normoxic control viability.

III.1.4. siRNA-mediated knockdown of OTR

III.1.4.1. Transfection efficiency determined using AF555-labelled negative control siRNA sequence

The knock down of the expression of OTR was performed with 1, 5 and 10 nM of two different commercially-available siRNA sequences complementary to OTR mRNA. For a

control and to optimize the transfection conditions, we used equimolar doses of a negative control siRNA sequence (scrambled). This reagent is labelled with a red fluorescent tag (Alexa Fluor 555) to enable the visualization of siRNA incorporation into the cells and has no silencing effect on any gene. Mock transfection, in which the siRNA sequences are provided in the absence of transfection reagent, were carried out in each optimization experiment as demonstrated in Figure 9.

Incubation of scrambled siRNA with cells was performed during 24 (Fig. 9A) and 48 hours (Fig. 9B). Analysis of the ratios of incorporated siRNA fluorescence to DAPI fluorescence emitted from the cells' nuclei recorded by inverted microscope demonstrated that a final concentration of 5 nM siRNA provided the optimal transfection efficiency at both time points (Fig. 9A and B). Overall siRNA incorporation was higher at 24 hours post-transfection than at 48 hours (Fig. 9C). This led us to introduce a new time condition of 48 hours with a re-transfection after 24 hours. In subsequent tests, this condition revealed optimal siRNA incorporation (Fig. 9D). The final protocol of siRNA experiments is presented in Figure 9E.
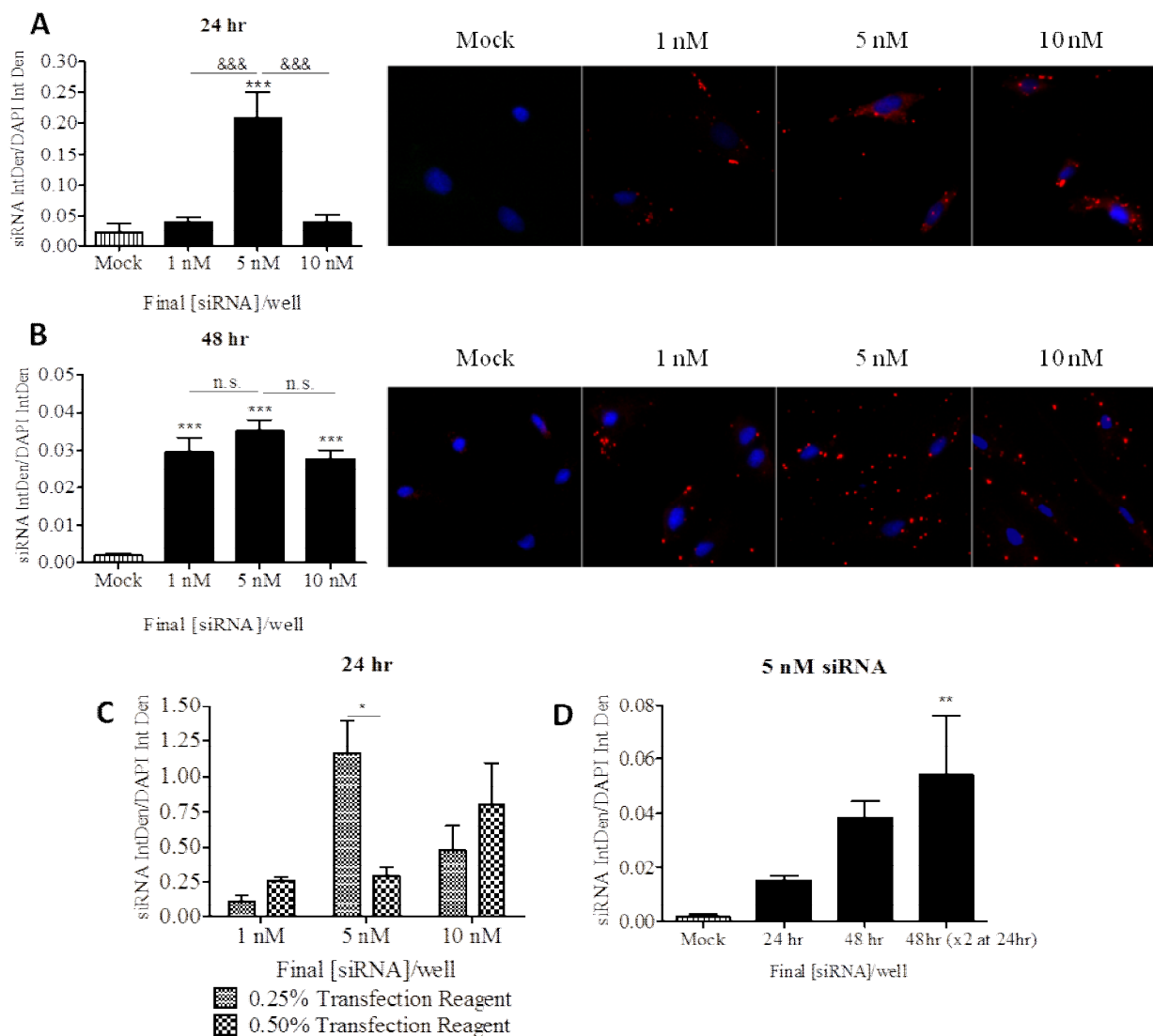
Figure 9. Optimization of siRNA-mediated knockdown of OTR. Effect of siRNA concentration on transfection efficiency at 24 and 48 hours post-transfection. The relative integrated density of the fluorescent siRNA sequence/DAPI fluorescence was used as measurement of the presence of siRNA within the cells after **A**. 24 and **B.** 48 hours with different concentrations of siRNA and 0.25% v/v transfection reagent used. **C.** Effect of the concentration of transfection reagent on transfection efficiency with different concentrations of siRNA. **D.** Effect of exposure time on siRNA (5 nM, 0.25 % v/v transfection reagent) incorporation within the cells. A double transfection with 5 nM and an incubation of 48 hr provided the optimal siRNA incorporation.

III.1.4.2. Confirmation of OTR knockdown

As demonstrated in Figure 10, immunofluorescent staining of transfected cells as well as Western blot were used to confirm the effective knockdown of OTR protein expression. Western blot analysis revealed a reduction in OTR expression of $65 \pm 7\%$ as compared to control siRNA-transfected cells (Fig. 10B).
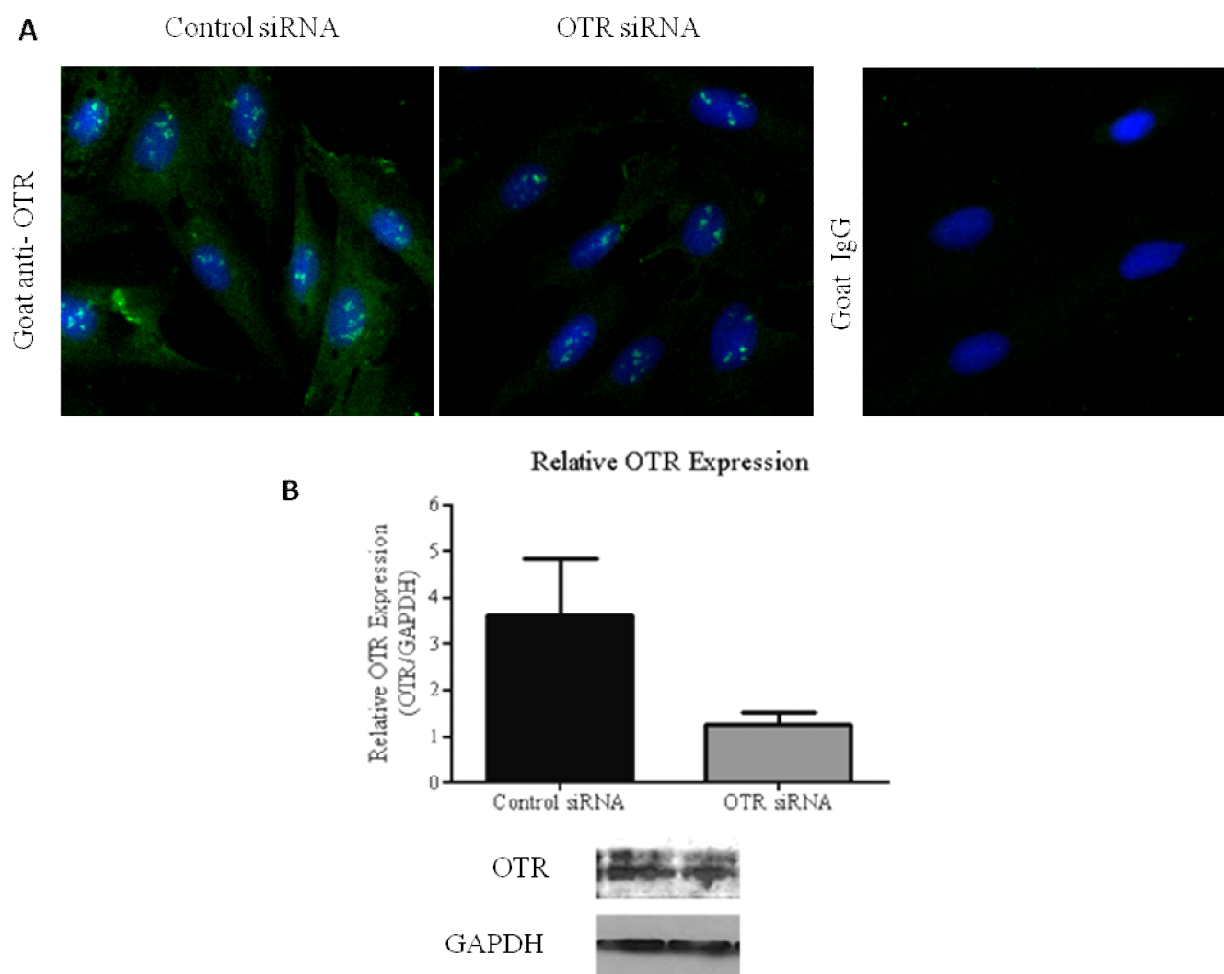
Figure 10. siRNA-mediated knockdown of OTR decreased OTR expression after a transfection with 5 nM siRNA every 24 hours for 48 hours using 0.25% v/v transfection reagent. A. Reduction of OTR-specific immunofluorescence by siRNA treatment. Staining of OTR (green) and DAPI (blue) **B.** Western-blot quantification of the control and OTR siRNA-treated H9c2 cells.

III.2. Oxytocin protects cardiomyocyte viability

III.2.1. Pre-treating H9c2 cells with oxytocin protects them from death after simulated ischemia-reperfusion

We[74] and others[70] had previously reported that OT preconditioning improves myocardial functional recovery in animal as well as *in vitro* models of cardiac ischemia - reperfusion. We thus investigated whether OT treatment in our experimental IR model could elicit protection of H9c2 cells against ischemia - reperfusion damage.

Figure 11A presents the treatment schedule of OT in the IR protocol. OT (1 nM) was administered beginning 15 minutes prior the induction of ischemia and maintained throughout the IR experiment. As presented in Figure 11B, OT administered at a concentration of 1 nM at all points of our IR protocol protected H9c2 cell metabolic viability as measured by the MTS test, restoring viability to 97.4 ± 2.3 % of normoxic control, as compared to 88.4 ± 1.5% in untreated IR ($p < 0.05$ vs. OT-treated).

To investigate whether the protection of viability induced by OT was attributable to decreased cell mortality, we evaluated cell death in IR with and without OT treatment. Using the TUNEL assay, we investigated whether OT treatment prevented cell death as evaluated by nuclear DNA fragmentation. In normal control conditions (normoxia), H9c2 cells displayed 1.69 ± 0.13 % TUNEL - positive nuclei (Fig. 11C). The cells exposed to IR displayed 2.74 ± 0.39 % of TUNEL - positive nuclei ($p < 0.05$ vs. Normoxic group), and supplementation with 1 nM of OT resulted in a decrease in the proportion of TUNEL - positive nuclei to 1.39 ± 0.19 % ($p = 0.0048$ vs. IR; $p = 0.2084$ vs. normoxia, Fig. 11C).

In order to verify the validity of our results obtained with H9c2 cells, we repeated the experiment using isolated adult rat ventricular cardiomyocytes (ARVCMs). As presented in Figure 11D, ARVCMs in culture displayed relatively higher numbers of dead cells as compared to H9c2 cells under basal (normoxic) conditions (18.2 ± 7.2 TUNEL-positive nuclei in ARVCMs normoxic control vs. 1.69 ± 0.13 % in H9c2 normoxic control). In ARVCMs exposed to IR, a 2-fold increase in cell death was noted, to 36.3 ± 11.2 % of cells. In response to treatment with 1 nM OT, the number of cells displaying dead nuclei decreased significantly vs. untreated IR control ($p < 0.05$) to 3.4 ± 2.3 %, and the results were statistically different from normoxic control (Fig. 11D).
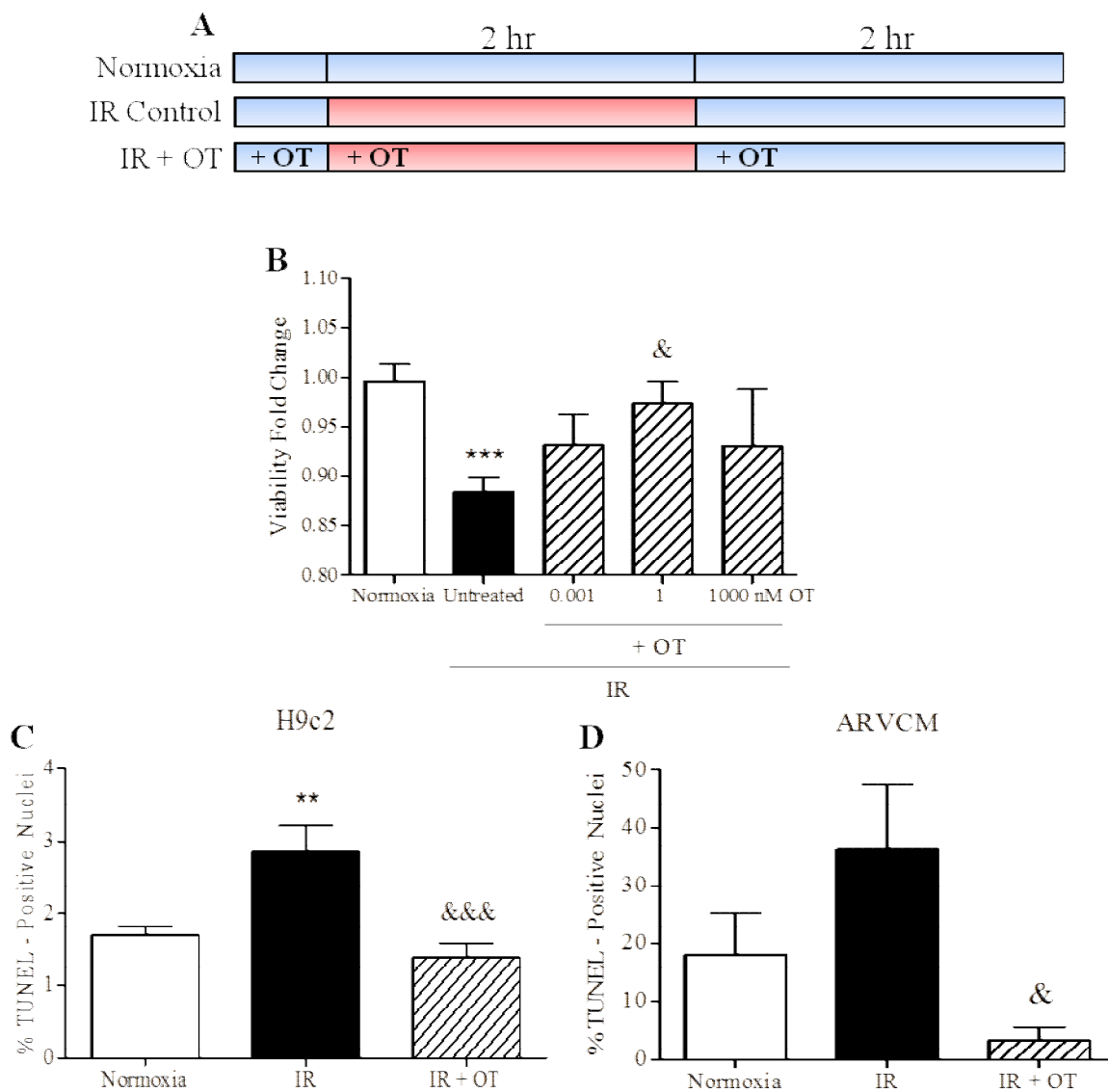
Figure 11. Preconditioning cardiomyocytes with 1 nM OT beginning 15 minutes prior to the onset of ischemia and maintained throughout the simulated ischemia-reperfusion (IR) experiment prevents cell death. **A**. IR protocol showing the times of OT addition as well as the controls. **B.** Viability after 2 hours of simulated ischemia and 2 hours of reperfusion, with and without OT treatment. Values reported as fold change with respect to normoxic control cells. *** $p < 0.001$ vs. normoxic control, & $p < 0.05$ vs. untreated IR. **C.** TUNEL assay of H9c2 cells and **D.** isolated adult rat ventricular cardiomyocytes (ARVCMs) following IR. ** $p < 0.01$ vs. normoxia; & $p < 0.05$ vs. untreated IR.

III.2.2. Oxytocin protects cell viability optimally if administered at the onset of reperfusion

In the preceding experiment, OT was administered throughout the simulated ischemia-reperfusion experiment, beginning at 15 minutes prior to the onset of ischemia, during ischemia and in the reperfusion medium. To investigate the specific point of OT action during IR, we added OT at three different points of the IR experiment. 1) In the OT pre-conditioning group, we added 1 nM of OT to H9c2 culture 15 minutes prior to the onset of ischemia (OT pre-con); 2) in OT-ischemia group, we added OT during the 2-hour ischemic period (OT ischemia); 3) in the OT postconditioning group, OT was added only at the onset of reperfusion, dissolved in reperfusion media (OT post-con). In group 4, OT was present during all three time points of the IR experiment (OT-all). As shown in Figure 12A, compared to untreated IR control (column 1), OT treatment before ischemia only (pre-con) had no effect on cell metabolic viability measured by formazan production (Fig. 12A, column 2); OT presence during ischemia increased cell viability by $9.7 \pm 2.5\%$ ($p < 0.05$, Fig. 12A, column 3); OT presence after ischemia (at post-con) increased cell viability by $15.8 \pm 3.5\%$ ($p < 0.001$, Fig. 12A, column 4), while OT-all increased viability by only $7.1 \pm 1.8\%$ ($p < 0.01$, Fig. 12A, column 5) compared to untreated IR.

Investigations of whether preconditioning of H9c2 cells with OT could increase the protection against IR with different combinations of OT administration brought negative results (Fig. 12B). Following the observation that protection was maximal if OT was supplied at reperfusion (post-con), different combinations of OT administrations during the pre-con and ischemic phases in combination with post-con were investigated (Figure 12). As shown in Figure 12C, the cells treated with OT during reperfusion only displayed optimal

viability ($15.8 \pm 3.6\%$ higher than untreated control, $p < 0.001$). OT administration at the ischemic and reperfusion periods as well as at all phases (OT-all) significantly improved viability (Fig. 12C columns 3 and 5, up by $11.5 \pm 3.5\%$ and $7.1 \pm 1.8\%$, $p < 0.05$ vs. untreated control). OT administered only at reperfusion provided significantly better protection than when done so in combination with an OT treatment prior to ischemia (Fig. 12C column 2 vs. 4 and 5).
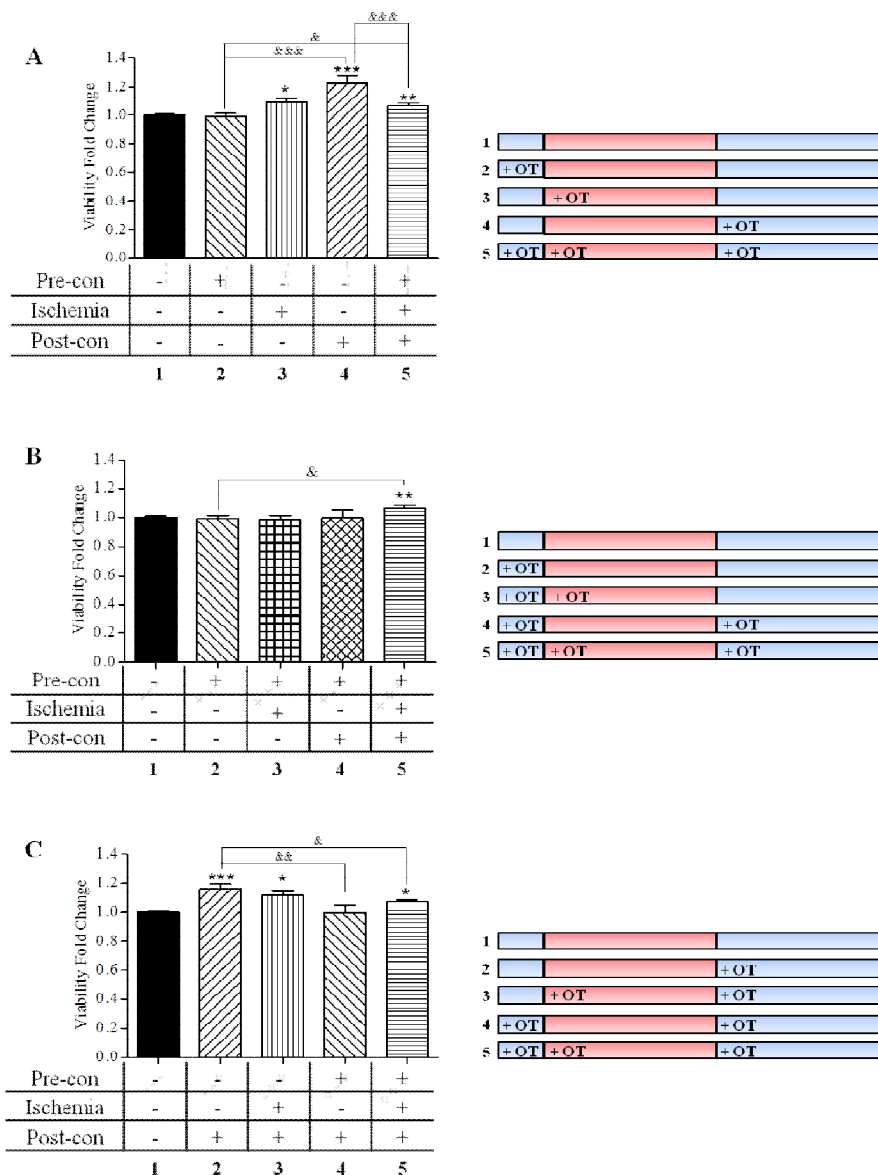
Figure 12. OT protects cardiomyocyte viability optimally if administered exclusively at reperfusion. A. A single dose of OT was administered either before ischemia (Pre-con, col. 2), during ischemia (Ischemia, col. 3), at reperfusion (post-con, col. 4) or at all three times (col.5). OT ischemia, post-con and OT-all treatments provided significant protection of viability, with OT post-con providing the strongest protection. **B.** OT pre-con with combinations of OT treatment during ischemia and reperfusion. *OT-all (col. 5) is the only condition in which OT treatment before ischemia resulted in a significant improvement in viability after IR.* **C.** OT Postconditioning with combinations of OT treatment prior to and during ischemia. OT administered only at reperfusion provided the strongest protection, however, OT present during ischemia as well as in reperfusion (column 3) also significantly improved viability. The numbers indicate the corresponding visual representation of the protocol followed for that column * $p < 0.05$, ** $p < 0.01$, *** $p < 0.001$ vs. untreated control; & $p < 0.05$, && $p < 0.01$, &&& $p < 0.001$.

III.2.2.1. OT administered at reperfusion protects optimally at concentrations ranging from 1 - 250 nM

Figure 13 presents the concentration-response analysis of OT administered at the post-con period. The results revealed significant protection starting at a concentration of 1 nM of OT, with an optimal protection at 62.5-125 nM (up by 55% compared to untreated IR, to 89.5 ± 3.2% of normoxic control, $p < 0.001$). Importantly, lowered OT protection was noted when OT concentration exceeded 500 nM.
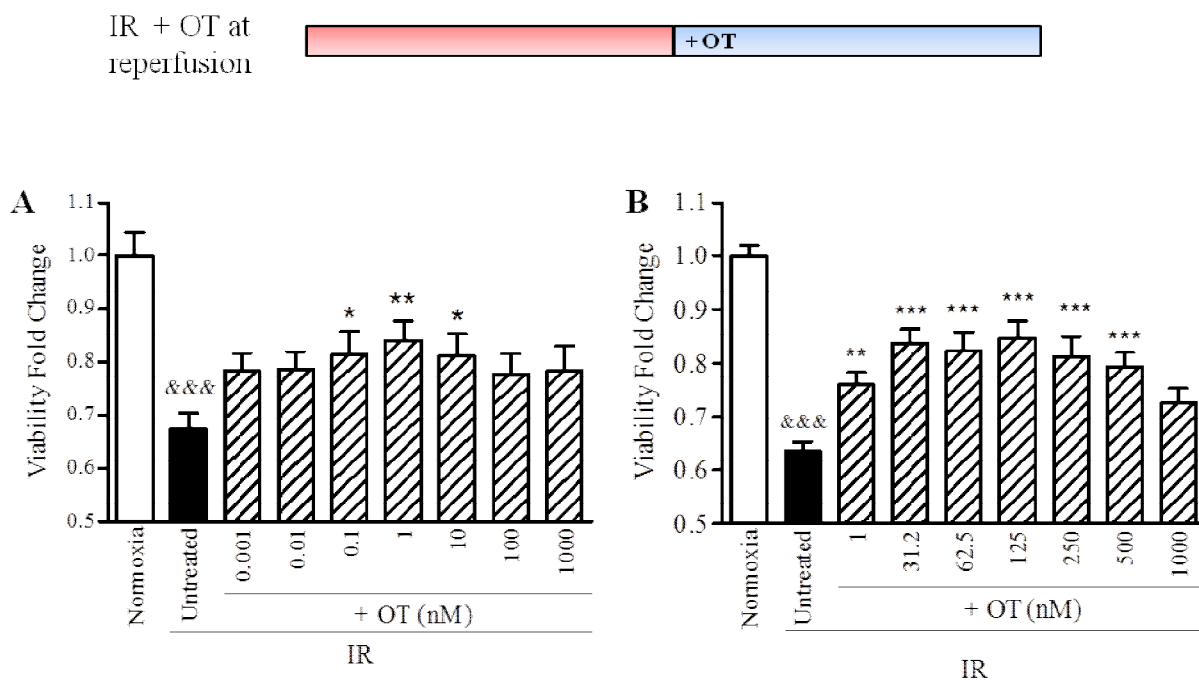
Figure 13. Concentration -response of oxytocin administered at reperfusion. A. Initial experiments revealed an optimal protection around a concentration of 1 nM OT. **B.** Serial dilution analysis using concentrations reported[112] to stimulate a known cardioprotective pathway (Pi3K-Akt) *** $p < 0.001$, ** $p < 0.01$, * $p < 0.05$ vs. Untreated IR; &&& $p < 0.001$ vs. normoxia.

III.3. The protection afforded by OT is mediated by oxytocin receptor

III.3.1. OTA concentration-dependently blocks the protective effect of OT

Oxytocin can trigger intracellular signaling via its interaction with oxytocin receptors (OTR) as well as through vasopressin receptors. To evaluate whether OTR-specific signaling was involved in the protection we observed upon OT treatment, experiments using an antagonist specific against OTR (OTA). As shown in Figure 14, the protective effect of 1 nM OT during the postconditioning period was abolished by the administration of OTA at concentrations of 0.1, 1 and 10 nM.
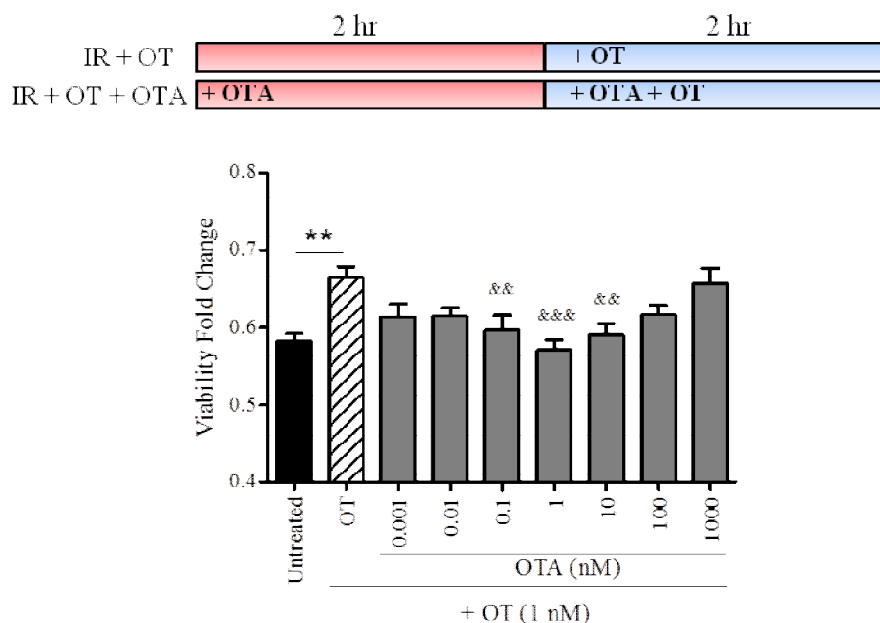
Figure 14. OT antagonist OTA concentration-dependently abolishes the protective effect of OT treatment at reperfusion. && p <0.01, &&& p < 0.001 vs. IR + OT 1 nM at reperfusion; ** p < 0.01.

III.3.2. OTR knockdown reverses the protective pattern observed by OT treatment on cell death

Figure 15 presents the results obtained from siRNA knockout experiments designed to evaluate the role of OTR in cell protection against IR. The standardization of the experiment has been presented in section III.1.4.1 (Figure 10).

H9c2 cells were transfected with siRNA sequences targeting OTR (siOTR, Fig. 15B) or with control scrambled siRNA (scr, Fig. 15A). After 48 h, the cells were exposed to IR and cell death was evaluated by DNA fragmentation detected by the TUNEL method. Under normoxia, scr cells (1.3 ± 0.7%) and siOTR cells (1.6 ± 0.6%) displayed a similar proportion of dead nuclei (Fig. 15A and B). In scr cells subjected to IR, the proportion of dead nuclei increased to 11.7 ± 4.5%; this increase was prevented by treatment with 1 nM of OT to 3.8 ± 0.8% (p = 0.0027, Fig. 15A). Upon IR conditions, siOTR-cells displayed an increase in cell death compared to normoxic control to 5.9 ± 1.9 %. Interestingly, OT treatment of siOTR cells increased cell death almost 3-fold to 16.7 ± 2.9 % (p< 0.05, Fig. 15B).
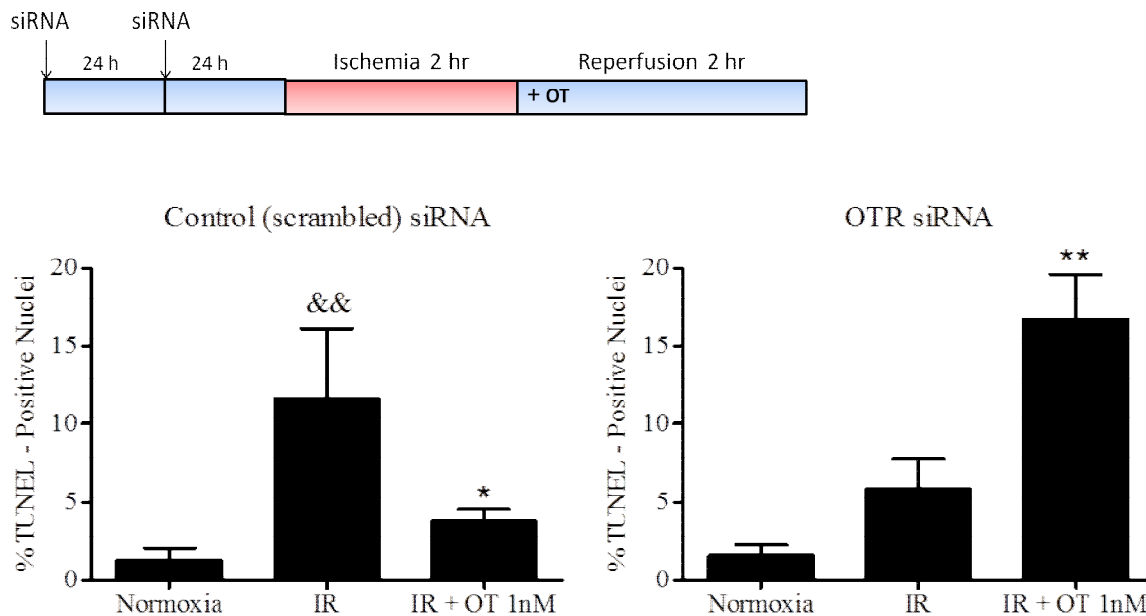
Figure 15. OTR signaling is necessary for OT-induced protection of viability. **A.** Control (scrambled) siRNA-transfected cells display a significant protection by OT. * p < 0.05, ** p < 0.01. **B.** siRNA-mediated OTR knockdown reverses the protective pattern observed by OT treatment on cell death. The siRNA transfection and experimental schedule of OT treatment is presented at the top panel ** p < 0.01 vs. IR untreated.

III.3.3. A high concentration of vasopressin, administered at reperfusion, exerts a mild protection of metabolic viability in H9c2 cells

Given the unexpected results obtained with OTR knockdown experiments, we hypothesized that in conditions of OTR down-regulation, OT may elicit a deleterious effect via vasopressin receptor 1a, which is expressed in H2c9 cells (See

Figure **5**). The effect of vasopressin (AVP) administration (0.1 - 1000 nM) during the reperfusion phase of the IR protocol is presented in Figure 16A. Data analysis indicates that AVP administered at reperfusion exerts no effects at concentrations of 0.1 – 100 nM, but

provides a significant cell protection at the highest concentration of AVP tested (1000 nM, to 84.0 ± 2.1 % of normoxic control vs. 76.8 ± 1.2 in AVP-untreated IR control, $p < 0.05$).

III.3.4. An antagonist to vasopressin receptors V1a and V2 protects viability only in the absence of oxytocin

For the study of the effects of AVP receptor blockade, Conivaptan, an antagonist of vasopressin receptors V1a and V2 has been employed. Figure 16B demonstrates that Conivaptan administration (50 nM) alone increased cell viability (to 77.9 ± 3.7% compared to 57.8 ± 2.7% in vehicle-treated control, $p = 0.0009$). Two-way ANOVA analysis revealed that the concentration of OT significantly influences cell protection ($p = 0.0449$) while the presence of Conivaptan tended to influence cell protection ($p = 0.0615$). Two-way ANOVA demonstrated a significant interaction between OT concentration and Conivaptan on cell viability using the MTS assay ($p = 0.0121$, Fig. 16B)

Detailed analysis by student t test demonstrated that the cells treated with vehicle (DMSO) and with OT at doses of 125, 250, 1000 ($p < 0.05$) and 500 nM ($p < 0.01$) displayed a significant improvement in viability. In the presence of Conivaptan, the protective effect of OT was reduced. The level of cell protection in samples treated by OT + Conivaptan was at the range observed in Conivaptan control (Fig. 16B).
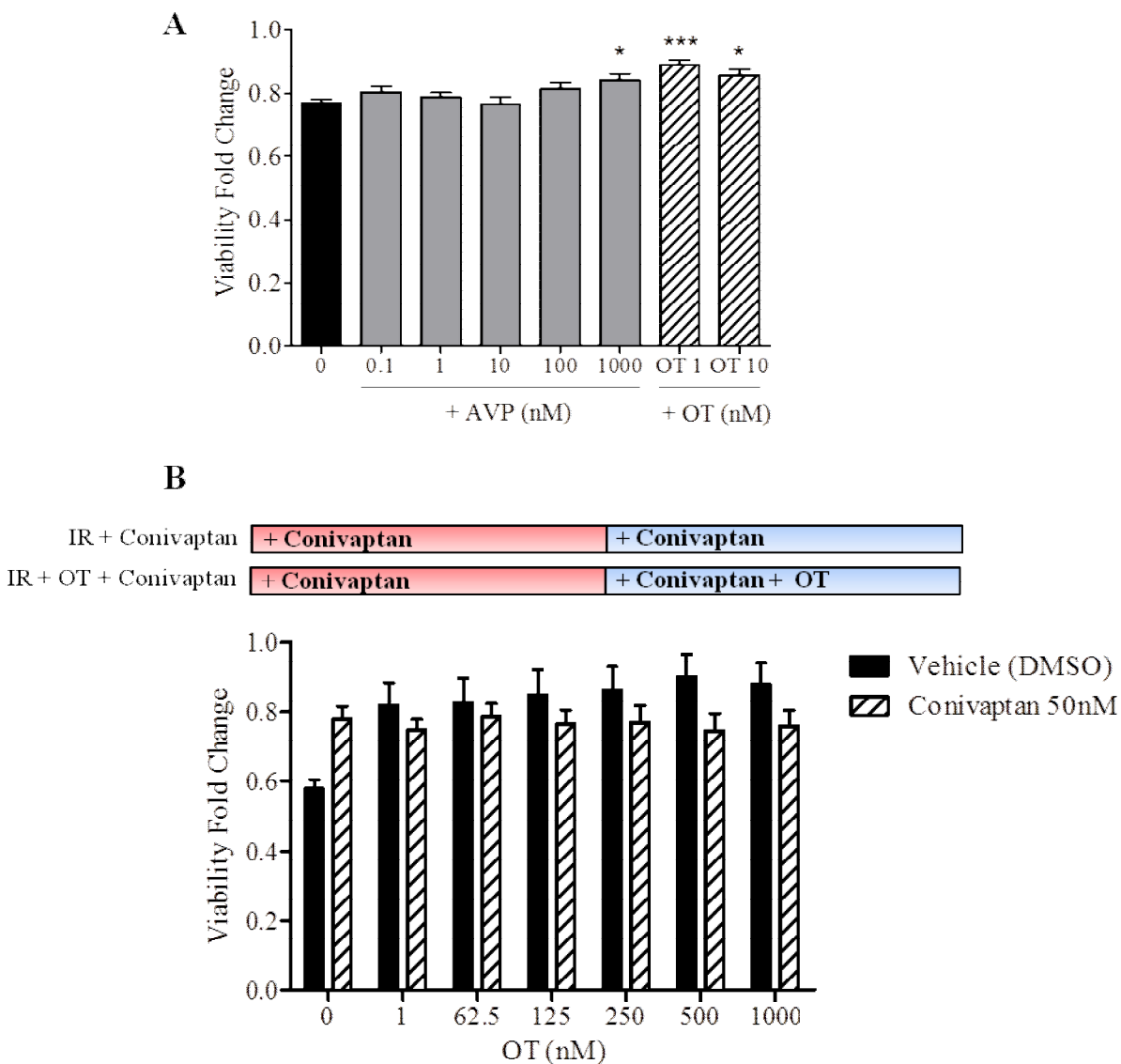
Figure 16. The role of vasopressin system in OT-mediated protection. A. Vasopressin administered at reperfusion protected cell viability only in the highest concentration tested (1000 nM). *** $p < 0.001$ vs. untreated IR. **B.** Vasopressin receptor V1a and V2 antagonist Conivaptan (50nM) protects cell viability in the absence of OT. There is a significant interaction ($p = 0.0121$) of OT and Conivaptan actions as estimated by two-way ANOVA. Experimental protocol of Conivaptan treatment in IR is presented at the top of the figure.

III.4. Mechanisms of oxytocin-induced cytoprotection

III.4.1. Oxytocin decreases the formation of reactive oxygen species (ROS) in cardiomyocytes exposed to IR

We hypothesized that modulation of oxidative stress may be one of the mechanisms of OT-induced protection. The determination of intracellular oxidative formation was based on the oxidation of 2 μM of 5-(and-6)-chloromethyl-2',7'-dichlorodihydrofluorescein diacetate, acetyl ester (CM-H$_2$DCFDA, Invitrogen). The acetate group in this cell-permeable probe is cleaved by intracellular esterases; subsequent oxidation releases fluorescent 2',7'-dichlorofluorescein that is retained within the cell, thus facilitating long-term studies on intracellular oxidative potential.

As shown in Figure 17A, intracellular ROS increased in ARVCMs upon simulated ischemia-reperfusion and was normalized by treatment with 1 nM OT beginning at 15 minutes prior to ischemia and maintained throughout the experiment (Fig. 17A).

To verify the hypothesis that OT exerts protection against ROS at reperfusion, H9c2 cells were treated with different concentrations of OT exclusively during the reperfusion period. As demonstrated in Figure 17B, the production of ROS was significantly attenuated at concentrations of 62.5-1000 nM of OT but not at a concentration of 1 nM after 2 hours of reperfusion.
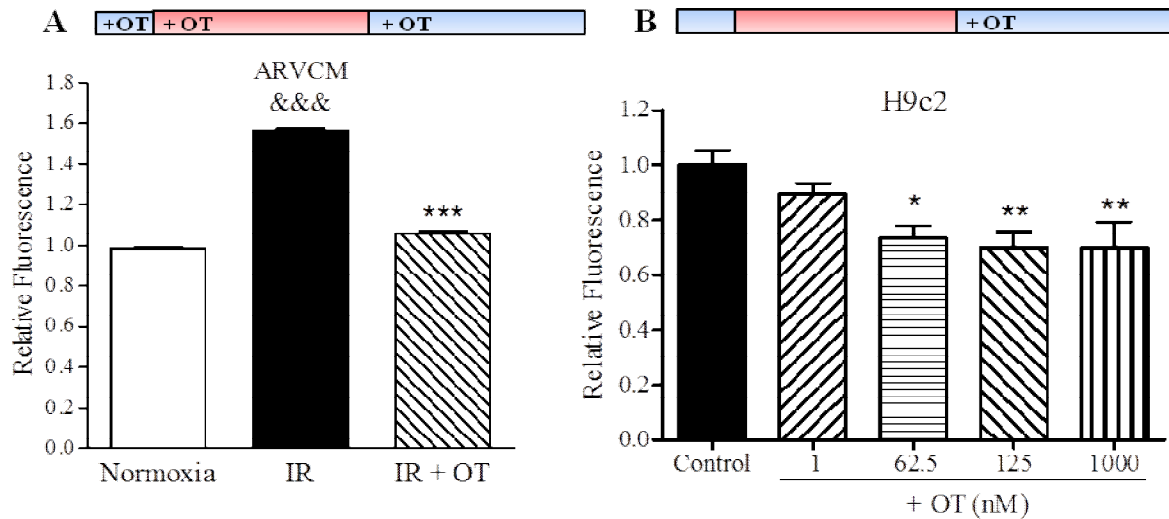
Figure 17. OT treatment prevents ROS formation following simulated ischemia-reperfusion. A. Intracellular ROS production in ARVCMs. Cells were incubated with the CM-H$_2$DCFDA probe in warm KRH buffer at 37°C for 30 minutes prior to IR protocol. Cells were then washed, and 1 nM of OT was added to the cells prior to the induction of ischemia, and maintained throughout the experimental time points. Fluorescence was measured after 1 hour of reperfusion. *** p < 0.001 **B.** Intracellular ROS production in H9c2 cells after 2 hours of reperfusion with OT treatment at the onset of reperfusion. After 1 hour of reperfusion in the presence of OT, cells were incubated with the CM-H$_2$DCFDA probe in warm KRH buffer at 37°C for 30 minutes. Cells were then washed and incubated in normal conditions for an additional 30 minutes (2 hours total reperfusion time). Fluorescence was measured using a microplate reader set at excitation 485/20 nm, emission 528/20 nm. * p < 0.05, ** p < 0.01 vs. control.

III.4.2. OT treatment in normoxic conditions causes an increase in intracellular ROS production

Interestingly, these experiments revealed that under normoxic conditions, OT treatment alone is sufficient to trigger a short-lived burst in intracellular ROS. H9c2 cells were incubated with the CM-H$_2$DCFDA probe, which becomes fluorescent upon oxidation by intracellular ROS and is retained within the cells. Figure 18A shows the effect of OT on ROS generation

after 5 minutes: a concentration of 1 nM OT increased intracellular ROS by 27.7 ± 6.1 % ($p < 0.001$ vs. control); 62.5 nM OT induced a 23.5 ± 6.2 % ($p < 0.01$ vs. control); 125 nM OT induced a 21.3 ± 3.9 % increase in ROS ($p < 0.01$ vs. control), whereas 1000 nM OT induced a 13.4 ± 4.1 % increase in intracellular ROS (n.s., Figure 18A). A similar pattern was observed after 15 minutes (Figure 18B), where OT increased ROS maximally at a concentration of 1 nM (up by 25.4 ± 5.7 % , $p < 0.01$ vs. control); but also significantly increased intracellular ROS by 23.6 ± 6.2 %, $p < 0.01$) with 62.5 nM OT, by 24.2 ± 4.7% with 125 nM OT ($p < 0.01$ vs. control) and by 18.5 ± 4.8 % with 1000 nM OT ($p < 0.05$ vs. control). As Figure 18C demonstrates, after 30 minutes of OT treatment only a concentration of 1000 nM was sufficient to induce a significant ROS production (up by 15.3 ± 4.5 %, $p < 0.05$ vs. control). At the early time points of 5 and 15 minutes, intracellular ROS production was optimally exerted in lower OT concentrations of 1 - 62.5 nM and less effective or absent when OT was added at 125-1000 nM; however, this pattern was not maintained after 30 minutes of treatment with OT (Fig. 18C). Thus, OT triggers a short-lived burst in ROS production. This phenomenon may be involved in OT signaling.
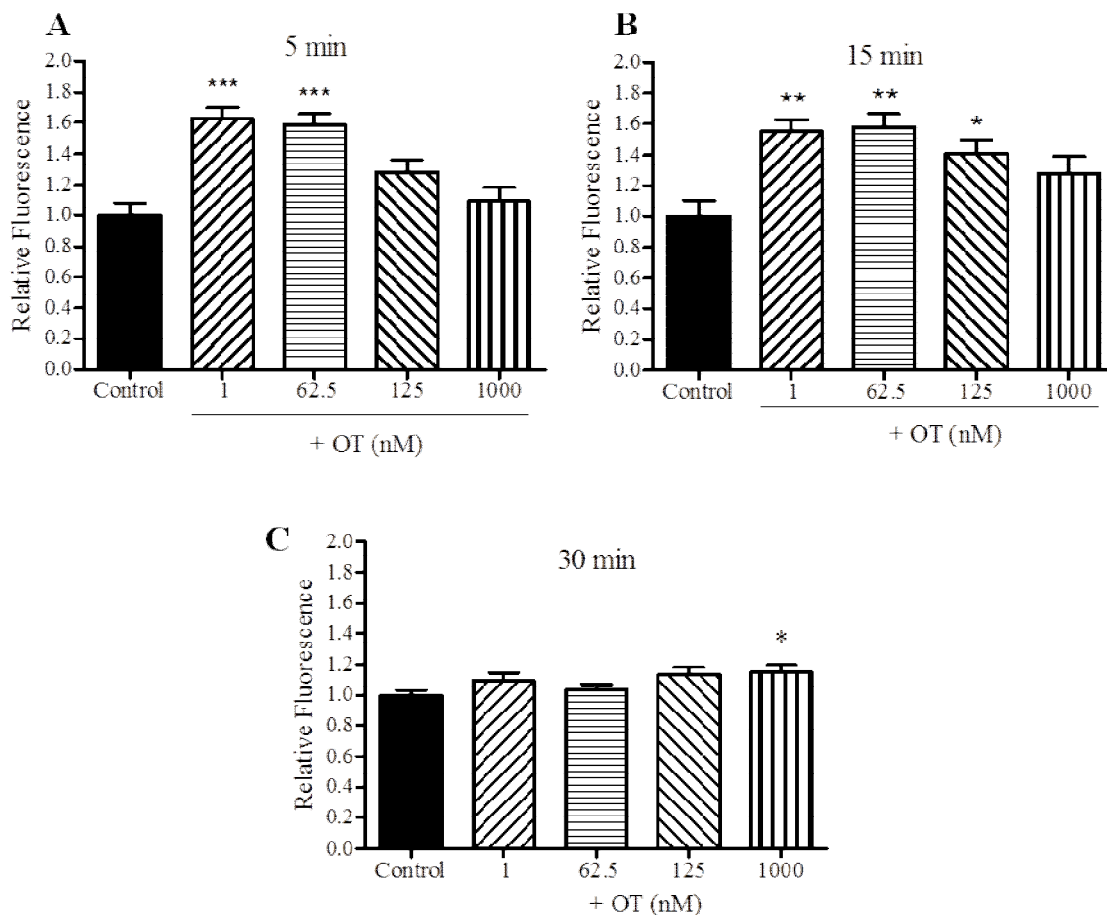
Figure 18. Intracellular ROS production after stimulation of H9c2 cells with OT. A. 5 minutes; **B.** 15 minutes, and **C.** 30 minutes of treatment with OT, under normoxic conditions. The treatment performed at different OT concentrations was assessed by fluorescence emitted by the oxidized probe CM-H$_2$DCFDA * p < 0.05, ** p < 0.01, *** p < 0.001 vs. control.

III.4.3. OT preconditioning of H9c2 cells protects them from doxorubicin-induced cytotoxicity

The stimulation of ROS by OT-preconditioned H9c2 cells led us to the hypothesis that reactive oxygen species released from the mitochondria during a brief OT treatment, induce preconditioning of cardiomyocytes and cell resistance to ischemia - reperfusion injury. To test this hypothesis we treated H9c2 cells with OT prior to exposure to Doxorubicin (Dox).

Dox is a drug commonly used for anti-cancer therapy but whose use is limited due to its cardiotoxicity targeting mitochondria[113]. Figure 19 demonstrates that a 24-hour Dox treatment (1 μM) induced a reduction in cell viability to $72.9 \pm 3.7\%$ of Dox-untreated control, $p < 0.0001$. Of the tested concentrations, 1000 nM OT had the maximal effect in protection of cells and increased viability to $86.7 \pm 4.1\%$ of Dox-untreated control. Two-way ANOVA reveals a significant effect of OT treatment ($p < 0.0001$) and of Dox treatment ($p < 0.0001$) but an insignificant interaction ($p = 0.9744$).

In the absence of Dox, OT treatment for 24 hours (62.5 and 1000 nM) also increased metabolic viability (up by $13.2 \pm 2.6\%$, $p < 0.001$ and $14.3 \pm 2.7\%$ $p < 0.001$ respectively vs. untreated control).
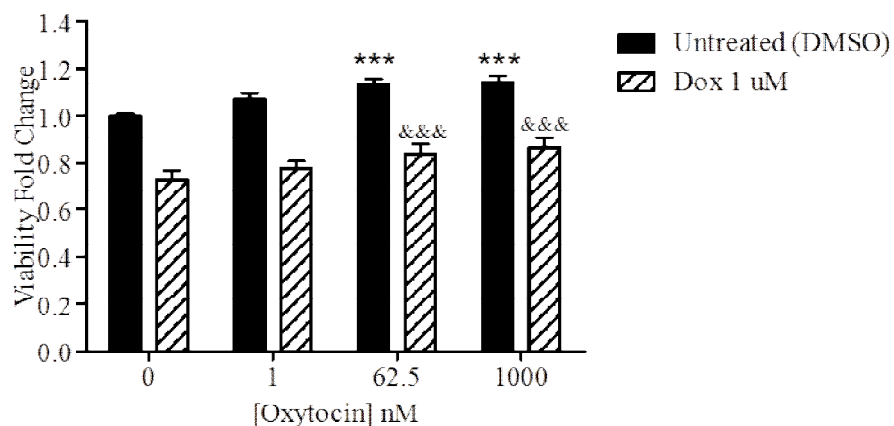
Figure 19. OT partially protects from doxorubicin - induced H9c2 cell death. Cells were pre-treated with varying doses of OT for 30 minutes prior to the addition of 1μM Dox for 24 hours (OT was not removed from the media prior to the addition of Dox). OT treatment for 24 hours induced a significant increase in viability both in the presence and absence of Dox. Two-way ANOVA reveals a significant effect of OT treatment ($p < 0.0001$), of Dox treatment ($p < 0.0001$) but insignificant interaction ($p = 0.9744$). *** $p < 0.001$ vs. Untreated vehicle; &&& $p < 0.001$ vs. Dox-treated, OT-untreated.

III.4.4. Pi3K-Akt-eNOS signaling is involved in OT-mediated protection from simulated ischemia - reperfusion

III.4.4.1. Pi3K inhibitor Wortmannin blocks the protective effect of oxytocin

Previous studies demonstrated that OT stimulates phosphatidylinositol-3-kinase (Pi3K)/Akt pathway in cardiomyocytes[76] and mesenchymal cells[114]. Activation of this pathway has been shown to be essential for the anti-apoptotic effects of H_2O_2-stimulated preconditioning of cardiomyocytes [115]. In addition, the maintenance of the activated form of Akt has been found to be protective against Dox-induced cardiomyopathy[116].

Experiments with Wortmannin (Wort), an irreversible covalent inhibitor of Pi3K, demonstrated that this pathway is necessary for OT-induced protection of metabolic viability as measured by formazan production in IR experiment using H9c2 cells (Fig. 20). ANOVA analysis demonstrated significant effect of interaction of OT and Wort treatments (p = 0.0068), OT effect (p < 0.001) and Wort dose effects (p < 0.001). Detailed analysis demonstrated that Wort at the concentration of 1-1000 nM did not influence metabolic viability of H9c2 cells in the absence of OT, which indicates lack of toxic effects of this compound on the cells at the concentrations used. As shown in Figure 20, OT treatment induced a 25.5 ± 4.4% increase in metabolic viability of H9c2 cells compared to untreated control; this protection decreased to 15.1 ± 1.5% in the presence of 10 nM Wort. Concentrations of 100 and 1000 nM Wort completely blocked the OT-induced protection of cells.
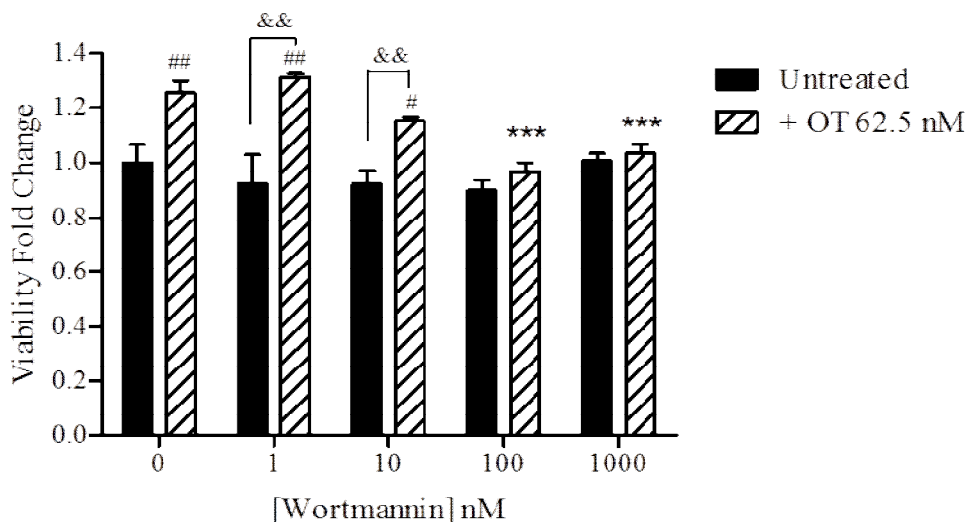
Figure 20. The phosphatidylinositol-3-OH kinase (Pi3K)-Akt pathway inhibitor, Wortmannin (Wort) blocked OT-mediated cell protection in IR conditions in a concentration - dependent manner. H9c2 cells were exposed to the indicated concentrations of Wortmannin in the ischemic buffer and again in the reperfusion medium, with or without OT. N=6 in each group/ Symbols: # $p < 0.05$, ## $p < 0.01$ effect of OT treatment; * $p < 0.05$ effect of OT treatment in presence of 1-1000 nM Wort vs. the OT in control.

III.4.4.2. OT stimulation causes Akt phosphorylation (Thr308) and co-localization with mitochondria in the perinuclear region

The protection from IR mediated by OT was blocked by the Pi3K-Akt pathway inhibitor Wortmannin in a concentration - dependent manner; therefore, we hypothesized that protection afforded by OT in IR experiment is related to Akt phosphorylation. Because there are reports suggesting that p-Akt translocation inside the cell structures is associated with enhanced cardiomyocyte viability[29,38] we performed immunofluorescence studies of p-Akt in cells stimulated with OT. Using inverted immunofluorescence microscopy, we noted that in normoxic conditions, cells treated for 30 min with 62.5 nM of OT, displayed increase of p-

Akt (Thr308) staining and specifically, p-Akt accumulated in intracellular structures apparently inside, or around, the cell nuclei (Fig. 21). We hypothesized that in some cells stimulated with OT, p-Akt will co-localize with mitochondria. Indeed, as presented in Figure 21, the co-staining with mitochondrial marker Cox IV showed partial co-localization of this protein with p-Akt (detected as yellow-orange staining in the merged photo) in the cytoplasm of OT-treated cells.

More details of the co-staining of p-Akt and Cox IV are presented at higher magnifications (Fig. 22) and by confocal microscopy (Fig. 23 and 24). Figures 22 and 23 present accumulated p-Akt apparently within the nuclei of OT - treated cells (white arrows). Detailed observation of these cells indicated that Cox IV protein, which was not seen in the nuclei of control cells, was transmitted to the nuclei of OT-stimulated cells where it co-localizes with p-Akt (Fig. 22-24). As marked by the arrows in Fig. 22, Cox IV staining was visible in the nuclear region, corresponding to the localization of p-Akt. In some micrographs, the structure composed of p-Akt and Cox IV appears associated with the nuclear envelope but not present inside the nuclei (yellow arrows in Fig. 23, 24), whereas in others (white arrows Fig. 22-24) p-Akt and Cox IV accumulated and co-localized in well-defined structures mostly in what appears to be the inside of the cells' nuclei in OT-treated cells.
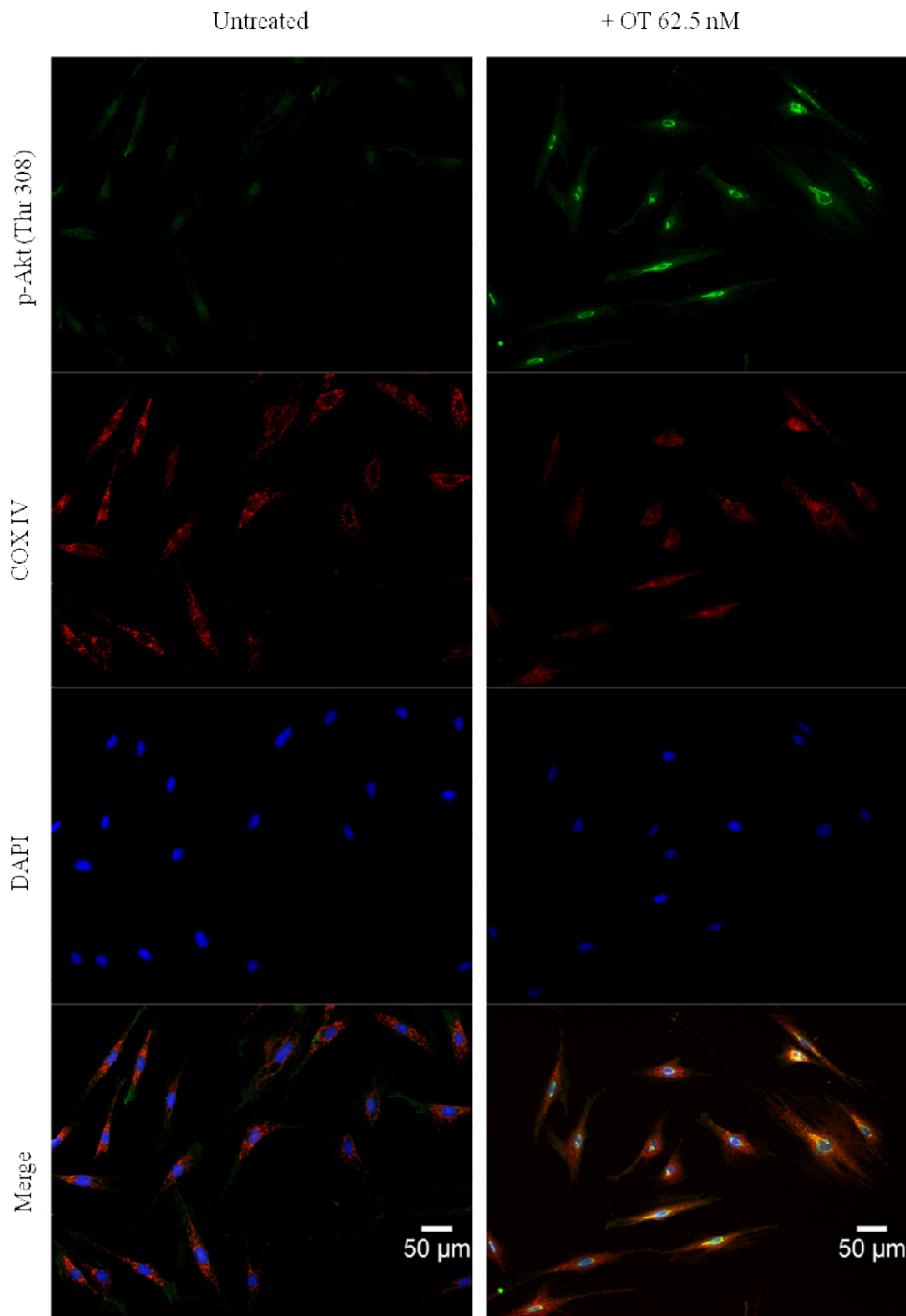
Figure 21. OT treatment causes Akt phosphorylation and accumulation in and around the nuclei of H9c2 cells. 10X magnification micrographs of H9c2 cells following 30 min of treatment with OT 62.5 nM. Cells were fixed and probed using antibodies against phosphorylated Akt (Thr308, green) and mitochondrial cytochrome c oxidase/respiratory complex IV present on the mitochondrial inner membrane (COX IV, red). Following OT treatment, p-Akt appears accumulated in a distinct structure *inside* (white arrows) and/or *around* (yellow arrows) the cells' nuclei.
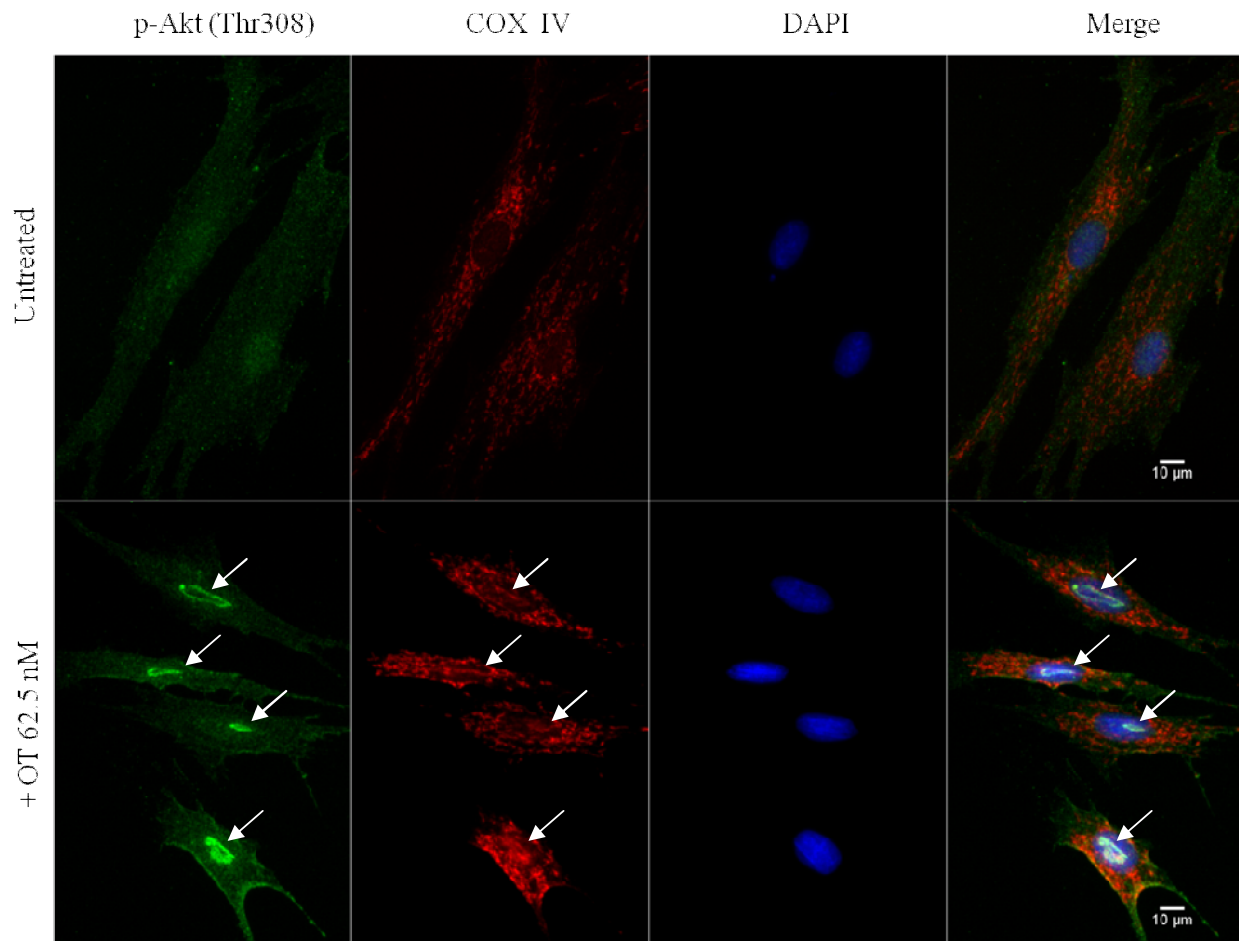
Figure 22. OT treatment causes p-Akt phosphorylation in a structure within the nuclei. Inverted microscope micrographs of H9c2 cells following 30 min of OT treatment and probed with p-Akt (T308, green) and mitochondrial complex IV (Cox IV, red).
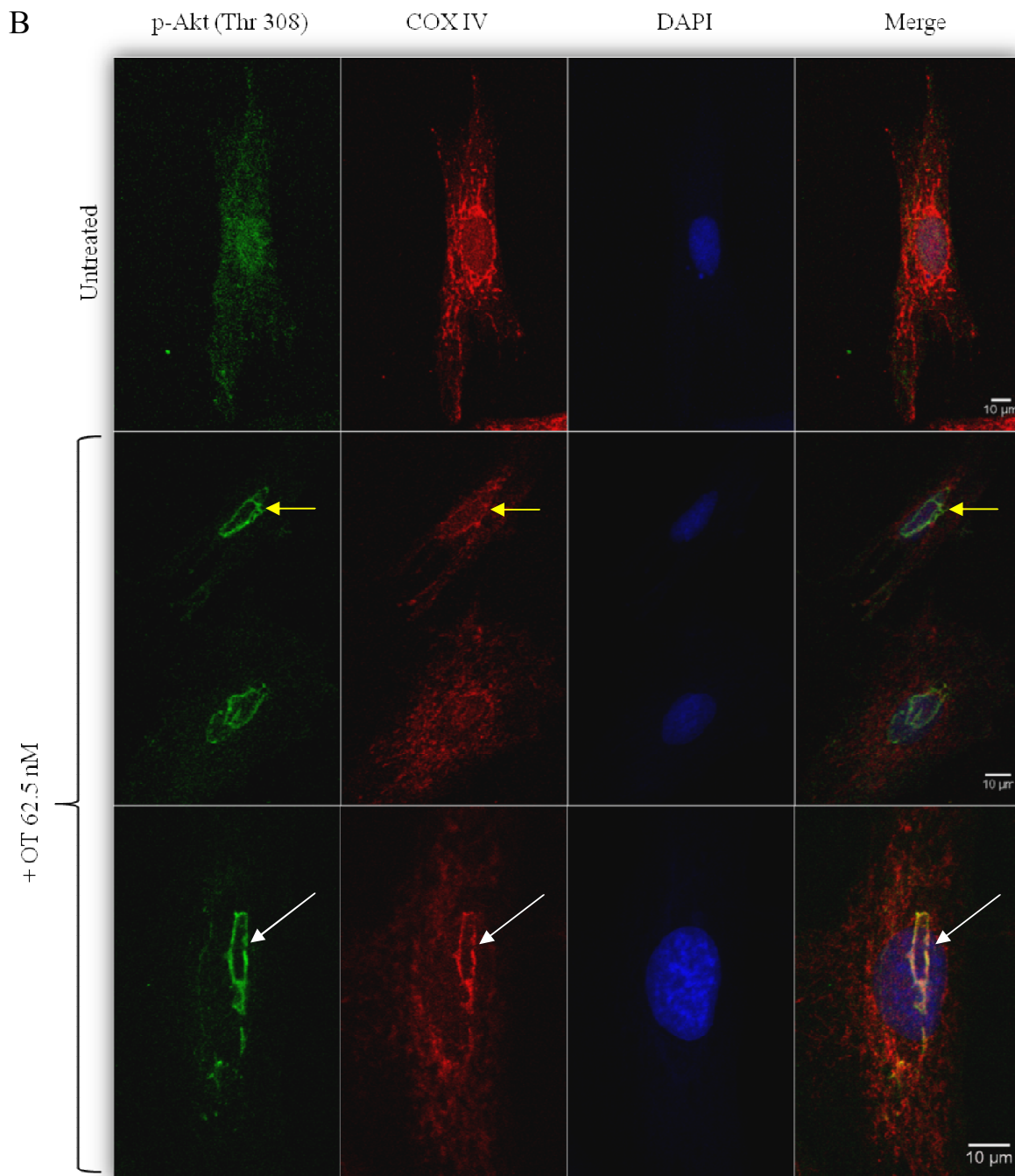
Figure 23. OT treatment causes p-Akt phosphorylation in a structure within the nuclei. Micrographs of H9c2 cells following 30 min of OT treatment and probed with p-Akt (T308. green) and mitochondrial complex IV (Cox IV, red). using **A.** Inverted microscope and **B.** Optical slices demonstrating precise c-localization of p-Akt (T308) and Cox IV apparently concentrated in a structure within and around the nuclei of H9c2 cells treated with OT (62.5 nM) in normoxic conditions.
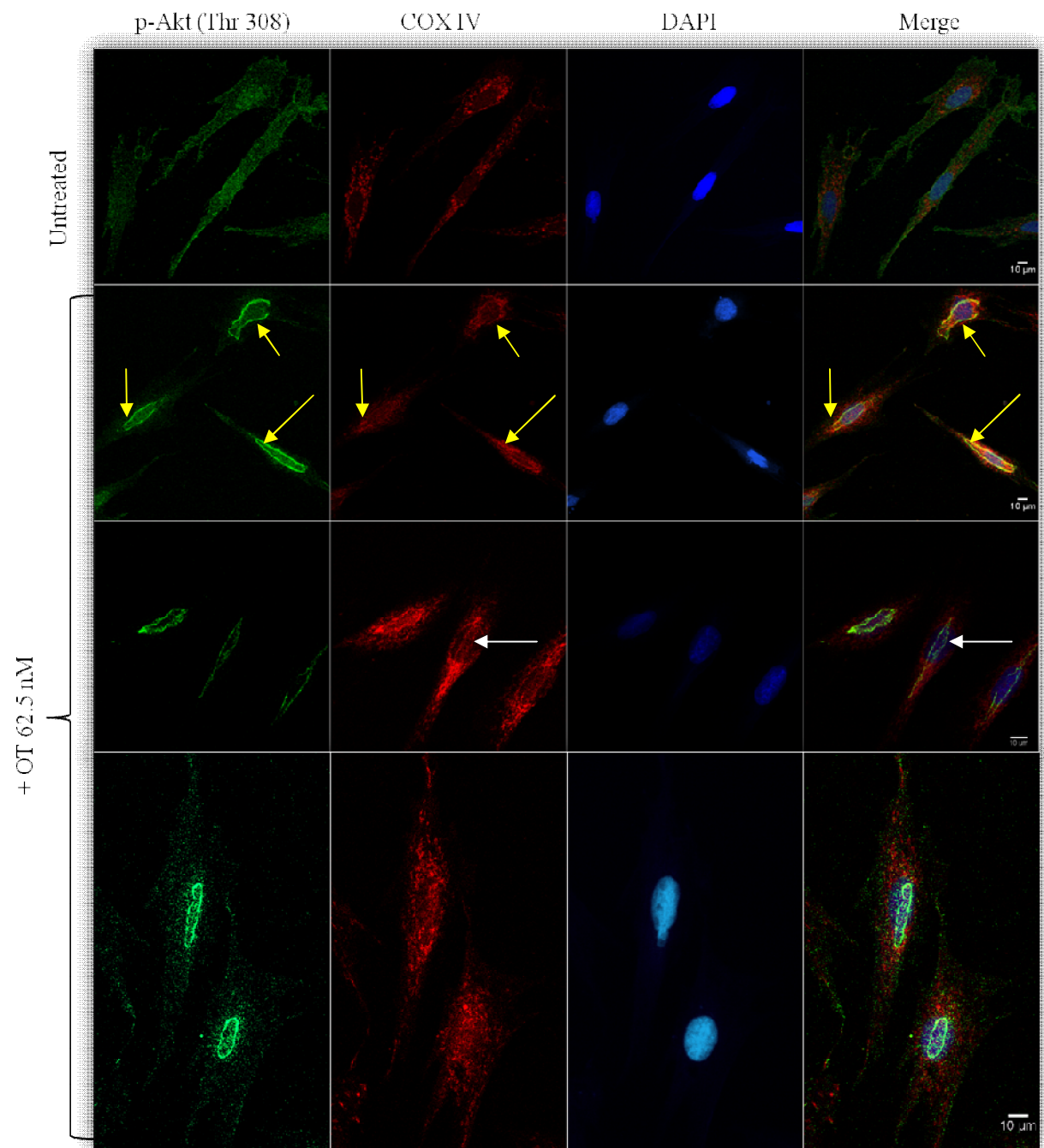
Figure 24. OT treatment causes p-Akt phosphorylation in a structure around the nuclei. Optical slices demonstrating precise co-localization of p-Akt (T308, green) and Cox IV (red) apparently concentrated in a structure around the nuclei of H9c2 cells following 30 min of OT treatment in normoxic conditions.

In conclusion, the confocal analysis presented in Figures 23 and 24 revealed that p-Akt co-localizes precisely with mitochondrial cytochrome C oxidase (Cox IV) in the perinuclear cell region. Although this phenomenon was also visible in some cells treated with different doses of OT (1, 500 and 1000 nM, results not shown), the effect was strongest at a dose of OT 62.5 nM. The observed structure is present most clearly in normoxic cells after 30 minutes of OT treatment (Fig. 21-24). However, it was also observed following the IR protocol, after 30 minutes of OT treatment during reperfusion (Fig. 25).
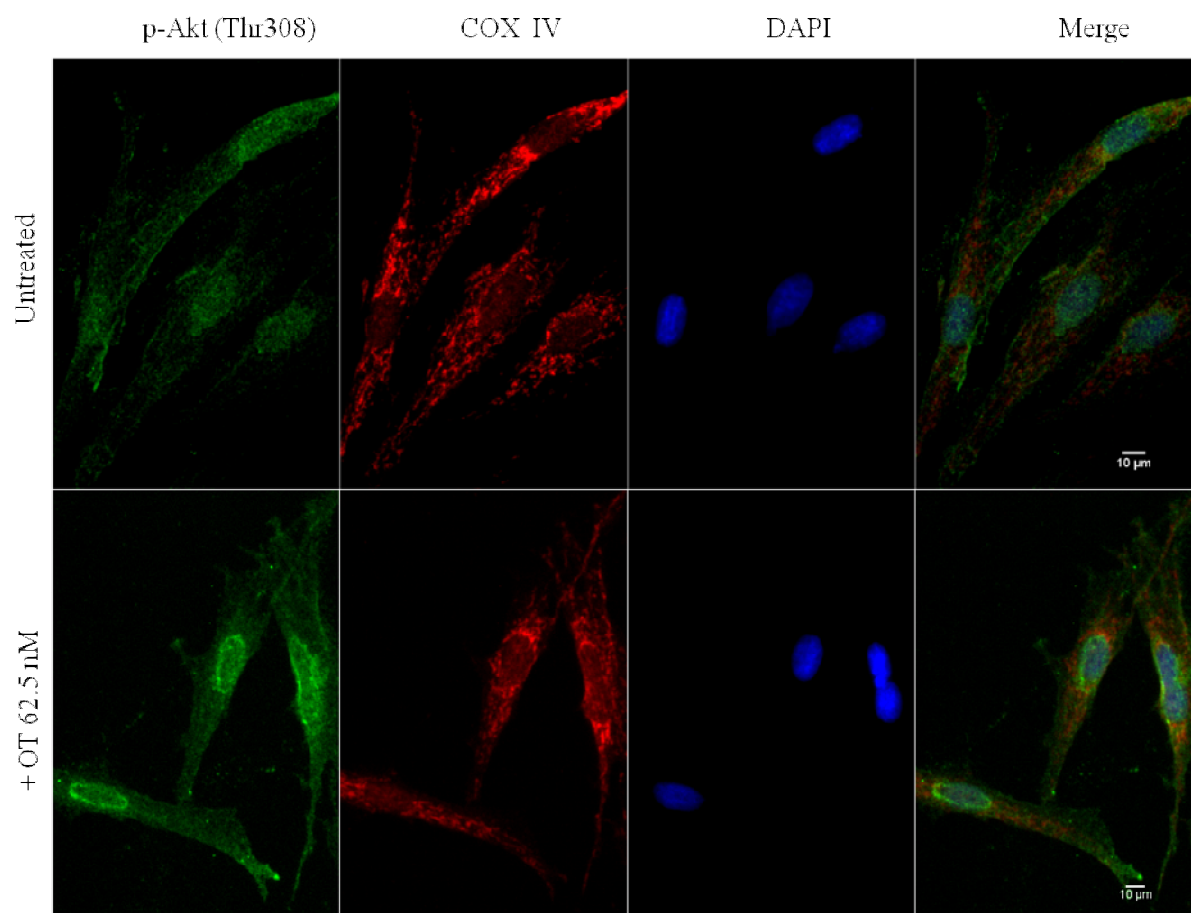
Figure 25. H9c2 cells subjected to hypoxia and treated with OT at reperfusion period display Akt phosphorylation and p-Akt and Cox IV translocation in the perinuclear region. Optical slices of untreated and after 30 min of OT (62.5 nM) treatment following simulated ischemia - reperfusion.

III.4.4.3. OT treatment causes eNOS phosphorylation (Ser1177) and nuclear co-localization with p-Akt (Thr308)

Given the evidence obtained that cGMP production via soluble GC was an essential part of OT-induced protection of cell viability, we performed investigations of endothelial nitric oxide (eNOS) phosphorylation status following different lengths of OT treatment under normoxic conditions.

Figure 26 presents confocal micrographs demonstrating the time course of eNOS phosphorylation (Ser1177, red) and nuclear accumulation after 0, 5, 15 and 30 minutes of treatment with OT 62.5 nM. Interestingly, closer analysis of nuclear p-eNOS revealed a distinct structure of p-eNOS (Ser1177) and p-Akt (Thr308) proteins co-localizing within the nuclei of H9c2 cells (Figure 27); this intra-nuclear structure appears very similar to the one observed previously (Figure 23, bottom panel).
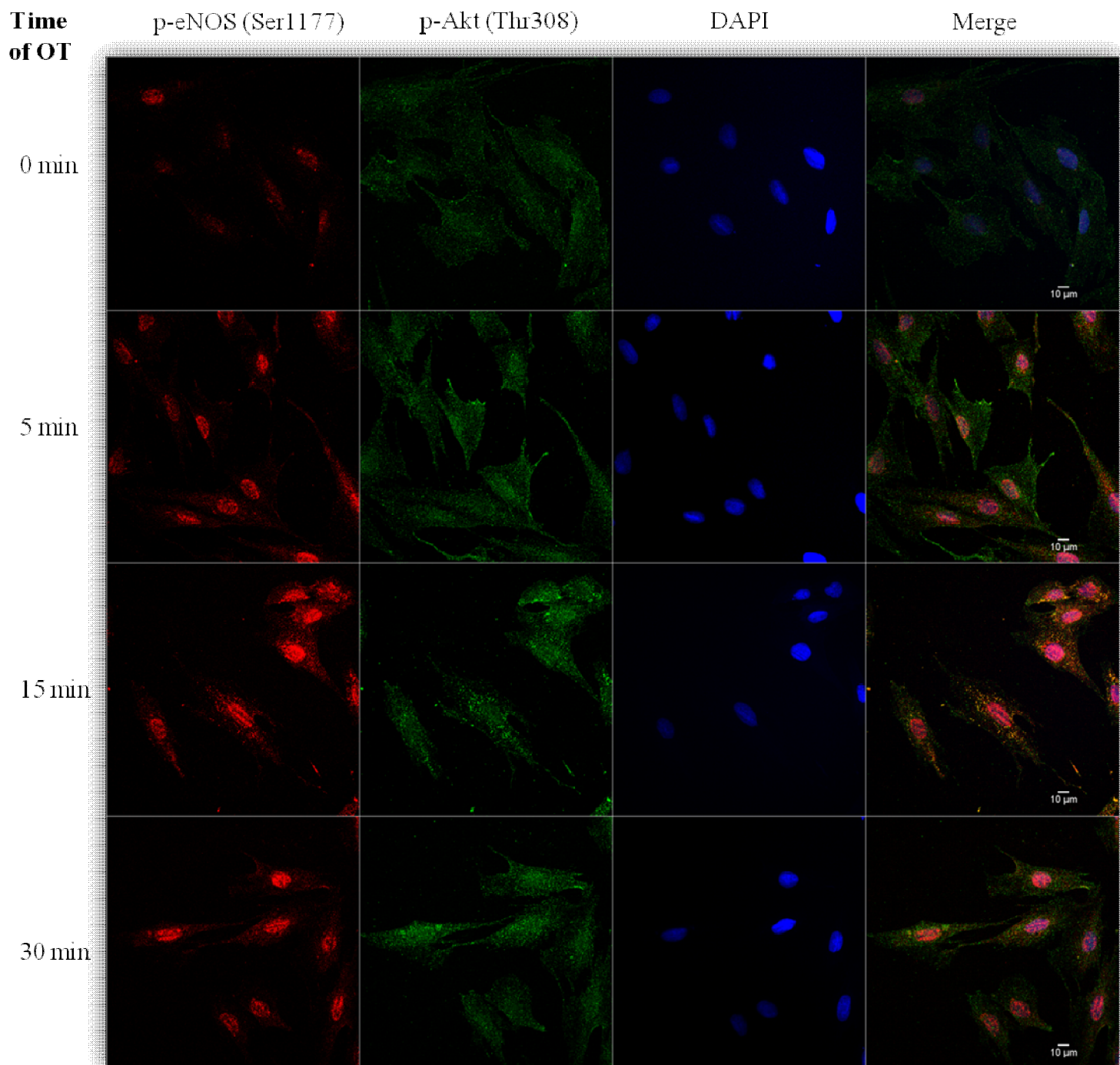
Figure 26. OT causes p-eNOS accumulation in the nuclei of H9c2 cells. Time-course of changes in the abundance and intracellular localization of phoshorylated forms of eNOS (Ser1177, red) and Akt (Thr308, green) during 30 min of OT treatment. Nuclei are stained with DAPI in blue. With time, the co-localized areas are stained mostly in cell nuclei and appear in orange color.

p-eNOS (Ser1177)	p-Akt (Thr308)	DAPI	Merge
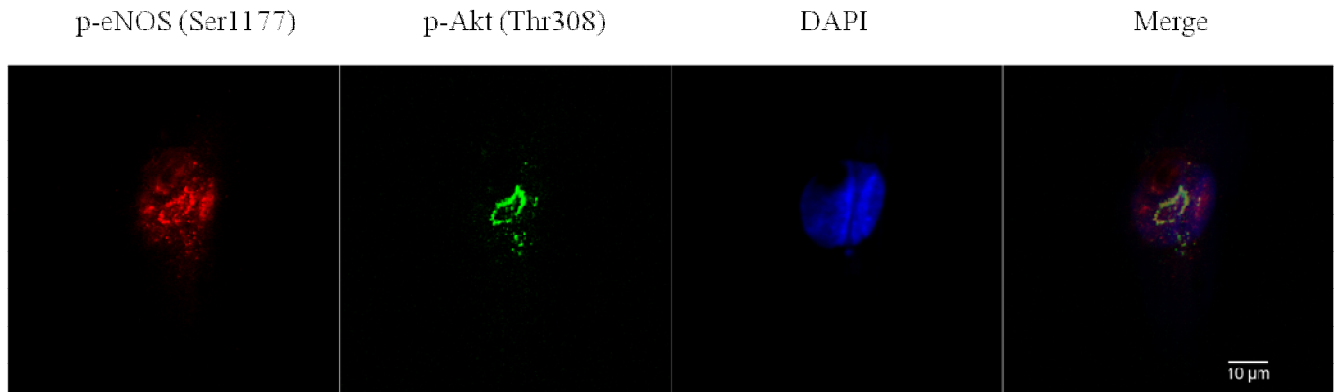
Figure 27. Co-localization of phosphorylated eNOS (p-eNOS, red) and phosphorylated Akt (p-Akt, green) in H9c2 cells stimulated with 62.5 nM of OT. Optical slice of H9c2 cell nucleus after 30 minutes of treatment with OT, and demonstrates the appearance of phosphorylated eNOS (Ser1177, red) and phosphorylated Akt (Thr308, green) structures in the nuclei of cells treated for 30 min with 62.5 nM of OT.

III.4.5. The cGMP/PKG pathway mediates OT-induced cardioprotection

III.4.5.1. cGMP-dependent protein kinase (PKG) activity

Previous experiments *in vivo* demonstrated that nitric oxide (NO) plays a role in OT-stimulated cardiac protection [71,74] and acts against cardiac ischemia-reperfusion injury in association with PI3K/Akt activation[71]. NO signaling is known to stimulate the activity of soluble guanylate cyclase (sGC), which results in an increase in cyclic GMP (cGMP) production and increased activity of the pro-survival cGMP - dependent protein kinase (PKG). To investigate the role played by PKG in OT-mediated cell protection against IR, H9c2 cells were treated with the PKG inhibitor KT-5823 (Figure 28) throughout the IR experiment, with or without 62.5 nM OT added at reperfusion. Figure 28 reveals that a concentration of 2 μM KT5823 blocks the protection induced by treatment with OT ($p = 0.0001$ vs. OT Vehicle). Two-way ANOVA revealed a significant interaction ($p = 0.0128$) of OT treatment ($p < 0.0001$) and KT5823 concentration ($p < 0.0001$).
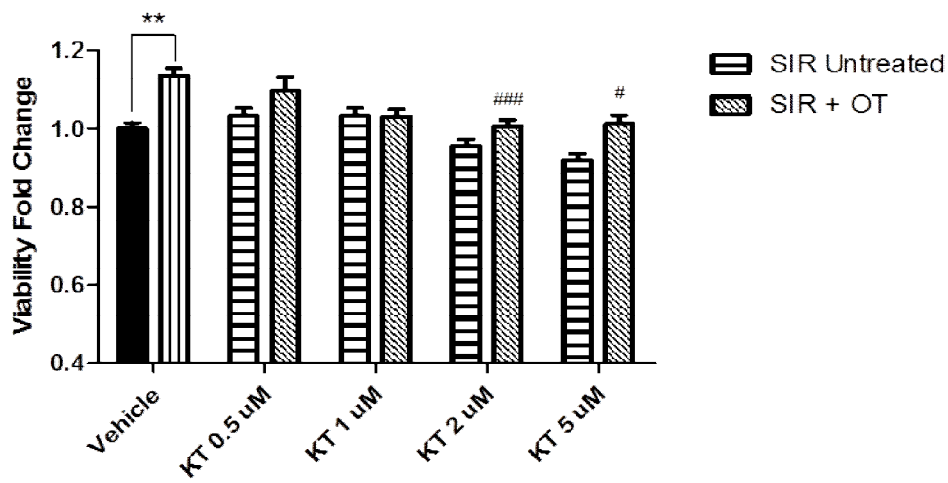
Figure 28. cGMP-dependent protein kinase (PKG) inhibitor KT-5823 blocks the protective effect of OT (62.5 nM) treatment at reperfusion. H9c2 cells were treated with the indicated concentrations of KT5823 throughout the duration of the IR experiment. A single administration of OT (62.5 nM) was done at the onset of reperfusion. Viability was determined after 4 hours of reperfusion. Significant interaction (p = 0.0128), OT treatment (p < 0.0001) and KT5823 concentration (p < 0.0001). ** p < 0.01; # p < 0.05, ## p < 0.001 vs. SIR + OT vehicle.

III.4.5.2. Guanylate cyclase activity

In cells, cGMP is the activating substrate for PKG, and is produced by two major classes of guanylate cyclases: soluble (sGC) and particulate (pGC). The activation of sGC is associated predominantly with NO, whereas pGC is activated by natriuretic peptides. In order to further explore the OT cytoprotective mechanism associated with NO activation, we investigated the role of sGC activity in cells subjected to SIR. Figure 29 shows that sGC inhibitor ODQ has a significant effect on OT-induced viability protection, with two-way ANOVA revealed significant interaction (p = 0.009), OT treatment (p = 0.0412), and ODQ treatment (p < 0.0001). OT treatment in the absence of ODQ induced a 19.0 ± 3.6 % increase in metabolic

viability (student t test p < 0.001 vs. untreated control, whereas the specific inhibition of sGC by the administration of 2μM ODQ blocked OT's protection of metabolic viability to 91.8 ± 3.5 % of untreated control (p = 0.0004 vs. OT-treated, ODQ-untreated).

Figure 29B demonstrates that a concentration of 0.2 μM of pGC inhibitor/natriuretic peptide antagonist A71915 prevents OT - induced protection of viability following IR. Two-way ANOVA reveals a significant interaction of OT and A71915 treatments (p = 0.0455). Student t test reveals that a treatment with 0.2 μM A71915 blocks OT's protective effect. OT alone increased viability (by 16.2 ± 5.0%, p < 0.001 vs. untreated control), whereas A71915 co-administered with OT had a tendency to decrease viability to 98.9 ± 2.6 % of untreated control (p = 0.0574 vs. OT alone). These results suggest that OT exerts its cardioprotective effect via the generation of cGMP.
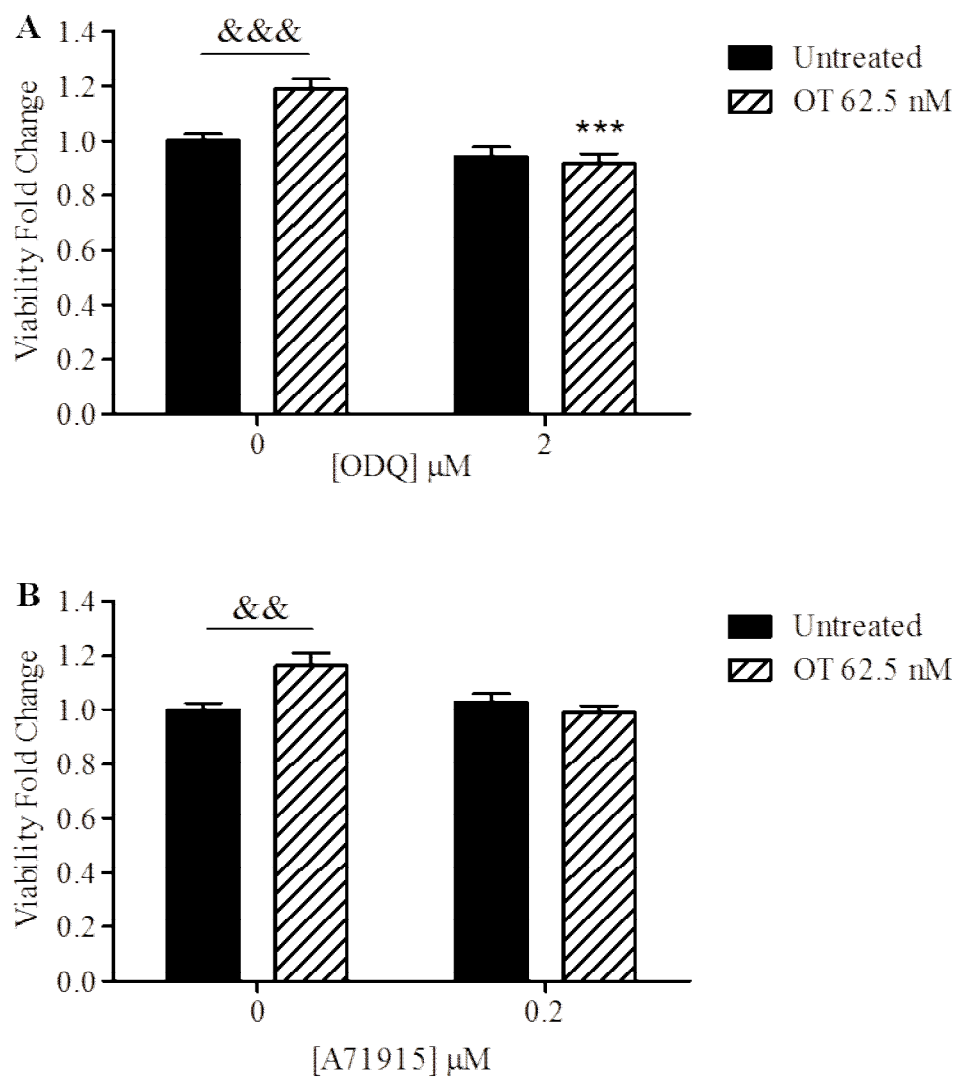
Figure 29. Inhibition of cGMP production blocks the protection induced by OT treatment at reperfusion. A. Soluble guanylate cyclase (sGC) inhibitor ODQ blocks the protective effect of OT at a concentration of 2 μM. &&& $p < 0.001$; *** $p < 0.001$ vs. OT-treated, ODQ untreated control. **B.** Particulate GC antagonist A71915 partially blocks the protective effect of OT at a concentration of 0.2 μM. && $p < 0.01$.

IV. DISCUSSION

Work from recent years has demonstrated that OT has the capacity to attenuate the myocardial damage resulting from myocardial ischemia -reperfusion injury. A variety of research groups around the world have reported impressive reductions in infarct size when the ischemic event was preceded by an administration of OT[70,74,77,80–82]. More interestingly from a clinical perspective, important reductions in infarct size are also observed when OT is administered at the onset of reperfusion[71], or just prior to it[83]. However, the molecular mechanism indicating how oxytocin protects the cardiac cells in from ischemia – reperfusion injury is far from being explained.

The results of this project demonstrate that oxytocin directly acts on cardiomyocytes to improve their survival during the acute phase of simulated ischemia - reperfusion. On the H9c2 cell line (a cardiomyocyte model) we revealed the pleiotropic mechanisms by which OT protection is induced. Using formazan production for the measurement of cell viability and metabolic activity, a significant cellular protection was observed at a concentration of 1 nM of OT, with an optimal protection at 62.5-125 nM. A specific OT antagonist concentration-dependently blocked the protective effect of OT. Using the TUNEL methodology, it has been shown that OT treatment of H9c2 cells transfected with OT receptor siRNA increased cell apoptosis 3-fold in comparison to the control. The OT-induced increase in cell mortality in OTR siRNA cells could be mediated by vasopressin receptors. Indeed, blockade of AVP receptors by Conivaptan increased cell viability in IR conditions. OT treatment decreased the fluorescence of CM-H_2DCFDA products in IR-treated cells indicating a decrease of intracellular reactive oxidative species (ROS). Interestingly, these experiments revealed that under normoxic conditions, OT treatment alone is sufficient to

trigger a short-lived burst in intracellular ROS. The OT protection of IR was blocked by the PI3K-Akt inhibitor Wortmannin. Correspondingly, using confocal microscopy, we noted that cells treated with OT displayed increased Akt (Thr308) phosphorylation and specifically, Akt was accumulated in ring-like structures associated with mitochondria and nuclei. The demonstration that KT-5823, inhibitor of protein kinase G (PKG) and ODQ, inhibitor of soluble guanylyl cyclase, reduced OT-mediated protection in IR, indicated the role of cGMP-dependent protein kinase (PKG). Consequently, confocal microscopy demonstrated the increase of eNOS phosphorylation and its nuclear accumulation in cells treated with OT. OT protection in IR was also inhibited by ANP receptor antagonist, A71915.

These data suggest that OT provides protection to the injured heart by pleiotropic mechanisms which include inhibition of ROS, inhibition of cardiomyocyte death and stimulation of cell protective Pi3K-Akt-PKG signaling and molecular trafficking.

IV.1. Experimental Models

IV.1.1. H9c2 cells are a good *in vitro* model of oxytocin signaling in cardiomyocyte ischemia - reperfusion

The use of *in vitro* models of ischemia - reperfusion injury is necessary in order to study mechanistic details of cell death and signaling. The cell line H9c2 is an accepted model of cardiomyocyte amenable to manipulations. Our data demonstrates that H9c2 cells express both OTR and AVP receptor 1a along with cardiomyocyte - specific markers GATA - 4 and troponin T. In addition, select experiments were performed in parallel in primary cultures of adult rat ventricular cardiomyocytes as well as in H9c2 cells, and the results demonstrate that

in our experimental model H9c2 cells behave in a way comparable to adult cardiomyocytes in culture.

As stated previously, ionic homeostasis and pH modulation are essential features of ischemia - reperfusion injury[8]. In our experiments, the use of an ischemic buffer proved indispensable for the consistent reduction of cell viability as a function of time of exposure of H9c2 cells to hypoxic conditions.

The use of two different sequences of small interfering RNA (siRNA) targeting OTR allowed us to decrease the amount of OTR protein expressed by H9c2 cells while minimizing off-target effects of each sequence. A scrambled siRNA control served to verify the experimental conditions, and in all cases tested the scrambled siRNA - treated cells responded in the same way as un-transfected cells, confirming that transfection with siRNA in itself was not enough to affect the phenotype of the cells.

IV.2. OT protects cardiomyocyte survival

IV.2.1. OT preconditioning directly protects cardiomyocyte survival

Cardioprotective treatments aim to salvage cardiac function by protecting the survival of contractile cardiac cells, the cardiomyocytes, from death following ischemia - reperfusion injury. While the majority of the volume of the myocardium is composed of cardiomyocytes, there are many different cell types present such as fibroblasts and endothelial cells, and cardioprotective stimuli likely confer effects in all the cell types of the myocardium[8]. Cell-cell interactions and paracrine signaling across cell types could confer the protected phenotype to cardiomyocytes without directly stimulating receptors on the cardiomyocytes

themselves. The presence of OTR on endothelial cells is well known, and oxytocin treatment stimulate angiogenesis[117]. To study whether oxytocin can directly trigger pro-survival signaling in cardiomyocytes, isolated primary cultures of rat cardiomyocytes as well as the cell line H9c2, derived from embryonic rat heart, were used in this study. With the use of an *in vitro* simulated ischemia - reperfusion protocol we were able to clearly demonstrate that treatment with OT beginning 15 minutes prior to the induction of ischemia and maintained throughout the experimental protocol can exert a protective effect on cardiomyocytes' metabolic viability and decrease the number of dead nuclei detected by TUNEL. Importantly, primary cultures of adult rat cardiomyocytes responded in the same pattern as H9c2 cells; confirming the validity of H9c2 cells as a model of adult cardiomyocyte. However, the relative proportion of dead cells was higher in primary cultures of adult cardiomyocytes compared to H9c2 cells.

IV.2.2. OT exerts an optimal protective effect if administered only at reperfusion

Our investigations into the specific point of OT action in the protection from ischemia - reperfusion revealed that OT protects optimally if administered at reperfusion. This observation is consistent with recent reports in the literature indicating a significant reduction in infarct size when OT is administered at the onset of reperfusion[71,83]. This agrees with the fact that the induction of cell death from ischemia - reperfusion injury is believed to take place in the first minutes of reperfusion[8], and that ischemic preconditioning is known to confer resistance to cell death from ischemia - reperfusion by activating pro - survival kinases at reperfusion[15]. Thus, when a single OT administration was performed, protection

improved the closer OT was administered to reperfusion; with OT administration during ischemia only providing a small measure of protection. This is probably due to the fact that the first few minutes of reperfusion are critical in determining cell fate. Protective signaling triggered by an OT treatment during ischemia might still play a role in early reperfusion.

Additionally, OTR signaling is known to become desensitized after prolonged OT stimulation[56]. Thus, in the case of multiple OT administrations (Fig. 12B and C), when OT is added prior to reperfusion as well as at the onset of reperfusion, OT signaling and thus kinase activation would be attenuated during the critical phase of reperfusion as compared to OT administration exclusively at reperfusion.

IV.2.3. The protection induced by OT is mediated by OTR

OT is almost identical to a second neurohypophyseal hormone, arginine vasopressin (AVP), differing from it by only 2 amino acid residues. Conceivably both hormones can act through both receptors, with different affinities. Based on the results obtained using an antagonist specific to OTR, OTA, we demonstrate that OT is cardioprotective if its signaling is mediated by OTR. OTR expression is down-regulated in hearts having undergone cardiac ischemia by 40-50%[73,74], and this reduction could be restored by treatment with OT[74]. Interestingly exercise training increased OTR mRNA expression by 4-6 times in both sham-operated and ovariectomized rat hearts, pointing to a possible involvement of OT signaling in the cardioprotective effects of exercise[72].

IV.2.3.1. OTR knockdown reverses the protective pattern seen by OT treatment

H9c2 cells treated with scrambled (non-silencing) siRNA sequences displayed an increase in cell death upon IR that was significantly attenuated upon treatment with OT at reperfusion. In the absence of OTR, IR in itself caused a more modest induction of cell death, and treatment with OT at reperfusion caused an increase in the number of TUNEL-positive nuclei compared to untreated cells. This suggests the possibility that in the absence of OTR, OT can trigger deleterious signaling via the related V1a and/or V2 receptors. This agrees with reports that low-dose AVP infusion after 1 hour of ischemia increased mortality and cardiac dysfunction in mice[73], and that cardiac-restricted over expression of V1a causes left ventricular dysfunction[118]. Furthermore, the use of an antagonist for AVP receptors V1a and V2 in itself proved to be protective in our model of simulated ischemia - reperfusion. We would thus expect that AVP signaling is deleterious in this context, and OT is favourable. However, treatment with AVP did not decrease cardiomyocyte viability at concentrations ranging from 0.1 to 100 nM, but improved viability at a concentration of 1000 nM. The protection elicited by the high concentration of AVP may reflect the fact that at higher concentrations AVP can trigger signaling via OTR. Similarly, reduced protection was observed when OT was administered at concentrations higher than 500 nM, suggesting that at high concentrations OT may trigger signaling via V1a.

IV.3. Mechanisms of OT - induced cardiomyocyte protection

IV.3.1. OT prevents the intracellular formation of reactive oxygen species after 1 and 2 hours of reperfusion

The formation and sustained opening of the mitochondrial permeability transition pore (mPTP) is considered the irreversible commitment of a cell to death[11]. Among the stimuli known to trigger its opening is the excess formation of reactive oxygen species within the cell, leading to oxidative stress[8,10,11]. It is believed that the reintroduction of oxygen into altered mitochondria (i.e., with high matrix Ca^{2+} and inorganic phosphate concentrations) at reperfusion causes an excessive production of ROS, leading to intracellular oxidative stress, which under the high Ca^{2+} concentrations causes death through opening of the mPTP[8]. This study demonstrated that when OT is administered at reperfusion, there is a 30 % decrease in intracellular ROS content after 2 hours of reperfusion.

IV.3.2. OT treatment under normoxic conditions causes a short - lived burst in ROS production

A short treatment with OT under normal conditions (i.e. not after ischemia - reperfusion) caused up to a 25% increase in ROS that was apparent after 5 and 15 but not 30 minutes of treatment with OT. This observation agrees with the proposed mechanism by which cardioprotective stimuli prevent mPTP formation, stating that protein kinase C-ε becomes activated by a burst of ROS production and subsequently inhibits the opening of the mPTP[14]. In this model, cardioprotective stimuli, such as bradykinin, opioids, natriuretic peptides and IPC[19], are believed to cause the opening of mitochondrial ATP-sensitive K^{+} channels, which trigger a burst in ROS, and this ROS is the signal that is transmitted to PKCε, and PKCε then

inhibits mPTP opening by unclear mechanisms[14]. The exogenous administration of H_2O_2 can in itself prevent mPTP formation[14]. Some authors have proposed that H_2O_2 treatment can act as a preconditioning stimuli because it causes a transient opening of mPTP which reduces mitochondrial ions and prevents the prolonged opening of the mPTP, which would be lethal[119]. Some authors have proposed that ligand triggers (such as adenosine, bradykinin and opioids) of pre- and postconditioning may generate a burst in ROS production that protect against the subsequent and more substantial generation of injury producing ROS during reperfusion[20]. The ROS scavenger N-acetylcysteine (NAC) blocks the cardioprotection induced by PC if administered in the first 3 minutes of reperfusion[8]. A recent report demonstrated that NAC abolished the protective effect of OT preconditioning in the anesthetized rat heart undergoing MI[81]. This observation agrees with our data that OT treatment in normoxia causes a short-lived ROS production, whereas OT administration at reperfusion causes a decrease in intracellular ROS generation after 1 and 2 hours of reperfusion.

IV.3.3. OT protects from doxorubicin - induced mitochondrial toxicity

The modulation in ROS production and the importance of mitochondria in cell death and survival decisions prompted us to investigate whether OT could directly protect mitochondrial function of cardiomyocytes. Doxorubicin is a commonly used chemotherapeutic agent for the treatment of neoplasms. However, its use is limited due to the fact that it causes major cardiac toxicity through mitochondrial dysfunction and caspase-3 activation[113] that is likely to be different from the antitumor mechanism[116]. Here we report that a 30 minute pre-treatment with OT (62.5 and 1000 nM) prior to the administration of

Dox for 24 hr resulted in improved viability of H9c2 cells. Our observations demonstrating that OT treatment of cardiomyocytes stimulates Akt phosphorylation and translocation into mitochondria is consistent with some mechanisms of protection against Dox-induced cardiac toxicity which include the increase in phosphorylated Akt and attenuation of Dox-induced oxidative stress[116].

IV.4. Signalisation involved in OT-mediated cardiomyocyte protection

IV.4.1. Pi3K/Akt signaling

GPCR are known to activate the Pi3K-Akt pathway, a major pro-survival pathway important in survival from ischemia - reperfusion injury, and OT-OTR signaling has been shown to involve Pi3K-Akt[76,112]. Furthermore, protection from Dox-induced cardiotoxicity by heat shock protein (Hsp) 20 involves Akt phosphorylation [116]. Wortmannin is a metabolite of the fungus *Penicillum funiculosum* and a potent inhibitor of Pi3Ks; Pi3Ks activate phosphorylation of Akt. Wortmannin concentrations of 100 and 1000 nM completely abrogated the protection induced by OT in a concentration - dependent manner without causing cell toxicity. This finding indicates that the protection induced by OT is mediated by the action of Pi3Ks, the kinase which also mediates glucose uptake in isolated neonatal rat cardiomyocyte culture[76].

IV.4.2. OT causes phosphorylated Akt (Thr308) to co-localize with mitochondria in or around the nucleus

Using formazan production for the measurement of cell viability and metabolic activity, a significant cellular protection was observed at a concentration of 1 nM of OT, with an optimal protection at 62.5-125 nM. This observation is consistent with a report by Klein *et al*. on Caco 2BB gut cells demonstrating that OT activates the Pi3K pathway maximally when given at a concentration of 62.5 nM. In our study, treatment of H9c2 cells with this concentration of OT resulted in the formation of clear intracellular structures of accumulated p-Akt. Confocal microscopy analysis revealed that these structures of p-Akt co-localize precisely with mitochondrial protein Cox IV.

Cardioprotective stimuli that open mitoK$_{ATP}$ channels such as BMS-191095 are thought to trigger mitoK$_{ATP}$ opening via the translocation of phosphorylated Akt to the mitochondria[36]. Activated mitochondrial Akt phosphorylates hexokinase-II and results in the prevention of mPTP opening due to ROS and Ca^{2+} overload[38]. Akt is also known to phosphorylate Bcl-2 family members: BAD phosphorylation at Ser136 by Akt is cardioprotective, and Bax phosphorylation at Ser184 by Akt prevents the conformational change necessary for Bax translocation to the mitochondria[35] where it triggers mPTP opening. Additionally, Akt causes the inhibition of the translocation of apoptosis initiating factor (AIF) to the nucleus where it induces DNA fragmentation; Akt also phosphorylates and inactivates caspase-9 (Ser 196)[30].

Activated Akt is known to be translocated actively to the nucleus, where it acts to regulate gene transcription by phosphorylating many different targets such as Forkhead transcription factors (FOXO), CREB[120] and Pim-1 kinase[121]. In the context of cardiac ischemia, nuclear Akt has been shown to be cardioprotective in hypoxia and ischemia-reperfusion [122].

Constitutive and sustained Akt activation is associated with cardiomyocyte hypertrophy[28], nuclear-targeted Akt does not induce hypertrophy in cardiomyocytes *in vivo* and *in vitro*[122] but rather antagonizes hypertrophy and causes an increase in atrial natriuretic peptide (ANP) expression[123]. Oxytocin is well known to cause an increase in ANP expression and release from the heart[63]. It is thus possible that the mechanism by which OT exerts its protection during reperfusion involves Akt phosphorylation and translocation to the nucleus, where it causes an increase in protective ANP synthesis and release. Our experiments supported this concept by the demonstration that the use of ANP receptor antagonist, A71915 resulted in the loss of OT-mediated protection of H9c2 cells exposed to IR. Although de novo ANP synthesis are unlikely to play a role in the acute phase of ischemia - reperfusion injury, ANP release from intracellular stores is a fast process counted in seconds and minutes. Furthermore, ANP release, known to be triggered in cardiomyocytes by the action of OT[63], also causes nuclear accumulation of phosphorylated Akt and pro-survival signaling[31]. ANP is an established cardioprotective agent[124]; it inhibits the release of renin and aldosterone synthesis, inhibits sympathetic nerve activity, ameliorates endothelial function, decreases fibrosis, inflammation and apoptosis in myocytes secondary to cGMP production[89].

IV.4.3. OT mediates cardioprotection through eNOS phosphorylation and cGMP-PKG signaling

The activity of cGMP - dependent protein kinase (PKG) is well - known to trigger protective signaling in the context of myocardial ischemia - reperfusion injury. PKG can directly prevent mPTP opening, possibly due to the opening of mitoK$_{ATP}$ and PKCε - mediated inhibition of the mPTP. The protective effect of preconditioning with oxytocin was abrogated

by the administration of 5-hydroxydecanoate, an inhibitor of mitoK[ATP] in anesthetized rat[80] and rabbit[82] hearts. Oxytocin could trigger PKG signaling by three different mechanisms. First, OT acting via OTR stimulates PLC-β to produce inositol-3,4,5-triphosphate (IP3) and DAG. IP3 leads to Ca^{2+} release from intracellular stores and the activation of Ca-Calmodulin (CaM), which activates eNOS to increase NO production. Secondly, OTR stimulates Pi3K activity to produce phosphatidylinositol-3,4,5-triphosphate (PIP3), which activates Akt signaling and in turn eNOS activity. NO produced from these two pathways stimulates soluble guanylate cyclase (sGC) to produce cGMP, which activates PKG[125]. Thirdly, as mentioned above, OT stimulates ANP release from intracellular stores via OTR-mediated Ca^{2+} mobilization secondary also to PLC production of IP3. ANP in turn increases cGMP production via natriuretic peptide receptor A (NPR-A), a membrane-bound guanylyl cyclase (pGC).

NO production has also been proposed as cardioprotective due to the attenuation of ROS production during reperfusion caused by the reversible inhibition of mitochondrial respiratory complex I by S-nitrosylation[19]. Phosphorylation of eNOS at Ser1177, which is protective in ischemia - reperfusion[45], is mediated by Akt[126]. Recent evidence indicates that the subcellular localization of eNOS is an important component in the regulation of the effect induced by NO[127], and vascular endothelial growth factor (VEGF) stimulation was shown to induce translocation of activated eNOS to the nucleus of vascular endothelial cells[128]. OT treatment has been shown to trigger NO production in stem cells[129], with increased eNOS expression in the peri-infarct area in rat MI following OT preconditioning[74] and increased eNOS phosphorylation in rabbits receiving OT at reperfusion[71]. Similarly, the protective

effect of OT preconditioning was abolished by the administration of L-NAME, a non-specific NOS inhibitor, in both anesthetized rat[81] and rabbit[82] hearts.
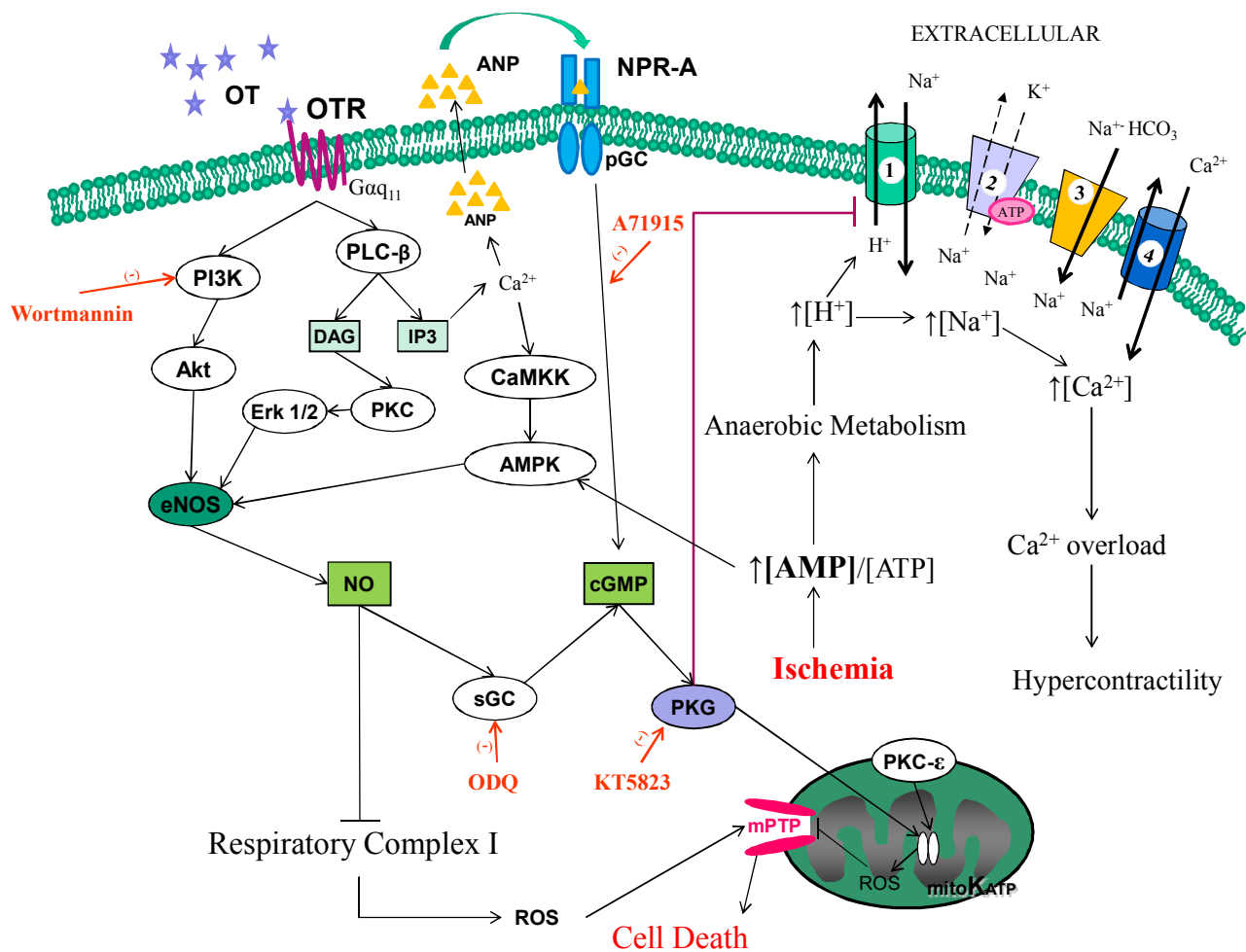
Figure 30. Proposed protective signaling triggered by OT in cardiomyocytes. OT acts via OTR, a sarcolemmal GPCR. The signal stimulates PLC-β and Pi3K/Akt pathways, which result in NO production and the modulation of ionic pump activity, resulting in the inhibition of mitochondrial permeability transition pore (mPTP) opening. OT also causes ANP release, which also causes cGMP production (through NPR-A) and cytoprotection. 1. NHE: Na^+/H^+ exchanger; 2. ATP-dependent Na^+/K^+ pump; 3. Na^+/bicarbonate co-transporter; 4. NCE: Na^+/Ca^{2+} exchanger. OT: oxytocin; OTR: OT Receptor; PLC-β: phospholipase C type β; DAG: diacylglycerol; IP3: inositol-3-phosphate; PKC: protein kinase C; Erk1/2 : extracellular-regulated kinases 1 and 2; PI3K phosphatidylinositol-3-kinase; eNOS: endothelial nitric oxide synthase; NO: nitric oxide; sGC: soluble guanylate cyclase; pGC: particulate guanylate cyclase; cGMP: cyclic guanosine monophosphate; PKG: cGMP-

dependent protein kinase; ROS: reactive oxidative species; mPTP: mitochondrial permeability transition pore; mitoK$_{ATP}$: mitochondrial ATP-sensitive K$^+$ channels; CaM: Ca^{2+}- Calmodulin; CaMKK: CaM kinase kinase; AMPK: AMP-activated protein kinase; NPR-A: natriuretic peptide receptor type A. Adapted from Ref. [130]

IV.5. Signalosome hypothesis

Signalosomes have recently been discovered as cardioprotective signaling complexes induced upon GPCR activation and pre- and postconditioning stimuli[51,52]. Based on our observations, we propose that OT stimulation triggers the formation of signalosomes. The basis for this comes from the observed co-localization of phosphorylated Akt with mitochondrial proteins as well as with the phosphorylated (Ser1177) form of eNOS in precise intracellular structures. The existence of these complexes may explain the co-localization of phosphorylated Akt with the mitochondria as well as with phosphorylated eNOS, and the formation of the observed intracellular structures. Indeed, the effect of signalosomes can be blocked by the administration of an inhibitor of PKG, KT-5823[51]; the same inhibitor completely blocks the OT - mediated protection of cardiomyocyte viability observed in our experiments. Furthermore, eNOS and OTR are both well-known to associate with caveolins (integral membrane proteins that define the structure of caveolae[131]), and the cardioprotective effect of eNOS can be blocked by chemically disrupting caveolae[132], pointing to the need for the caveolar signaling platform for eNOS-mediated cardioprotection. Further experiments are necessary to determine whether OT treatment causes protective signalosome formation. Such experiments might include the isolation of these structures by ultracentrifugation as well as immunoprecipitation of caveolar structures.
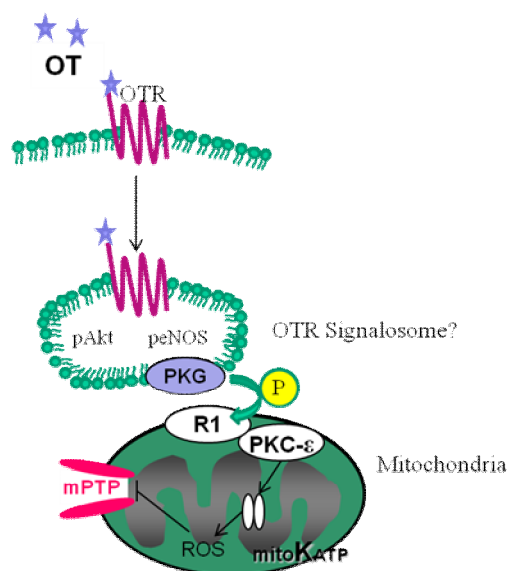
Figure 31. OTR signalosome hypothesis. Upon OT stimulation, a caveolar assembly containing OTR, p-Akt and p-eNOS is formed, which migrates to cell's mitochondria and causes mitoK$_{ATP}$ opening.

Overall, OT is emerging as an exciting candidate for cardioprotection at the time of reperfusion. Repeated observations of the cardioprotection induced by OT *in vivo* as well as *in vitro*, along with a more detailed mechanistic analysis presented in this thesis point to a great potential of this hormone for clinical use. Further potential advantages of OT administration to MI patients include the reduction in stress-induced cardiovascular responses following MI in rats[133], the observation that OT induces cardiomyogenesis of mouse embryonic stem cells through an NO-dependent mechanism[134] as well as of adult sca-1-positive stem cells[135] prevents cardiac hypertrophy (A. Menaouar, unpublished results) and enhances the protective potential of mesenchymal stem cells[114].

V. CONCLUSIONS

The results presented in this thesis clearly indicate that oxytocin (OT) directly triggers protective signaling in cardiomyocytes exposed to simulated ischemia - reperfusion through signaling via oxytocin receptor. Furthermore, the loss of OT receptor expression results in increased cell death following treatment with OT, indicating that the expression level of OTR is a critical determinant of the effect elicited by OT. It is possible that in the absence of OTR, deleterious signaling proceeds via vasopressin receptors present on cardiomyocytes. While OT and OTR knockout mice present slightly altered cardiovascular regulation, to our knowledge no studies have addressed the implications of OT or OTR deficiency in cardiac salvage following ischemia - reperfusion injury. New experiments must be carried out in these knockout models to determine the effects of OT signaling in the absence of OTR in the context of cardiac ischemia - reperfusion.

Oxytocin exerts an optimal protective effect in simulated ischemia - reperfusion (IR) if administered exclusively at the onset of reperfusion, as a postconditioning stimulus. This may reflect the fact that OTR desensitization causes an attenuated response to OT signaling at the critical moment of early reperfusion.

The protection of mitochondrial integrity in early reperfusion is critical for cell survival. Supporting a role for OT protection of mitochondrial integrity is the observation that oxytocin preconditioning protects cardiomyocytes against doxorubicin - induced mitochondrial toxicity in a concentration - dependent manner.

Oxytocin treatment of cardiomyocytes results in Akt and eNOS phosphorylation and their translocations to the cells' nuclei. Additionally, upon oxytocin treatment, the phosphorylated form of Akt co-localizes with cell mitochondria and generates specific structures within or around cell nuclei. To our knowledge this is the first report describing the formation of these structures. Their significance in cardioprotective signaling remains to be further studied.

Based on data obtained from the use of specific inhibitors, we can conclude that the protection induced by oxytocin to cardiomyocytes undergoing IR requires signaling through Pi3K-Akt, the generation of cGMP through particulate, and the activation soluble guanylate cyclase cGMP dependent protein kinase (PKG).

Bibliography

1. Yellon, D. M. & Hausenloy, D. J. Myocardial reperfusion injury. *The New England journal of medicine* **357**, 1121–35 (2007).

2. Piper, H. M., García-Dorado, D. & Ovize, M. A fresh look at reperfusion injury. *Cardiovascular research* **38**, 291–300 (1998).

3. Hausenloy, D. J. & Yellon, D. M. The therapeutic potential of ischemic conditioning: an update. *Nature reviews. Cardiology* **8**, 619–29 (2011).

4. Bell, R. M. & Yellon, D. M. Conditioning the whole heart--not just the cardiomyocyte. *Journal of molecular and cellular cardiology* **53**, 24–32 (2012).

5. Perrelli, M., Pagliaro, P. & Penna, C. Ischemia/reperfusion injury and cardioprotective mechanisms: Role of mitochondria and reactive oxygen species. *World Journal of Cardiology* **3**, 186–200 (2011).

6. Jaswal, J. S., Keung, W., Wang, W., Ussher, J. R. & Lopaschuk, G. D. Targeting fatty acid and carbohydrate oxidation--a novel therapeutic intervention in the ischemic and failing heart. *Biochimica et biophysica acta* **1813**, 1333–50 (2011).

7. Sanada, S., Komuro, I. & Kitakaze, M. Pathophysiology of myocardial reperfusion injury: preconditioning, postconditioning, and translational aspects of protective measures. *American journal of physiology. Heart and circulatory physiology* **301**, H1723–41 (2011).

8. Ovize, M. *et al.* Postconditioning and protection from reperfusion injury: where do we stand? Position paper from the Working Group of Cellular Biology of the Heart of the European Society of Cardiology. *Cardiovascular research* **87**, 406–23 (2010).

9. Murphy, E. & Steenbergen, C. Mechanisms Underlying Acute Protection From Cardiac Ischemia-Reperfusion Injury. *Physiological reviews* **88**, 581–609 (2008).

10. Heusch, G., Boengler, K. & Schulz, R. Inhibition of mitochondrial permeability transition pore opening: the Holy Grail of cardioprotection. *Basic research in cardiology* **105**, 151–4 (2010).

11. Halestrap, A. P., Clarke, S. J. & Javadov, S. A. Mitochondrial permeability transition pore opening during myocardial reperfusion--a target for cardioprotection. *Cardiovascular research* **61**, 372–85 (2004).

12. Murry, C. E., Jennings, R. B. & Reimer, K. a. Preconditioning with ischemia: a delay of lethal cell injury in ischemic myocardium. *Circulation* **74**, 1124–1136 (1986).

13. Yang, X., Cohen, M. V & Downey, J. M. Mechanism of cardioprotection by early ischemic preconditioning. *Cardiovascular drugs and therapy* **24**, 225–34 (2010).

14. Costa, A. D. T. *et al.* The mechanism by which the mitochondrial ATP-sensitive K+ channel opening and H2O2 inhibit the mitochondrial permeability transition. *The Journal of biological chemistry* **281**, 20801–8 (2006).

15. Hausenloy, D. J., Tsang, a, Mocanu, M. M. & Yellon, D. M. Ischemic preconditioning protects by activating prosurvival kinases at reperfusion. *American journal of physiology. Heart and circulatory physiology* **288**, H971–6 (2005).

16. Zhao, Z.-Q. *et al.* Inhibition of myocardial injury by ischemic postconditioning during reperfusion: comparison with ischemic preconditioning. *American journal of physiology. Heart and circulatory physiology* **285**, H579–88 (2003).

17. Tsang, A., Hausenloy, D. J. & Yellon, D. M. Myocardial postconditioning: reperfusion injury revisited. *American journal of physiology. Heart and circulatory physiology* **289**, H2–7 (2005).

18. Hausenloy, D. J. & Yellon, D. M. Preconditioning and postconditioning: united at reperfusion. *Pharmacology & therapeutics* **116**, 173–91 (2007).

19. Heusch, G., Boengler, K. & Schulz, R. Cardioprotection: nitric oxide, protein kinases, and mitochondria. *Circulation* **118**, 1915–9 (2008).

20. Gross, E. R. & Gross, G. J. Ligand triggers of classical preconditioning and postconditioning. *Cardiovascular research* **70**, 212–21 (2006).

21. Leevers, S. J., Vanhaesebroeck, B. & Waterfield, M. D. Signalling through phosphoinositide 3-kinases: the lipids take centre stage. *Current opinion in cell biology* **11**, 219–25 (1999).

22. Sussman, M. a *et al.* Myocardial AKT: the omnipresent nexus. *Physiological reviews* **91**, 1023–70 (2011).

23. Fayard, E., Xue, G., Parcellier, A., Bozulic, L. & Hemmings, B. A. Protein Kinase B (PKB / Akt), a Key Mediator of the PI3K Signaling Pathway. *Current topics in microbiology and immunology* **346**, 31–56 (2010).

24.   Visnjic, D. & Banfic, H. Nuclear phospholipid signaling: phosphatidylinositol-specific phospholipase C and phosphoinositide 3-kinase. *Pflügers Archiv : European journal of physiology* **455**, 19–30 (2007).

25.   Lemmon, M. A., Falasca, M., Schlessinger, J. & Ferguson, K. Regulatory recruitment of signalling molecules to the cell membrane by pleckstrin homology domains. *Trends in cell biology* **7**, 237–42 (1997).

26.   Yoon, H., Hajduk, P. & Petros, A. Solution structure of a pleckstrin-homology domain. *Nature* **369**, 672–675 (1994).

27.   Pawson, T. Protein modules and signalling networks. *Nature* **373**, 573–580 (1995).

28.   Miyamoto, S., Rubio, M. & Sussman, M. a Nuclear and mitochondrial signalling Akts in cardiomyocytes. *Cardiovascular research* **82**, 272–85 (2009).

29.   Su, C.-C., Yang, J.-Y., Leu, H.-B., Chen, Y. & Wang, P. H. Mitochondrial Akt-regulated mitochondrial apoptosis signaling in cardiac muscle cells. *American journal of physiology. Heart and circulatory physiology* **302**, H716–23 (2012).

30.   Parcellier, A., Tintignac, L. a, Zhuravleva, E. & Hemmings, B. a PKB and the mitochondria: AKTing on apoptosis. *Cellular signalling* **20**, 21–30 (2008).

31.   Kato, T. *et al.* Atrial natriuretic peptide promotes cardiomyocyte survival by cGMP-dependent nuclear accumulation of zyxin and Akt. *Journal of clinical investigations* **115**, 2716–30 (2005).

32.   Webster, K. a Aktion in the nucleus. *Circulation research* **94**, 856–9 (2004).

33.   Armstrong, S. C. Protein kinase activation and myocardial ischemia/reperfusion injury. *Cardiovascular research* **61**, 427–36 (2004).

34.   Bijur, G. N. & Jope, R. S. Rapid accumulation of Akt in mitochondria following phosphatidylinositol 3-kinase activation. *Journal of Neurochemistry* **87**, 1427–1435 (2003).

35.   Miyamoto, S., Murphy, A. & Brown, J. Akt mediated mitochondrial protection in the heart: metabolic and survival pathways to the rescue. *Journal of bioenergetics and …* 169–180 (2009).doi:10.1007/s10863-009-9205-y

36.   Ahmad, N. *et al.* Cardiac protection by mitoKATP channels is dependent on Akt translocation from cytosol to mitochondria during late preconditioning. *American journal of physiology. Heart and circulatory physiology* **290**, H2402–8 (2006).

37.   Yang, J.-Y., Yeh, H.-Y., Lin, K. & Wang, P. H. Insulin stimulates Akt translocation to mitochondria: implications on dysregulation of mitochondrial oxidative phosphorylation in diabetic myocardium. *Journal of molecular and cellular cardiology* **46**, 919–26 (2009).

38.   Miyamoto, S., Murphy, a N. & Brown, J. H. Akt mediates mitochondrial protection in cardiomyocytes through phosphorylation of mitochondrial hexokinase-II. *Cell death and differentiation* **15**, 521–9 (2008).

39.   Finocchietto, P. *et al.* Control of muscle mitochondria by insulin entails activation of Akt2-mtNOS pathway: implications for the metabolic syndrome. *PloS one* **3**, e1749 (2008).

40.   Burley, D. S., Ferdinandy, P. & Baxter, G. F. Cyclic GMP and protein kinase-G in myocardial ischaemia-reperfusion: opportunities and obstacles for survival signaling. *British journal of pharmacology* **152**, 855–69 (2007).

41.   Inserte, J. *et al.* cGMP/PKG pathway mediates myocardial postconditioning protection in rat hearts by delaying normalization of intracellular acidosis during reperfusion. *Journal of molecular and cellular cardiology* **50**, 903–9 (2011).

42.   Abdallah, Y. *et al.* Insulin protects cardiomyocytes against reoxygenation-induced hypercontracture by a survival pathway targeting SR Ca2+ storage. *Cardiovascular research* **70**, 346–53 (2006).

43.   Gorbe, A. *et al.* Role of cGMP-PKG signaling in the protection of neonatal rat cardiac myocytes subjected to simulated ischemia/reoxygenation. *Basic research in cardiology* **105**, 643–50 (2010).

44.   Cohen, M. V, Yang, X.-M., Liu, Y., Solenkova, N. V & Downey, J. M. Cardioprotective PKG-independent NO signaling at reperfusion. *American journal of physiology. Heart and circulatory physiology* **299**, H2028–36 (2010).

45.   Sun, J. & Murphy, E. Protein S-Nitrosylation and Cardioprotection. *Circulation research* **106**, 285–296 (2010).

46.   Xuan, Y. T., Guo, Y., Han, H., Zhu, Y. & Bolli, R. An essential role of the JAK-STAT pathway in ischemic preconditioning. *Proceedings of the National Academy of Sciences of the United States of America* **98**, 9050–5 (2001).

47.   Mohr, A. *et al.* Dynamics and non-canonical aspects of JAK/STAT signalling. *European journal of cell biology* **91**, 524–32 (2012).

48. Lecour, S. Activation of the protective Survivor Activating Factor Enhancement (SAFE) pathway against reperfusion injury: Does it go beyond the RISK pathway? *Journal of molecular and cellular cardiology* **47**, 32–40 (2009).

49. Argaud, L. *et al.* Postconditioning inhibits mitochondrial permeability transition. *Circulation* **111**, 194–7 (2005).

50. Davidson, S. M., Hausenloy, D., Duchen, M. R. & Yellon, D. M. Signalling via the reperfusion injury signalling kinase (RISK) pathway links closure of the mitochondrial permeability transition pore to cardioprotection. *The international journal of biochemistry & cell biology* **38**, 414–9 (2006).

51. Garlid, K. D., Costa, A. D. T., Quinlan, C. L., Pierre, S. V & Dos Santos, P. Cardioprotective signaling to mitochondria. *Journal of molecular and cellular cardiology* **46**, 858–66 (2009).

52. Quinlan, C. L. *et al.* Conditioning the heart induces formation of signalosomes that interact with mitochondria to open mitoKATP channels. *American journal of physiology. Heart and circulatory physiology* **295**, H953–H961 (2008).

53. Gutkowska, J. & Jankowski, M. Oxytocin: Old Hormone, New Drug. *Pharmaceuticals* **2**, 168–183 (2009).

54. World Health Organisation *WHO Model List of Essential Medications*. (2011).

55. Du Vigneaud, V., Ressler, C. & Trippett, S. The sequence of amino acids in oxytocin, with a proposal for the structure of oxytocin. *Journal of Biological Chemistry* 949–957 (1953).at <http://www.jbc.org/content/205/2/949.short>

56. Gimpl, G. & Fahrenholz, F. The oxytocin receptor system: structure, function, and regulation. *Physiological reviews* **81**, 629–83 (2001).

57. Kimura, T. *et al.* Molecular regulation of the oxytocin receptor in peripheral organs. *Journal of Molecular Endocrinology* **30**, 109–115 (2003).

58. Danalache, B. a, Gutkowska, J., Slusarz, M. J., Berezowska, I. & Jankowski, M. Oxytocin-Gly-Lys-Arg: a novel cardiomyogenic peptide. *PloS one* **5**, e13643 (2010).

59. Gutkowska, J. & Jankowski, M. Oxytocin revisited: its role in cardiovascular regulation. *Journal of neuroendocrinology* **24**, 599–608 (2012).

60. Zingg, H. H. Vasopressin and oxytocin receptors. *Baillière's Clinical Endocrinology and Metabolism* **10**, 75–96 (1996).

61. Mukaddam-Daher, S., Yin, Y.-L., Roy, J., Gutkowska, J. & Cardinal, R. Negative Inotropic and Chronotropic Effects of Oxytocin. *Hypertension* **38**, 292–296 (2001).

62. Gutkowska, J. & Jankowski, M. Oxytocin revisited: It is also a cardiovascular hormone. *Journal of the American Society of Hypertension : JASH* **2**, 318–25 (2008).

63. Gutkowska, J. *et al.* Oxytocin releases atrial natriuretic peptide by combining with oxytocin receptors in the heart. *Proceedings of the National Academy of Sciences of the United States of America* **94**, 11704–9 (1997).

64. Manning, M. *et al.* Oxytocin and vasopressin agonists and antagonists as research tools and potential therapeutics. *Journal of neuroendocrinology* **24**, 609–28 (2012).

65. Petersson, M., Lundeberg, T., Sohlström, a, Wiberg, U. & Uvnäs-Moberg, K. Oxytocin increases the survival of musculocutaneous flaps. *Naunyn-Schmiedeberg's archives of pharmacology* **357**, 701–4 (1998).

66. Tuğtepe, H. *et al.* The protective effect of oxytocin on renal ischemia/reperfusion injury in rats. *Regulatory peptides* **140**, 101–8 (2007).

67. Düşünceli, F. *et al.* Oxytocin alleviates hepatic ischemia-reperfusion injury in rats. *Peptides* **29**, 1216–22 (2008).

68. Ceanga, M., Spataru, A. & Zagrean, A.-M. Oxytocin is neuroprotective against oxygen-glucose deprivation and reoxygenation in immature hippocampal cultures. *Neuroscience letters* **477**, 15–8 (2010).

69. Jankowski, M. *et al.* Rat heart: a site of oxytocin production and action. *Proceedings of the National Academy of Sciences of the United States of America* **95**, 14558–63 (1998).

70. Ondrejcakova, M., Ravingerova, T., Bakos, J., Pancza, D. & Jezova, D. Oxytocin exerts protective effects on in vitro myocardial injury induced by ischemia and reperfusion. *Canadian journal of physiology and pharmacology* **87**, 137–42 (2009).

71. Kobayashi, H. *et al.* Postinfarct treatment with oxytocin improves cardiac function and remodeling via activating cell-survival signals and angiogenesis. *Journal of cardiovascular pharmacology* **54**, 510–9 (2009).

72. Gutkowska, J., Paquette, A., Wang, D., Lavoie, J.-M. & Jankowski, M. Effect of exercise training on cardiac oxytocin and natriuretic peptide systems in ovariectomized rats. *American journal of physiology. Regulatory, integrative and comparative physiology* **293**, R267–75 (2007).

73. Indrambarya, T., Boyd, J. H., Wang, Y., McConechy, M. & Walley, K. R. Low-dose vasopressin infusion results in increased mortality and cardiac dysfunction following ischemia-reperfusion injury in mice. *Critical care* **13**, R98 (2009).

74. Jankowski, M. *et al.* Anti-inflammatory effect of oxytocin in rat myocardial infarction. *Basic research in cardiology* **105**, 205–18 (2010).

75. Szeto, A. *et al.* Oxytocin attenuates NADPH-dependent superoxide activity and IL-6 secretion in macrophages and vascular cells. *American journal of physiology. Endocrinology and metabolism* **295**, E1495–501 (2008).

76. Florian, M., Jankowski, M. & Gutkowska, J. Oxytocin increases glucose uptake in neonatal rat cardiomyocytes. *Endocrinology* **151**, 482–91 (2010).

77. Alizadeh, A. M. *et al.* Oxytocin protects rat heart against ischemia-reperfusion injury via pathway involving mitochondrial ATP-dependent potassium channel. *Peptides* **31**, 1341–5 (2010).

78. Skyschally, A., Schulz, R. & Heusch, G. Pathophysiology of myocardial infarction: protection by ischemic pre- and postconditioning. *Herz* **33**, 88–100 (2008).

79. Alizadeh, A. M., Faghihi, M., Sadeghipour, H. R., Mohammadghasemi, F. & Khori, V. Role of endogenous oxytocin in cardiac ischemic preconditioning. *Regulatory peptides* **167**, 86–90 (2011).

80. Alizadeh, A. M. *et al.* Oxytocin protects cardiomyocytes from apoptosis induced by ischemia-reperfusion in rat heart: role of mitochondrial ATP-dependent potassium channel and permeability transition pore. *Peptides* **36**, 71–7 (2012).

81. Faghihi, M., Alizadeh, A. M., Khori, V., Latifpour, M. & Khodayari, S. The role of nitric oxide, reactive oxygen species, and protein kinase C in oxytocin-induced cardioprotection in ischemic rat heart. *Peptides* **37**, 314–9 (2012).

82. Das, B. & Sarkar, C. Is preconditioning by oxytocin administration mediated by iNOS and/or mitochondrial K(ATP) channel activation in the in vivo anesthetized rabbit heart? *Life sciences* **90**, 763–9 (2012).

83. Anvari, M. A. *et al.* The administration of oxytocin during early reperfusion, dose-dependently protects the isolated male rat heart against ischemia/reperfusion injury. *European journal of pharmacology* **682**, 137–41 (2012).

84. Flynn, T., Bold, M. de & Bold, A. de The amino acid sequence of an atrial peptide with potent diuretic and natriuretic properties. *Biochemical and biophysical research communications* **117**, 859–865 (1983).

85. Nishikimi, T., Maeda, N. & Matsuoka, H. The role of natriuretic peptides in cardioprotection. *Cardiovascular research* **69**, 318–28 (2006).

86. De Vito, P., Incerpi, S., Pedersen, J. Z. & Luly, P. Atrial natriuretic peptide and oxidative stress. *Peptides* **31**, 1412–9 (2010).

87. Inagami, T. Atrial natriuretic factor. *Journal of Biological Chemistry* **264**, 3043–3046 (1989).

88. Dietz, J. R. Mechanisms of atrial natriuretic peptide secretion from the atrium. *Cardiovascular research* **68**, 8–17 (2005).

89. Kasama, S., Furuya, M., Toyama, T., Ichikawa, S. & Kurabayashi, M. Effect of atrial natriuretic peptide on left ventricular remodelling in patients with acute myocardial infarction. *European heart journal* **29**, 1485–94 (2008).

90. Calderone, a, Thaik, C. M., Takahashi, N., Chang, D. L. & Colucci, W. S. Nitric oxide, atrial natriuretic peptide, and cyclic GMP inhibit the growth-promoting effects of norepinephrine in cardiac myocytes and fibroblasts. *The Journal of clinical investigation* **101**, 812–8 (1998).

91. Oliver, P. M. *et al.* Hypertension, cardiac hypertrophy, and sudden death in mice lacking natriuretic peptide receptor A. *Proceedings of the National Academy of Sciences of the United States of America* **94**, 14730–5 (1997).

92. Kitakaze, M. *et al.* Human atrial natriuretic peptide and nicorandil as adjuncts to reperfusion treatment for acute myocardial infarction (J-WIND): two randomised trials. *Lancet* **370**, 1483–93 (2007).

93. Nishimori, K. *et al.* Oxytocin is required for nursing but is not essential for parturition or reproductive behavior. *Proceedings of the National Academy of Sciences of the United States of America* **93**, 11699–704 (1996).

94. Lee, H.-J., Caldwell, H. K., Macbeth, A. H., Tolu, S. G. & Young, W. S. A conditional knockout mouse line of the oxytocin receptor. *Endocrinology* **149**, 3256–63 (2008).

95. Camerino, C. Low sympathetic tone and obese phenotype in oxytocin-deficient mice. *Obesity (Silver Spring)* **17**, 980–4 (2009).

96.   Nishimori, K. *et al.* New aspects of oxytocin receptor function revealed by knockout mice: sociosexual behaviour and control of energy balance. *Progress in brain research* **170**, 79–90 (2008).

97.   Takayanagi, Y. *et al.* Oxytocin receptor-deficient mice developed late-onset obesity. *Neuroreport* **19**, 951–955 (2008).

98.   Young, W. S. *et al.* Deficiency in mouse oxytocin prevents milk ejection, but not fertility or parturition. *Journal of neuroendocrinology* **8**, 847–53 (1996).

99.   Michelini, L. C., Marcelo, M. C., Amico, J. & Morris, M. Oxytocinergic regulation of cardiovascular function: studies in oxytocin-deficient mice. *American journal of physiology. Heart and circulatory physiology* **284**, H2269–76 (2003).

100.   Amico, J. A., Morris, M. & Vollmer, R. R. Mice deficient in oxytocin manifest increased saline consumption following overnight fluid deprivation. *American journal of physiology. Regulatory integrative and comparative physiology* **281**, R1368–73 (2013).

101.   Puryear, R., Rigatto, K. V, Amico, J. a & Morris, M. Enhanced salt intake in oxytocin deficient mice. *Experimental neurology* **171**, 323–8 (2001).

102.   Rigatto, K., Puryear, R., Bernatova, I. & Morris, M. Salt appetite and the renin-angiotensin system: effect of oxytocin deficiency. *Hypertension* **42**, 793–7 (2003).

103.   Bernatova, I., Rigatto, K. V, Key, M. P. & Morris, M. Stress-induced pressor and corticosterone responses in oxytocin-deficient mice. *Experimental physiology* **89**, 549–57 (2004).

104.   Winslow, J. T. & Insel, T. R. The social deficits of the oxytocin knockout mouse. *Neuropeptides* **36**, 221–229 (2002).

105.   Takayanagi, Y. *et al.* Pervasive social deficits, but normal parturition, in oxytocin receptor-deficient mice. *Proceedings of the National Academy of Sciences of the United States of America* **102**, 16096–101 (2005).

106.   Banerjee, I., Fuseler, J. W., Price, R. L., Borg, T. K. & Baudino, T. Determination of cell types and numbers during cardiac development in the neonatal and adult rat and mouse. *American journal of physiology. Heart and circulatory physiology* **293**, H1883–91 (2007).

107.   Teng, R., Calvert, J. & Sibmooh, N. Acute erythropoietin cardioprotection is mediated by endothelial response. *Basic research in cardiology* **106**, 343–354 (2011).

108. Ikonomidis, J. S., Tumiati, L. C., Weisel, R. D., Mickle, D. A. G. & Li, R.-K. Preconditioning human ventricular cardiomyocytes with brief periods of simulated ischaemia. *Cardiovascular Research* **28** , 1285–1291 (1994).

109. Diaz, R. J. & Wilson, G. J. Studying ischemic preconditioning in isolated cardiomyocyte models. *Cardiovascular research* **70**, 286–96 (2006).

110. Gomez, L. a, Alekseev, a E., Aleksandrova, L. a, Brady, P. a & Terzic, a Use of the MTT assay in adult ventricular cardiomyocytes to assess viability: effects of adenosine and potassium on cellular survival. *Journal of molecular and cellular cardiology* **29**, 1255–66 (1997).

111. Zhang, X. *et al.* Synergistic effects of the GATA-4-mediated miR-144/451 cluster in protection against simulated ischemia/reperfusion-induced cardiomyocyte death. *Journal of Molecular and Cellular Cardiology* **49**, 841–850 (2010).

112. Klein, B. Y., Tamir, H. & Welch, M. G. PI3K/Akt responses to oxytocin stimulation in Caco2BB gut cells. *Journal of cellular biochemistry* **112**, 3216–26 (2011).

113. Green, P. S. & Leeuwenburgh, C. Mitochondrial dysfunction is an early indicator of doxorubicin-induced apoptosis. *Biochimica et biophysica acta* **1588**, 94–101 (2002).

114. Noiseux, N. *et al.* Preconditioning of stem cells by oxytocin to improve their therapeutic potential. *Endocrinology* **153**, 5361–72 (2012).

115. Angeloni, C. *et al.* H2O2 preconditioning modulates phase II enzymes through p38 MAPK and PI3K/Akt activation. *American journal of physiology. Heart and circulatory physiology* **300**, H2196–205 (2011).

116. Fan, G.-C. *et al.* Heat shock protein 20 interacting with phosphorylated Akt reduces doxorubicin-triggered oxidative stress and cardiotoxicity. *Circulation research* **103**, 1270–9 (2008).

117. Cattaneo, M. G., Lucci, G. & Vicentini, L. M. Oxytocin stimulates in vitro angiogenesis via a Pyk-2/Src-dependent mechanism. *Experimental cell research* **315**, 3210–9 (2009).

118. Li, X. *et al.* Controlled and cardiac-restricted overexpression of the arginine vasopressin V1A receptor causes reversible left ventricular dysfunction through Gαq-mediated cell signaling. *Circulation* **124**, 572–81 (2011).

119. Saotome, M. *et al.* Transient opening of mitochondrial permeability transition pore by reactive oxygen species protects myocardium from ischemia-reperfusion injury. *American journal of physiology. Heart and circulatory physiology* **296**, H1125–32 (2009).

120. Du, K. & Montminy, M. CREB is a regulatory target for the protein kinase Akt/PKB. *Journal of Biological Chemistry* **273**, 32377–9 (1998).

121. Muraski, J. a *et al.* Pim-1 regulates cardiomyocyte survival downstream of Akt. *Nature medicine* **13**, 1467–75 (2007).

122. Shiraishi, I. *et al.* Nuclear targeting of Akt enhances kinase activity and survival of cardiomyocytes. *Circulation research* **94**, 884–91 (2004).

123. Tsujita, Y. *et al.* Nuclear targeting of Akt antagonizes aspects of cardiomyocyte hypertrophy. *Proceedings of the National Academy of Sciences of the United States of America* **103**, 11946–51 (2006).

124. Burley, D. S., Hamid, S. a & Baxter, G. F. Cardioprotective actions of peptide hormones in myocardial ischemia. *Heart failure reviews* **12**, 279–91 (2007).

125. Xu, Z., Ji, X. & Boysen, P. G. Exogenous nitric oxide generates ROS and induces cardioprotection: involvement of PKG, mitochondrial KATP channels, and ERK. *American journal of physiology. Heart and circulatory physiology* **286**, H1433–40 (2004).

126. Klinz, F.-J. *et al.* Phospho-eNOS Ser-114 in human mesenchymal stem cells: constitutive phosphorylation, nuclear localization and upregulation during mitosis. *European Journal of Cell Biology* **84**, 809–818 (2005).

127. Gobeil, F. *et al.* Nitric oxide signaling via nuclearized endothelial nitric-oxide synthase modulates expression of the immediate early genes iNOS and mPGES-1. *The Journal of biological chemistry* **281**, 16058–67 (2006).

128. Feng, Y., Venema, V. J., Venema, R. C., Tsai, N. & Caldwell, R. B. VEGF Induces Nuclear Translocation of Flk-1/KDR, Endothelial Nitric Oxide Synthase, and Caveolin-1 in Vascular Endothelial Cells. *Biochemical and Biophysical Research Communications* **256**, 192–197 (1999).

129. Danalache, B. a *et al.* Nitric oxide signaling in oxytocin-mediated cardiomyogenesis. *Stem cells* **25**, 679–88 (2007).

130. Gonzalez Reyes, A., Gutkowska, J. & Jankowski, M. L ' ocytocine : un facteur de protection cardiaque. *Médecine Sciences Amérique* (2011).

131. Quest, A. F. G., Gutierrez-Pajares, J. L. & Torres, V. a Caveolin-1: an ambiguous partner in cell signalling and cancer. *Journal of cellular and molecular medicine* **12**, 1130–50 (2008).

132. Sun, J. *et al.* Disruption of caveolae blocks ischemic preconditioning-mediated S-nitrosylation of mitochondrial proteins. *Antioxidants & redox signaling* **16**, 45–56 (2012).

133. Wsół, A., Cudnoch-Je drzejewska, A., Szczepanska-Sadowska, E., Kowalewski, S. & Dobruch, J. Central oxytocin modulation of acute stress-induced cardiovascular responses after myocardial infarction in the rat. *Stress (Amsterdam, Netherlands)* **12**, 517–25 (2009).

134. Paquin, J., Danalache, B. a, Jankowski, M., McCann, S. M. & Gutkowska, J. Oxytocin induces differentiation of P19 embryonic stem cells to cardiomyocytes. *Proceedings of the National Academy of Sciences of the United States of America* **99**, 9550–5 (2002).

135. Matsuura, K. *et al.* Adult cardiac Sca-1-positive cells differentiate into beating cardiomyocytes. *The Journal of biological chemistry* **279**, 11384–91 (2004).